2015

LOSS OF MULTIDRUG RESISTANCE-ASSOCIATED PROTEIN 1 (MRP1/ABCC1) POTENTIATES DOXORUBICIN-INDUCED CARDIOTOXICITY IN MICE

Wei Zhang
University of Kentucky, zhangwei1104@gmail.com

STUDENT AGREEMENT:

I represent that my thesis or dissertation and abstract are my original work. Proper attribution has been given to all outside sources. I understand that I am solely responsible for obtaining any needed copyright permissions. I have obtained needed written permission statement(s) from the owner(s) of each third-party copyrighted matter to be included in my work, allowing electronic distribution (if such use is not permitted by the fair use doctrine) which will be submitted to UKnowledge as Additional File.

I hereby grant to The University of Kentucky and its agents the irrevocable, non-exclusive, and royalty-free license to archive and make accessible my work in whole or in part in all forms of media, now or hereafter known. I agree that the document mentioned above may be made available immediately for worldwide access unless an embargo applies.

I retain all other ownership rights to the copyright of my work. I also retain the right to use in future works (such as articles or books) all or part of my work. I understand that I am free to register the copyright to my work.

REVIEW, APPROVAL AND ACCEPTANCE

The document mentioned above has been reviewed and accepted by the student's advisor, on behalf of the advisory committee, and by the Director of Graduate Studies (DGS), on behalf of the program; we verify that this is the final, approved version of the student's thesis including all changes required by the advisory committee. The undersigned agree to abide by the statements above.

Wei Zhang, Student

Dr. Mary Vore, Major Professor

Dr. Isabel Mellon, Director of Graduate Studies

LOSS OF MULTIDRUG RESISTANCE-ASSOCIATED PROTEIN 1 (MRP1/ABCC1) POTENTIATES DOXORUBICIN-INDUCED CARDIOTOXICITY IN MICE

DISSERTATION

A dissertation submitted in partial fulfillment of the requirements for the degree of Doctor of Philosophy in the Graduate School at the University of Kentucky

By

Wei Zhang

Lexington, KY

Co-Director: Dr. Mary Vore, Professor of Toxicology

and Dr. Daret St Clair, Professor of Toxicology

University of Kentucky

Lexington, KY

2015

ABSTRACT OF DISSERTATION

LOSS OF MRP1 POTENTIATES DOXORUBICIN-INDUCED CARDIOTOXICITY IN MICE

Doxorubicin (DOX) is a broad-spectrum and effective chemotherapeutic agent, but its use in oncologic practice is limited by dose-dependent cumulative cardiotoxicity. DOX-induced cardiotoxicity is in large part due to its ability to cause oxidative stress. Multidrug resistance associated protein 1 (MRP1/ABCC1) is a member of the ATP-binding cassette (ABC) transporter superfamily. By effluxing a wide variety of endogenous and exogenous substrates, Mrp1 plays important physiological roles in multiple tissues and also protects normal tissues against toxicants. However, the role of MRP1 in heart is largely unknown.

The role of Mrp1 in DOX-induced cardiotoxicity was investigated in Mrp1 null (Mrp1-/-) and their C57BL (WT) littermates. Chronic DOX caused body weight loss and hemotoxicity, and these adverse effects were significantly exacerbated in Mrp1-/- vs WT mice. Importantly, loss of Mrp1 potentiated DOX-induced cardiotoxicity, presenting as worsened cardiac function and more cellular apoptosis in DOX treated Mrp1-/- mice. Mrp1 also protected neonatal mouse cardiomyocytes (CM) and cardiac fibroblasts (CF) culture against DOX cytotoxicity *in vitro*. This was demonstrated by the decreased cell survival, more apoptosis and more DNA damage in DOX treated Mrp1-/- vs WT cells.

In addition, the effects of deletion of Mrp1 was studied on glutathione (GSH)/glutathione disulfide (GSSG) homeostasis, glutathione conjugate of 4-hydroxy-2-nonenal (GS-HNE) accumulation, protein oxidative damage and expression of antioxidant enzymes. Loss of Mrp1 led to significantly higher GSH and GSSG basal levels in heart. Following DOX treatment, Mrp1-/- CM and CF showed increased GSH and GSSG levels vs WT cells. Meanwhile, DOX increased expression of the GSH synthesis enzymes in Mrp1-/- but not WT cells. Thus, increased GSH synthesis may contribute to the further increase in the GSH pool in DOX-treated Mrp1-/- cells. DOX induced comparable increases of GS-HNE concentration in WT and Mrp1-/- mice hearts. Finally, expression of

extracellular superoxide dismutase (ECSOD/SOD3) was significantly lower in Mrp1-/- vs. WT CM treated with either saline or DOX.

In summary, this study is the first to document a protective role of Mrp1 in DOX-induced cardiotoxicity. It gives critical information regarding the potential adverse sequelae of introduction of MRP1 inhibitors as adjuncts to clinical chemotherapy of multidrug resistant tumors.

KEYWORDS: Mrp1, doxorubicin, cardiotoxicity, glutathione, GS-HNE.

Wei Zhang

Student's signature

08/10/2015

Date

LOSS OF MULTIDRUG RESISTANCE-ASSOCIATED PROTEIN 1 (MRP1/ABCC1) POTENTIATES DOXORUBICIN-INDUCED CARDIOTOXICITY IN MICE

By

Wei Zhang

Dr. Mary Vore
Co-Director of Dissertation

Dr. Daret St Clair
Co-Director of Dissertation

Dr. Isabel Mellon
Director of Graduate Studies

08/10/2015
Date

Acknowledgements

This project throughout my graduate training would not have been possible without the support of many people. First, I express my deepest thanks to my Ph.D. advisor, Professor Dr. Mary Vore, for providing me this wonderful opportunity to work in her laboratory and learn from her how to be a better scientist and a better person. Throughout my Ph.D. study, she always encouraged me to develop independent thinking and research skills. She continually and greatly assisted me with the scientific writing skills. I will always be grateful for the time, patience, attention, guidance, mentorship and support she has provided. I have my special thanks to the Co-chair of my committee Dr. Daret St Clair, who provided timely and instructive comments and evaluation at every stage of my research process, allowing me to complete this project successfully. I would like to acknowledge my committee members, Dr. Allan Butterfield and Dr. Zhigang Wang for their constructive comments, help and guidance. I am also grateful for Dr. Jonathon Satin for agreeing to be my outside examiner.

I appreciate the assistance of Dr. Andrew Morris and Dr. Manjula Sunkara with LC/MS assays, Dr. Brandon Fornwalt, Dr. Moriel Vandsburger and Dr. Ahmed Abdel-Latif with the echocardiography study, Dr. Jonathon Satin and Gail Sievert with the neonatal mouse cardiomyocytes isolation, Dr. Chi Wang with the statistical analysis, and Dr. Mihail Mitov and Michael Alstott with the slot blot assay. I would also like to thank Dr. Xianglin Shi, Dr. Joy Zhang, Dr. Bernhard

Hennig forgenerously providing experimental materials and instruments used in this study.

I am grateful to the members of Dr. Vore' Lab and Dr. St Clair' lab, past and present, for all of their generous help, scientific advice, friendship and company. They are Baoxiang Yan, Dr. Jun Deng, Dr. Donna Coy, Dr. Tianyong Zhao, Dr. Paiboon Jungsuwadee, Dr. Caixia Hou, Teresa Noel, Dr. Luksana Chaiswing, Chontida Yarana, Dr. Yanming Zhao and Dr. Sangjit K Dhar. All my friends and colleagues at the University of Kentucky will be sorely missed.

Finally, I am forever grateful to my parents, Yu Zhang and Jun Cai for their love and always encouraging me to pursue higher education. And last, but not least, I owe special thanks to my husband, Xiabin Chen, for his continuous love, encouragement and support through our time in Kentucky.

TABLE OF CONTENTS

LIST OF TABLES

LIST OF FIGURES

Chapter One

Introduction

Overview

Chemotherapy usually refers to the use of chemical substances to treat cancer. It is one of the three main methods utilized to treat cancer, and may be used in conjunction with two other methods, radiation therapy and surgery. However, side effects induced by chemotherapy occurring in off-target organs sometimes significantly limit its clinic use. Acute toxicity induced by chemotherapy is usually due to the toxic effects on rapidly dividing normal cells, like hematological toxicity and gastrointestinal toxicity. In contrast, the late toxicity of chemotherapy is more complex and more difficult to be treated. Actually, in the last few decades, because of the advances in cancer treatment, more patients are becoming long-term survivors of this disease. Therefore, it is becoming increasingly important to understand how chemotherapy causes long-term adverse effects and how we might prevent them. The long-term effects of chemotherapy mainly include cardiac toxicity, pulmonary toxicity, impairment of fertility and secondary cancers. Among them, cardiac toxicity is one of the most severe side effects. It can occur within days, months or even years after treatment and it leads to an important increase of morbidity and mortality in patients receiving chemotherapy.

Doxorubicin (DOX) is a commonly used anthracycline chemotherapy agent for a wide variety of cancers. Large scale clinical studies show that DOX

significantly increases the incidence of heart failure in cancer patients. Studies in animal models and in vitro cell culture also demonstrate that DOX promotes the generation of reactive oxygen species (ROS) and causes oxidative stress in heart tissue or cardiomyocytes. Understanding the defense mechanisms of normal heart tissue against DOX toxicity will be very helpful to identify susceptible patients in the clinic and also identify potential ways to relieve or even prevent DOX-induced adverse effects in heart.

Multidrug resistance-associated protein 1 (MRP1/ABCC1) is a member of ATP-binding cassette (ABC) transporter superfamily. It is ubiquitously expressed in multiple tissues and utilizes the energy of ATP hydrolysis to actively transport a wide variety of compounds across biological membranes (cell or organelle membranes). It has been demonstrated to mediate a protective role in multiple organs through the excretion of toxic compounds and their metabolites. Recently, there is growing evidence showing that single nucleotide polymorphisms (SNPs) of MRP1 are associated with cancer patients' susceptibility to DOX-induced cardiotoxicity. But the underlying mechanism is not clear. Previous work in our laboratory found that one of these SNPs (Gly671Val) impairs by more than 85% MRP1's activity in effluxing glutathione conjugated 4-Hydroxy-2-nonenal (GS-HNE), and HEK cells that overexpress MRP1 (Gly671Val) are more sensitive to DOX toxicity compared to WT MRP1. Additional previous work in our laboratory found that after a single intravenous administration of DOX, Mrp1 null (Mrp1-/-) mice have more nuclear injury in heart compared to their wild type (WT) littermates. Thus, I hypothesize that MRP1 protects the heart against DOX

toxicity by effluxing the toxic products. This study explored the potential protective function of Mrp1 in DOX-induced cardiotoxicity *in vivo* and in *vitro*.

Doxorubicin (DOX)

DOX and its medical use in cancer treatment

DOX, also known by its trade name Adriamycin, is an anthracycline antibiotic chemotherapeutic drug derived from the bacterium *Streptomyces peucetius var. caesius* (Arcamone et al., 1969). It is one of the most potent anti-cancer agents and it is prescribed in isolation or in association with other drugs. DOX is used to treat a wide variety of cancers in multiple organs, including gynecological (breast, endometrium, ovary), urogenital (bladder, testicle), endocrine (thyroid, pancreas), gastrointestinal (stomach), and lung cancer. It is also effective in sarcomas (neuroblastoma, Ewing sarcoma, and osteosarcoma), acute lymphocytic and myeloid leukemia, and lymphomas (Minotti et al., 2004; Octavia et al., 2012). In the clinic, DOX is administered strictly by intravenous infusion. If the medication escapes from the vein, it can cause tissue irritation or damage. The dose and how often the medicine is given depends on patients' body size, blood counts, hepatic function, and the type of cancer being treated.

DOX induces cardiotoxicity

Despite its excellent clinical efficacy as a chemotherapeutic agent, the clinical usage of DOX has been restricted due to its potential to induce serious side effects in cancer patients, including low white blood cell counts with increased

risk of infection, low platelet counts with increased risk of bleeding, hair loss or thinning, nausea, vomiting and the most severe one - cardiotoxicity (Minotti et al., 2004; Dolye et al., 2005). Clinical studies clearly show that the incidence of heart failure rises rapidly once the cumulative dose of DOX exceeds 550 mg/m^2 in cancer patients (Von Hoff et al., 1979; Swain et al., 2003). For example, the incidence of heart failure is nearly 2% with a cumulative DOX dose of 300 mg/m^2 but rapidly increases to 20% at cumulative doses in excess of 550 mg/m^2 (Christiansen et al., 2006). In addition, the risk of heart failure is higher in individuals with a history of cardiomyopathy, mediastinal irradiation and heart disease (Chatterjee et al., 2010). Since the incidence of heart failure is highly dependent on how long these patients are being followed, it is now well-accepted that there is no absolutely safe dose of DOX for the heart. This means that the risk of developing heart failure in cancer patients treated with DOX remains a life-long threat.

Clinically, DOX-induced cardiotoxicity can occur acutely (during administration or on the day when treatment is given), subacutely (several days to months following administration), or be delayed (years to decades following exposure). Acute cardiotoxicity is uncommon. The incidence particularly increases when the cumulative dose exceeds 550 mg/m^2. It can consist of arrhythmias, a peri-myocarditis syndrome or electrocardiographic abnormalities. The subacute damage develops more insidiously over months, with increasing fatigue, tachycardia and eventually pulmonary edema and right heart congestive symptoms. The chronic/delayed cardiotoxicity is the most clinically relevant. It

can result in ventricular dysfunction, heart failure, and arrhythmias years or even decades after exposure. This suggests the need for a continuous follow-up of the cardiac status of patients who receive DOX. Chronic heart damage induced by DOX is usually considered to be irreversible. Thus, DOX-induced chronic/delayed cardiac toxicity strongly impacts cancer patients' quality of life and even survival and thus also significantly limits the therapeutic options.

Mechanisms of DOX-induced cardiotoxicity

The cancer therapeutic effect of DOX is mainly mediated by its intercalation into DNA or to act as a "topoisomerase poison" in dividing cells, causing DNA fragmentation, polymerase inhibition, and decreased DNA, RNA and protein synthesis (Rabbani et al., 2005). This mechanism is unlikely to be the major contributor in myocardial injury, since the replication of myocytes in heart is less active. A number of mechanisms have been proposed to explain the development of DOX-induced cardiotoxicity, including disruption of intracellular iron homeostasis (Ducroq et al., 2010), free radical and reactive oxygen species (ROS) formation (Minotti et al., 2004; Yen et al., 1996), reduction in the activity of endogenous antioxidant enzymes (Li et al., 2000), mitochondrial damage (Green et al., 2002), direct interaction with cell death triggers or down-regulation of cell survival genes (Poizat et al., 2005; Liu et al., 2008; Park et al., 2011), and activation of innate immunity (Nozaki et al., 2004; Riad et al., 2008). Although the mechanism of DOX-induced cardiotoxicity is likely complex and multifactorial, one of the most well-accepted hypothesis is that DOX-induced oxidative stress in

cardiac tissue through the generation of ROS is a major contributor.

This hypothesis states that the superoxide anion ($\bullet O_2^-$) and other reactive ROS generated by DOX, which cycles between the quinone and semiquinone, contribute significantly to cardiac pathology (Gewirtz, 1999; Minotti et al., 2004). First, a DOX molecule accepts one electron from NADH or NADPH to form the reduced semiquinone radical of DOX. In heart, enzymes that can catalyze this reaction include mitochondrial NADH dehydrogenases present in the sarcoplasmic reticulum and mitochondria as well as cytosolic enzymes such as NADPH dehydrogenase, xanthine oxidase and nitric oxide synthases (Pawłowska et al., 2003; Nohl et al., 1998; Vásquez-Vivar et al., 1997; Fogli et al., 2004). Then, the unpaired electron is donated to molecular oxygen by DOX-semiquinone, forming $\bullet O_2^-$ (Figure 1.1). Once the $\bullet O_2^-$ is produced, the dismutation of $\bullet O_2^-$ to hydrogen peroxide (H_2O_2) is catalyzed by superoxide dismutase (SOD) or may occur spontaneously. H_2O_2 is a relatively stable and low-toxicity molecule, and can be eliminated by catalase, glutathione peroxidase (Gpx) and thioredoxin peroxidase (Tpx) under physiological conditions. However, in the presence of transition metal ions, especially iron ions, the overproduction of H_2O_2 and $\bullet O_2^-$ can be converted through Fenton and Haber-Weiss reaction to a large amount of hydroxyl radical (•OH), which has a very short half-life and is extremely reactive and toxic. It reacts with almost any oxidizable compound in its vicinity and thus induces damage to all types of macromolecules, including lipids, nucleic acids, and proteins. Among these macromolecular damages, lipid peroxidation is probably the most important. The lipid peroxidation can result in

severe membrane dysfunction and significant damage to mitochondrial structural integrity and function. Therefore, it is the ROS released by this DOX redox cycling, rather than DOX itself that is most likely responsible for drug induced adverse cardiotoxicity.

A body of evidence in animal models supports the hypothesis that ROS contributes to DOX-induced cardiotoxicity. For example: chronic DOX cardiotoxicity has been associated with a marked drop in expression of the antioxidant enzyme manganese superoxide dismutase (MnSOD) (Li et al., 2000; Stěrba et al., 2011), while overexpression of MnSOD protects mitochondrial complex I against DOX-induced cardiotoxicity in MnSOD transgenic mice (Yen et al., 1996; Yen et al., 1999). The overexpression of glutathione peroxidase (Gpx) protects the isolated mouse heart from toxicity induced by DOX perfusion, as well as heart damage in mice treated with single high dose of DOX (15 mg/kg) (Xiong et al., 2006). Furthermore, multiple antioxidant molecules show promising protective effects in myocyte cell culture study or small animal studies (Oliveira et al., 2004; Lou et al., 2005; Singal et al., 2000).

This importance of antioxidant enzymes and molecules in protecting against DOX-induced cardiotoxicity also provides some explanation of why the heart is particularly susceptible to DOX. First, the heart has a large density/volume of mitochondria because it requires large amounts of energy. However, mitochondria are both important sources of ROS formation and susceptible targets of ROS damage. The abundance of mitochondria existing in heart could cause extensive production of ROS and exacerbate the ROS-induced tissue

damage, which is related to mitochondrial dysfunction (Hansen at al., 2006). Second, the heart has relatively lower amounts of antioxidant enzymes like SOD and catalase compared to other tissues, such as the liver (Gao et al., 2008). In fact, after exposure to DOX, cardiomyocytes show a further decrease in the content/activity of antioxidant enzymes, including GPx, cytosolic Cu,ZnSOD and mitochondrial MnSOD, at least at some specific time points (Li et a., 2000).

Current treatment for DOX induced cardiotoxicity

At present, there are three major approaches for primary prevention of DOX-induced cardiotoxicity. One strategy is to reduce cardiotoxic potency by administering DOX via continuous infusion instead of one bolus injection. The idea behind this approach is that the DOX concentration in the heart is lower when a continuous infusion is given, leading to lower clinical cardiotoxicity, while DOX concentrations in tumor tissue are the same with continuous or bolus administration (Pacciarini et al., 1978). Thus, increasing infusion duration clearly reduced cardiotoxicity without compromising oncological efficacy. Another strategy is to use liposomal encapsulation, or using a less cardiotoxic derivative (e.g., epirubicin or idarubicin). Liposomal DOX is trapped within the internal aqueous compartment by the ion gradient difference and helps to restrict DOX inside the vessel wall of organs with tight capillary junctions (normal tissues such as the heart), but allows DOX to more readily penetrate through tumor vasculature, which is more fragile and permeable than healthy tissue. Thus, liposomal DOX can significantly decrease the DOX concentration in the heart

without impairment of its anti-cancer efficacy (Rahman et al., 2007; Safra et al., 2000). However, because of its high cost, liposomal DOX is not widely used yet. In addition to changing the way of administration and drug formulation, another approach to relieve DOX-induced cardiotoxicity is to use a cardioprotective agent in conjunction with DOX treatment. Dexrazoxane is the only cardioprotective drug currently available in the clinic. Dexrazoxane's ability to chelate iron was previously thought to be the primary mechanism of cardioprotection. However, the lack of similar effects when other even stronger iron chelators are used has questioned this mechanism (Simůnek et al., 2009). Finally, because there is some concern that dexrazoxane may attenuate the chemotherapeutic efficacy of DOX, it is recommended that its use be initiated only after a patient has received more than 300 mg/m^2 of DOX.

At present, scientists continue to identify additional optimal ways to address this problem, and some potential candidates are under investigation. One major category is antioxidant chemicals and free radical scavengers. For example, Carvedilol, a clinically approved adrenergic blocking agent with potent anti-oxidant activity, has been found to be protective against DOX-induced ROS generation and apoptosis in rat heart in vivo (Oliveira et al., 2004). Another antioxidant, probucol, has been shown to prevent the left ventricular ejection fraction (LVEF) decrease in DOX-treated rats (Li et al., 2000; Lou et al., 2005; Singal et al., 2000). However, while the animal model studies and in vitro experiments have generally shown the favorable effects of antioxidant therapy, the results of clinical studies of antioxidants in patients have been inconsistent

due to differences in the antioxidant agent used, timing of therapy, type of malignancy and chemotherapeutic regimen. Continuous efforts in elucidating the pathogenic mechanisms, as well as identifying new therapeutic targets, will certainly be necessary for the development of more effective therapies.

ATP-binding cassette (ABC) transporter superfamily

The ATP-binding cassette (ABC) transporter superfamily is one of the largest and most broadly expressed transmembrane protein superfamilies known. The members are classified as ABC transporters based on the sequence and organization of their ATP-binding domain, also known as NBDs (nucleotide binding domains). ABC transporters are ubiquitous integral membrane proteins and the vast majority of them utilize the energy of ATP hydrolysis to actively transport a wide variety of substrates across extra- and intracellular membranes. Their substrates include phospholipids, ions, peptides, steroids, polysaccharides, amino acids, organic anions, bile acids, drugs, and other xenobiotics (Linton et al., 2007; Higgins et al., 2001). These transport activities are critical for most aspects of cell physiology and broadly impact human health and disease. Genetic variation in these genes is the cause or contributor to a wide variety of human disorders, including cystic fibrosis, neurological disease, retinal degeneration, cholesterol and bile transport defects, anemia, and drug response phenotypes (Mendoza et al., 2007; Leonard et al., 2003; Kim et al., 2009; Lambrechts et al., 2015).

ABC transporter subfamilies and structure

Phylogenetic analysis places the 48 known human ABC transporters into seven distinct subfamilies (ABCA through ABCG) (Table 1.1). All ABC transporters share a common architecture comprising two hydrophilic nucleotide-binding domains (NBDs) and two hydrophobic transmembrane domains (TMDs) / membrane spanning domains (MSDs) (Linton et al., 2007).

NBDs are located in the cytoplasm and each NBD contains three conserved domains: Walker A and Walker B motifs, found in all ATP-binding proteins, and a signature (C) motif, located just upstream of the Walker B site. The C motif is specific to ABC transporters and distinguishes them from other ATP-binding proteins. NBDs are the sites which bind and hydrolyze ATP and also are involved in coupling the energy released by binding and hydrolysis of ATP to processes of cross membrane transport. TMDs are usually composed of at least six transmembrane (TM) α-helices. They form the pathway through which solute crosses the membrane and also determine the specificity of the transporter through substrate-binding sites (Higgins et al., 2001; Linton et al., 2007).

Based on the position and orientation of membrane spanning segments and other domains (predicted by computer modeling and laborious biochemical experiments), there are three most plausible membrane topology models for the key ABC transporters. As shown in Figure 1.2, ABCB1 (MDR1/Pgp) is a "full transporter" with six TM helices in both TMDs, each followed by an NBD. A similar membrane topology has been predicted for ABCB4 (MDR3), ABCC4 (MRP4), ABCC5 (MRP5), and ABCB11 (BSEP) as well. In addition to an MDR1-

like core, MRP1 contains an additional N-terminal segment of about 280 amino acids. A major part of this region is membrane-embedded with five transmembrane helices (TMD0), while a small cytoplasmic loop of about 80 amino acids (CL) connects this area to the core region. Transporters with similar structure include ABCC2 (MRP2), ABCC3 (MRP3), and ABCC6 (MRP6). The last category includes half-size transporters which have only one TMD fused to one NBD, for example, ABCG2 (BCRP) subfamily. These transporters dimerize to form a biologically active ABC-transporter.

Mechanisms of the transport process

ABC transporters are mostly unidirectional. In bacteria, ABC transporters are predominantly involved in the import of essential compounds (sugars, vitamins, metal ions, etc.) into the cell, while in eukaryotes, most ABC transporters move compounds from the cytoplasm to the outside of the cell or into an intracellular compartment, such as endoplasmic reticulum, mitochondria, peroxisome (Saurin et al., 1999). Despite the diversity of localization and substrate specificity, ABC transporters share a common basic mechanism of transport: two NBDs bind and hydrolyze ATP, and energize unidirectional substrate transport, which occurs through a translocation pathway provided by two MSDs.

For ABC transporters that efflux the substrate from mammalian cells, an ATP-switch model (Higgins et al., 2004; Dong et al., 2005) is popularly used to explain this transport process in four steps (Figure 1.3). (a) The transport cycle is initiated by the interaction of substrate with the TMDs from the intracellular face

of the membrane. (b) The substrate binding induces a conformational change in the TMDs, and this conformational change is transmitted to the NBDs to initiate binding of two molecules of ATP. Basically, two NBDs interact with each other to form two composite nucleotide binding sites. At each nucleotide binding site, one ATP molecule is sandwiched between the Walker A and Walker B motifs from one NBD and the LSGGQ ABC signature motif (C-motif) from the other NBD. (c) ATP binding induces further conformational changes in the NBDs, which are transduced to the TMDs: a high-affinity substrate binding site at the inside of the membrane is reoriented to be exposed to the outside of the membrane. Simultaneously its affinity to substrate is reduced, resulting in extracellular release of the substrate. (d) Finally, ATP hydrolysis causes the transporter to be reset and the binding site reoriented back to face the inside of the membrane and affinity restored. It is clear that both NBDs are required, and both must hydrolyze ATP, and they do so by an 'alternating catalytic cycle' mechanism in which only one NBD hydrolyses one ATP at a time.

ABC transporters in cancer and normal tissues

Overexpression of certain ABC transporters has been associated with chemotherapy resistance in many cancer types, like leukemia, breast cancer, lung cancer and ovarian cancer. The mechanisms involved are revealed by biochemistry studies that demonstrate that some ABC transporters efflux cytotoxic drugs out of the cell, thus keeping intracellular drug concentrations below the cell-killing threshold. These ABC transporters are called multidrug

resistant (MDR) proteins. They include, but are not limited to, transporters such as P-glycoprotein (Pgp), MPR1, MRP2, and BCRP.

Although initially being found in drug resistance tumor cells, some ABC transporters are ubiquitously expressed in many normal tissues, including blood-brain barrier, liver, kidney, placenta, etc. Recently, there is a growing body of evidence showing the importance of ABC transporters in multiple normal organs' defense, such as regulating central nervous system permeability, protecting testicular tissue and the developing fetus. They are also involved in the toxin excretion from the liver, gastrointestinal tract and kidney, to protect the entire organism. These protective roles are conducted mainly through the excretion of toxic compounds and their metabolites (Leslie et al., 2005; Fromm, 2004; Sarkadi et al., 2004).

Multidrug resistance-associated protein 1 (MRP1/ABCC1)

Multidrug resistance-associated protein 1 (MRP1/ABCC1) is a member of the ABCC subfamily. The murine (Mrp1) and human (MRP1) orthologues of MRP1 are 88% identical. MRP1 was first discovered in a drug-selected human small cell lung carcinoma cell line, H69AR, which had developed drug resistance to DOX without the increase in expression of Pgp (Cole et al., 1992). MRP1 is a 190 kDa heavily glycosylated ABC transporter that contains three TMDs and two NBDs. The additional transmembrane domain TMD0, and the intra-cellular loop between TMD0 and TMD1, are important for trafficking and insertion of MRP1 in the plasma membrane (Westlake et al., 2005). With extensive investigation in

past two decades, MRP1 has been demonstrated to play an important role in the development of drug resistance of various types of cancer (Hsia et al., 2002; Triller et al., 2006; Nooter et al., 1997a; Nooter et al., 1997b; Sullivan et al., 1998). It does not appear to play a significant role in the absorption or eliminations of drugs, but does seem to be an important modulator of drug tissue exposure and metabolite cellular elimination.

MRP1 tissue distribution and intracellular localization

Beyond the tumor tissues, constitutive MRP1 is ubiquitously expressed in most normal tissues, especially in heart, skin, lung, brain capillary endothelial cells, and small intestine (Flens et al., 1996; Nies et al., 2004). In polarized epithelial cells, MRP1 is usually found in the basolateral membrane. While being primarily located in the plasma membrane, MRP1 is also found in the membrane of intracellular organelles such as endocytic vesicles, lysosomes located near the nucleus, trans-Golgi vesicles, and the mitochondria (Rajagopal et al., 2003; Gennuso et al., 2004; Jungsuwadee et al., 2009).

Substrates of MRP1

MRP1 effluxes a wide range of endobiotics and xenobiotics (Figure 1.4). These substrates are usually amphiphilic anionic compounds, including glutathione (GSH) and glutathione disulfide (GSSG) as well as GSH, glucuronide and sulfate conjugated organic anions, such as leukotriene C4 (LTC4) and GS-HNE (Leier et al., 1994; Cole and Deeley. 1998; Renes et al., 2000; Leslie et al.,

2001; Jungsuwadee et al., 2012). MRP1 also transports nonconjugated hydrophobic compounds in the presence of GSH, such as the natural product type chemotherapeutic agents Vinca Alkaloids and mutagens, such as aflatoxin B1 (Cole and Deeley., 2006).

MRP1 protects normal tissues against toxic effects of xenobiotics

In normal polarized epithelial cells, MRP1 is usually found on the basolateral membrane, and thus may serve to efflux substrates into the bloodstream or interstitial space. Generation and characterization of Mrp1-/- mice demonstrated that this protein is not essential for normal viability and fertility of mice (Wijnholds et al., 1997; Lorico et al., 1997). However, these Mrp1-/- mice show impaired ability to transport some endobiotics and xenobiotics. For example, Mrp1-/- mice are hypersensitive to the anticancer drug etoposide, and exhibit reduced inflammatory responses attributed to disrupted leukotriene homeostasis caused by the inability of these mice to efflux LTC4 (Wijnholds J et al., 1997). Detailed analysis of the etoposide toxicity indicates that Mrp1 contributes to the protection of the oropharyngeal mucosal layer and the seminiferous tubules of the testis, and it appears very likely that normally Mrp1 restricts access of etoposide to these tissues (Wijnholds et al., 1998). Mrp1-/- mice also show impairment in the efflux of [^{14}C] grepafloxacin and Fluo 3 in the skin (Li et al., 2005). In addition, a role for Mrp1 was demonstrated in cerebral amyloid-β (Aβ) clearance and brain accumulation, being identified as a potential target for treatment or preventing Alzheimer's disease and cerebral amyloid angiopathy (Krohn et al., 2011). Mrp1-

/- mice are also hypersensitive to sodium arsenite, sodium arsenate, and antimony potassium tartrate (Rappa et al., 1997). These data demonstrate that Mrp1 protects the normal tissues by effluxing endobiotics and xenobiotics and thus prevents the toxicants' accumulation in cell or tissue. However, it is largely unknown how Mrp1 functions in heart, especially when the heart is under stress, such as that induced by DOX treatment.

Clinical association between genetic variants of MRP1 and anthracycline induced cardiotoxicity

Genetic variations at the level of single nucleotide polymorphisms (SNPs) are well demonstrated to be associated with the differences of disease susceptibility and therapy response among the population. More recently, inter-individual difference in genes encoding the drug transporters have received considerable attention because of their ability to contribute to differences in drug absorption, distribution, and elimination that ultimately affect both drug efficacy and toxicity (Cole, 2014a). Accumulating case-control clinical studies have shown that several MRP1 SNPs are associated with the susceptibility to cardiotoxicity observed in cancer patients treated with anthracycline (Table 1.2) (Wojnowski et al., 2005; Semsei et al., 2012; Visscher et al., 2012). Although the biological function of these SNPs are not fully understood, we expect these SNPs could potentially change the expression and function of MRP1 and further impair the efflux of substrates, and finally contribute to the susceptibility to DOX-induced cardiotoxicity. Prior studies by our laboratory focused on one of these SNPs

(Gly671Val). Our laboratory demonstrated that HEK cells that overexpress MRP1 (Gly671Val) are more sensitive to DOX toxicity compared to cells that overexpress WT MRP1. Although human MRP1 can efflux DOX, this mutant MRP1 does not significantly increase the intracellular concentration of DOX in HEK cells, but impaired by more than 85% MRP1's activity in effluxing GS-HNE, which is an important toxic metabolite of lipid peroxidation (Jungsuwadee et al., 2012). This implies that MRP1 could play an important role in heart defense against DOX toxicity by effluxing toxic substrates other than DOX. Here, we will focus on MRP1's substrates that are related to oxidative stress.

Oxidative stress

Oxidative stress refers to a harmful condition that occurs when there is an excess of ROS, a failure of antioxidant defense systems, or both (Sies, 1997; Dasuri et al., 2012). ROS include free radicals, such as $\bullet O_2^-$ and •OH, and nonradicals capable of generating free radicals, such as H_2O_2. These ROS can be derived from several intracellular sources, including mitochondria, NAD(P)H oxidase, xanthine oxidase, and uncoupled nitric oxide synthase, as well as from exogenous factors such as DOX exposure. To protect cells from the damage caused by ROS, organisms have evolved a variety of antioxidant systems to rapidly and efficiently remove ROS or inhibit their activities and maintain appropriate redox homeostasis (Figure 1.5). The main antioxidant enzymes include superoxide dismutase (SOD), catalase, glutathione peroxidase (GPx), peroxiredoxin (Prx) and glutathione S-transferase (GST). SOD converts two

$\bullet O_2^-$ into one molecule of H_2O_2 and one molecule of O_2, while catalase further catalyzes the decomposition of H_2O_2 into H_2O and O_2. The main reactions that GPx and Prx catalyze are to reduce H_2O_2 to H_2O by consumption of reduced GSH or reduced thioredoxin (Trx). In addition to these antioxidant enzymes, there are also small antioxidant molecules such as GSH, peroxiredoxin (Prx), thioredoxin (Trx), vitamin C, and vitamin E. Oxidative stress has been implicated in numerous diseases at multiple organs, while heart is particularly vulnerable to oxidative stress induced damage due to relatively low expression/activity of antioxidant enzymes, and the low regeneration ability of the highly differentiated cardiomyocytes. Here, this dissertation mainly focuses on GSH/GSSG homeostasis and the lipid peroxidation product 4-Hydroyx-2-nonenal (HNE), because GSH, GSSG and GS-HNE are all substrates of MRP1.

GSH and GSSG homeostasis in cells

GSH is a tripeptide - γ-glutamyl-cysteinyl-glycine with a gamma peptide linkage between the carboxyl group of the glutamate side chain and the amine group of cysteine, which is attached by normal peptide linkage to a glycine. Reduced GSH is the most abundant intracellular non-protein thiol in almost all aerobic species. Due to its cysteinyl moiety, GSH is a nucleophile that provides electrons to electrophilic species to form GSSG. GSSG can be catalytically reduced back to GSH by the NAD(P)H dependent GSH reductase (GR) (Figure 1.6). The continued function of the redox cycle activity is dependent on the availability of NADPH, of which the pentose phosphate pathway is a major

source (Lushchak, 2012). Under physiological conditions, reduced GSH is the major form, with its concentration from 10 – 100 fold higher than the oxidized form, present as mixed disulfide (mainly GS-S-protein) and the disulfide (GSSG). However, this ratio will decrease in the presence of ROS, due to the rapid oxidation from GSH to GSSG. Therefore, the GSH/GSSG ratio is an important indicator of the redox environment. Maintenance of GSH homeostasis plays a vital role in a multitude of cellular processes, including drug and free radical detoxification, cell differentiation, proliferation and apoptosis (Jones, 2008).

In addition to its role in elimination of ROS, GSH is also a signaling molecule. It is added to proteins as a post-translational modification (Pompella et al., 2003) to form S-glutathionylated proteins. It interacts with nitric oxide (NO) to modify its bioavailability (Hogg et al., 2002). It also modifies the activity of neurotransmitter receptors and may itself be active as a neurotransmitter (Oja et al., 2000). In conclusion, GSH is a multifunctional molecule with diverse and still emerging functions.

GSH synthesis and metabolism

GSH is synthesized in all mammalian cells, and the liver is a major site. The synthesis from the precursor amino acids cysteine, glutamate and glycine is accomplished by a consecutive action of two ATP-dependent enzymes (Figure 1.7). First, gamma-glutamate-cysteine ligase (GCL), a heterodimer of a catalytic subunit (GCLc) and a modulatory subunit (GCLm), forms an unusual peptide bond between the γ-carboxyl of glutamate and the amino group of cysteine using

the energy provided by the hydrolysis of ATP (Lu, 2013). This is the rate-limiting step of GSH synthesis in vivo. The second step is addition of glycine to γ-glutamylcysteine. This reaction is catalyzed by glutathione synthase (GSS) and driven by the hydrolysis of another ATP. After its synthesis, GSH is delivered to some intracellular compartments, including mitochondria, endoplasmic reticulum, nucleus, and to the extracellular space (e.g., blood plasma and bile) for utilization by other cells and tissues (Forman et al., 2004).

The overall rate of GSH synthesis is controlled by several factors, including: (i) availability of the substrate, mainly L-cysteine. This is determined by membrane transport activities of the three sulfur amino acids cysteine, cystine and methionine, and the conversion of methionine to cysteine via the trans-sulfuration pathway (Grimble et al., 1992); (ii) the activity of the rate-limiting enzyme - GCL. This is determined by the expression level and relative ratio between its two subunits GCLc and GCLm (Chen et al., 2005). In most tissues, GCLc is found in excess compared to GCLm, while the binding of GCLc to GCLm dramatically decreases the sensitivity of the holoenzyme to GSH inhibition, presumably by changing the conformation of the enzyme; (iii) extent of feedback inhibition of GCL, especially GCLc by GSH (Taylor et al., 1996). Additionally, in some cases, the provision of ATP for GSH synthesis could represent another limiting factor. It is worth noting that both GCL and GS are sensitive to oxidative stress, and their expression is mainly under the regulation of the Nuclear factor (erythroid-derived 2)-like 2 (Nrf2), a transcription factor that regulates a wide array of antioxidant responsive element-driven genes in various cell types (Lu, 2009).

Although GSH is synthesized intracellularly in all the cell types, its biodegradation occurs outside of cells (Figure 1.8). Since GSH is not susceptible to proteolysis due to its unusual γ–carboxyl peptide linkage, GSH is resistant to intracellular degradation and its degradation only occurs in cell types that have gamma-glutamyl transpeptidase (γGT), an ectoenzyme on the cell membrane. γGT removes the γ–glutamyl moiety from GSH under physiological conditions, and then dipeptidase removes the glycyl moiety (Ballatori et al., 2009). The breakdown products (glutamate, glycine, and cysteine) can be taken up into the cell for GSH synthesis. In yeast, an alternative pathway of GSH degradation is mediated by a novel cytosolic protein complex involving three new genes Dug1, Dug2 and Dug3 (Ganguli et al., 2007; Baudouin-Cornu et al., 2012).

MRP1 and GSH/GSSG homeostasis

The relationship between GSH and MRP1 is complex. On one hand, GSH influences MRP1's ATP-dependent transport activity by either its direct conjugation to the substrates or binding MRP1 and stimulating its transport activity. On the other hand, MRP1 is able to efflux GSH directly (Cole, 2014b). GSH itself is a low affinity substrate of MRP1 (Km = 1-5 mM), but it is a suitable substrate for MRP1 under physiological conditions, considering that the physiological concentration of GSH is in the mM range in most cells. Co-transport of GSH with another substrate is another mechanism of GSH transport through MRP1. For example, depleting GSH with BSO inhibits transport of daunorubicin, vincristine, and aflatoxin B1 (Versantvoort et al., 1995; Rappa et al.,

1997; Salerno and Garnier-Suillerot, 2001). In addition, the ability of MRP1 to transport GSH can be markedly enhanced in vitro by a variety of xenobiotics (e.g., verapamil, vincristine, the antivirals indinavir and nelfinavir), including bioflavonoids (e.g., apigenin) (Loe et al., 2000; Cole., 2014b).

Whereas the role of GSH in preventing oxidative stress is well understood, the precise dynamics of MRP1 in regulating cellular GSH levels require clarification. It has been observed that the GSH content in cells overexpressing MRP1 is much lower than that of control cells, while Mrp1-/- mice have increased basal levels of GSH in multiple tissues (Rappa et al., 1997; Wijnholds et al., 1997). Minich et al (2006) also reported that astrocytes isolated from Mrp1-/- mice have 50% more intracellular GSH. Further, inhibiting MRP1 or selectively knocking down MRP1 causes a decrease in GSH release in both unstressed and stressed conditions (Minich et al., 2006; Sreekumar et al., 2012). This means that the basal intracellular level of GSH is affected by its efflux through MRP1. This is further demonstrated by the observation that the basal level of GSH export in Mrp1-/- mice stem cells is approximately one half of that observed in wild type cells (Cole et al., 1990; Rappa et al., 1997). The MRP1-mediated GSH transport in different cell types in specific tissue/organ has also received considerable attention. For example, in the brain, astrocytes maintain the redox balance of the cellular milieu by the MRP1-mediated extrusion of GSH (Minich et al., 2006).

In addition to GSH, GSSG has also been shown to be effluxed across the plasma membrane through MRP transporters (Hirrlinger et al., 2001; 2005; Minich et al., 2006; Cole and Deeley, 2006). As discussed above, GSSG tends

to accumulate in cells under conditions of oxidative stress. Because of its deleterious pro-oxidant activities, maintenance of low levels of GSSG (and an appropriately low GSSG/GSH ratio) is important for normal cellular function. This maintenance is accomplished mostly by a combination of the reduction of GSSG back to GSH by GR and the efflux of GSSG by MRP1 (and MRP2). MRP1's affinity for GSSG (Km ~100 μM) is significantly higher than that for GSH (Km ~ 1-5 mM) (Cole SP et al, 2006). MRP1-mediated GSSG efflux occurs during oxidative stress in several cell types, including astrocytes and endothelial cells (Minich et al., 2006; Ellison and Richie et al., 2012). A recent study implicates MRP1 as a neuroprotective factor against stroke and attributes this ability to MRP1-mediated efflux of GSSG, a known trigger of neuronal cell death (Park et al., 2011). These data indicate the role of MRP1 in the cellular response to oxidative stress. Thus, loss of MRP1 influences the intracellular level of GSH and GSSG, may disrupt the balance of the GSH/GSSG redox couple, and finally impair normal tissues' ability to defend against oxidative stress-induced injury.

Lipid peroxidation

The free radical-mediated peroxidation of lipids has received a great deal of attention in connection with oxidative stress in vivo. Free radicals, for example hydroxyl radical (OH·) generated from H_2O_2 via the Fenton– and Haber–Weiss reactions, mediate the removal of a hydrogen atom (H•) from a lipid (LH), which yields a lipid radical (L•). In the propagation phase, L• reacts with O_2 and forms a lipoperoxyl radical (LOO•), which in turn reacts with another polyunsaturated

fatty acids (PUFA) to yield a new L• and a lipid hydroperoxide (LOOH) (Figure 1.9A). Thus, one free radical can generate a high number of lipid hydroperoxides until the chain reaction is terminated by a chain-breaking antioxidant. Lipid peroxidation has been implicated in various diseases and aging, including inflammation, atherosclerosis, cataract formation, chronic degenerative diseases of the nervous system, and chronic liver disease (Sultana et al., 2013; Yadav et al., 2013; Parola et al., 1996).

HNE formation

Since lipid hydroperoxides (LOOH) produced by the chain reaction of lipid peroxidation are unstable, they decompose to various secondary products of lipid peroxidation, including malondialdehyde (MDA) and HNE (Figure 1.9B). The physiological concentration of HNE is in the submicromolar range (<0.1 μM), while in oxidative stress, even micromolar levels can be observed (Esterbauer et al., 1991; Butterfield and Stadtman, 1997). Thus, HNE can be regarded as a biomarker of oxidative stress.

HNE is very hydrophobic, so that it is mostly associated with the membranes where it is produced from the peroxidation of arachidonic and linoleic acids. Since HNE is relatively stable, it can diffuse remarkable distances from the site of formation to different cellular compartments. It has three main functional groups: an aldehyde, a double bond (alkene) between carbon C2 and C3, and a secondary alcohol at carbon C4 (Figure 1.10). HNE is a highly electrophilic molecule that easily reacts with glutathione, proteins and, at higher

concentrations, with DNA. HNE reacts with cysteine, histidine, and lysine residues of proteins, likely resulting in functional impairment (Esterbauer et al. 1991) (Figure 1.11).

To protect macromolecules from modification or adduction by HNE, mammalian cells metabolize 4-HNE rapidly (Figure 1.12). One important pathway of detoxification is through conjugation with GSH, either spontaneously or through GSH-S-transferases (GST) to form GS-HNE, which must be effluxed to alleviate intracellular toxicity (Volkel et al., 2005). In addition, HNE metabolism includes reduction to the corresponding alcohol, 1,4-dihydroxy-2-nonene (DHN) or oxidation to the corresponding acid, 4-hydroxy-2-nonenoic acid (HNA) (Alary et al., 2003; Volkel et al, 2005). GS-HNE can also be metabolized via an NADH-dependent alcohol dehydrogenase (ADH)-catalyzed reduction to GS-DHN and/or aldehyde dehydrogenase-catalyzed oxidation to GS-HNA. The biological activities of these GSH conjugates are not yet well characterized.

MRP1 and HNE detoxification

As discussed above, the GSH/GST system is a well-known mechanism in the cellular defense against oxidative stress. The excretion of GSH conjugates is important in decreasing intracellular concentrations of toxins because conjugation reactions can be reversible. In addition, some metabolites become more toxic on conjugation with GSH.

The conjugation of HNE with GSH forms a less toxic metabolite, GS-HNE, but its accumulation inside the cell can still generate toxicity due to end-product

inhibition of relevant GST, with subsequent accumulation of HNE and ensuing toxicity (Diah et al., 1999; Renes et al., 2000). Thus, the extrusion of GS-HNE is required for preventing these adverse toxicities. Evidence for a significant role of MRP1 as a transmembrane efflux transporter for GS-HNE conjugates has been reported, and the Km is in the μM range. In a human small cell lung cancer cell line, the expression of MRP1 was associated with protection against HNE toxicity (Renes et al., 2000). Our laboratory reported that mutant MRP1 (Gly671Val) impaired MRP1's ability to efflux GS-HNE by more than 80%, and caused a higher sensitivity to DOX toxicity in HEK cells (Jungsuwadee et al., 2012). That study also found that HNE-adducted protein is increased in mouse heart after DOX treatment and that sarcolemmal membrane vesicles from Mrp1-/- mice are unable to transport GS-HNE, indicating that Mrp1 is the only ATP-dependent efflux transporter in the mouse heart (Jungsuwadee et al., 2006). Thus, understanding of MRP1's effects on GS-HNE efflux and intracellular GS-HNE accumulation are needed to clarify the potential role of MRP1 in normal heart tissue defense against oxidative stress.

Research Objectives

This study explored the potential protective function of Mrp1 in DOX-induced cardiotoxicity. Mrp1-/- mice and their WT littermates were used as a study model. Although Mrp1 is highly conserved between human and rodents with 88% sequence homology, the human isoform (MRP1) is able to transport DOX, whereas murine Mrp1 has only a negligible ability to transport this anthracycline

(Stride et al., 1997). Therefore, the Mrp1-/- mouse provides a good model to study the role of Mrp1 in DOX cardiotoxicity separately from the effects of DOX retention. Of course, the diiference of human MRP1 and murine Mrp1 regarding the efflux of DOX could limite the translation from experimental finding in mouse model to clinical research.

In this study, after giving the mice chronic DOX treatment, the left ventricle function, heart apoptosis and heart fibrosis were evaluated. Effects of Mrp1 on DOX cytotoxicity were also investigated in two major cell components of heart: neonatal mouse cardiomyocytes and neonatal cardiac fibroblasts, including the effects on cell survival, cell apoptosis, and DNA damage. The mechanisms of Mrp1-mediated protection were further investigated based on known functions of Mrp1, mainly focusing on glutathione homeostasis, GS-HNE accumulation, and protein oxidative damage.

The results of the current study demonstrate that Mrp1 protects mouse heart against DOX-induced cardiotoxicity. Clinical studies show an association between multiple genetic variants of *MRP1* gene and cancer patients' susceptibility to DOX induced cardiotoxicity. Thus, our study may provide explanations for these clinical observations if any SNPs impair MRP1's expression or activity. It will further help to identify these susceptible patients and modify chemotherapy strategies for them, and thus prevent such drug-induced toxicity.

This dissertation research was conducted to test the following hypotheses:

1. Loss of Mrp1 will potentiate chronic DOX-induced cardiac dysfunction in mice;

2. Loss of Mrp1 will sensitize cardiomyocytes and/or cardiac fibroblasts to DOX cytotoxicity;
3. GSH/GSSG homeostasis will be disrupted in Mrp1-/- mouse heart.
4. Loss of Mrp1 will cause GS-HNE accumulation in mouse heart tissue after DOX administration.

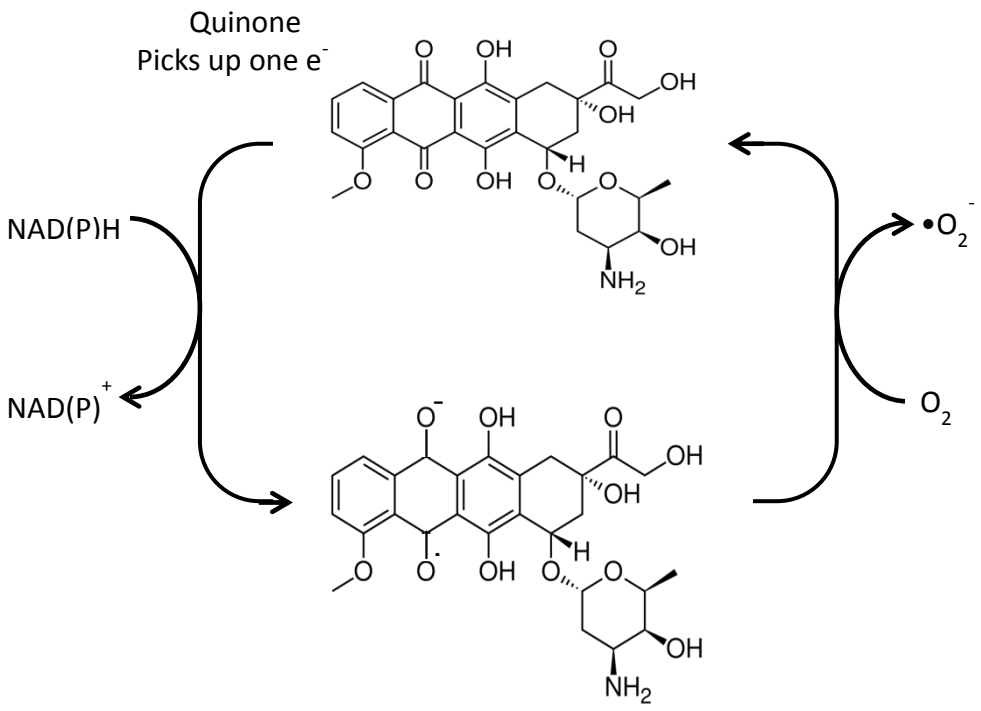

Figure 1.1. Schematic illustration of redox cycling of DOX. The quinone moiety of DOX accepts one electron from NAD(P)H to form a semiquinone that quickly regenerates its parent quinone by reducing oxygen to form superoxide ($\bullet O_2^-$); NAD(P), nicotinamide adenine dinucleotide (phosphate); $\bullet O_2^-$, superoxide (Stěrba et al., 2013)

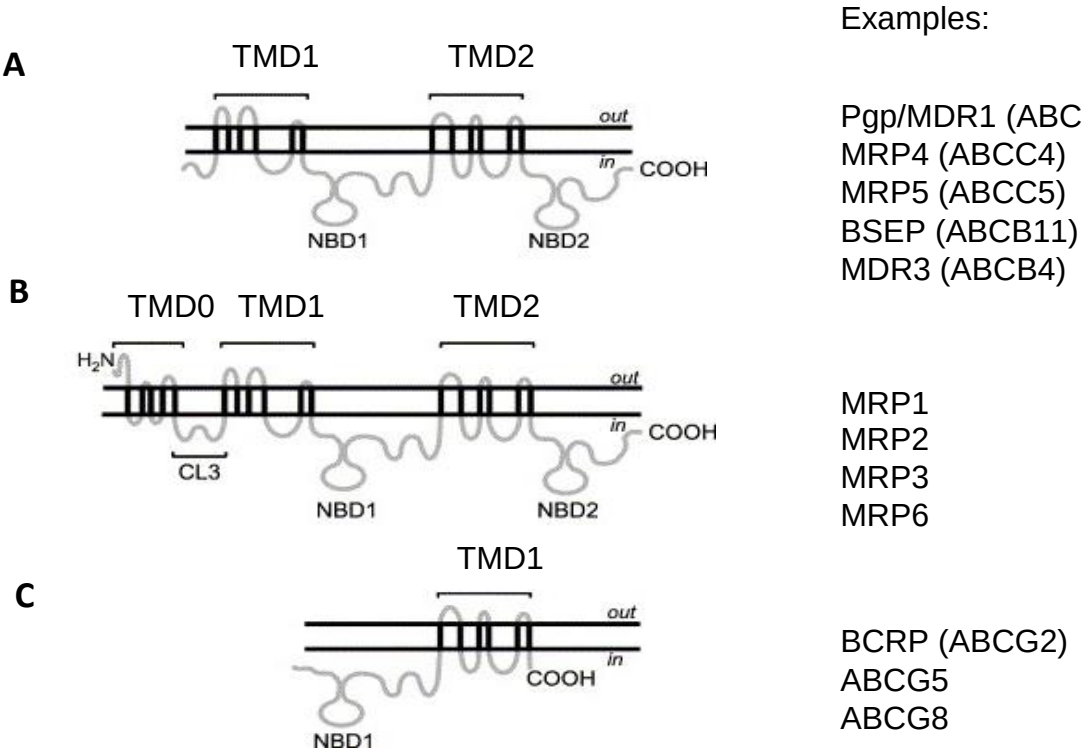

Figure 1.2. Structures of three categories of ABC transporters. Schematic representation of the predicted domain arrangement of (A) full length transporter; (B) extended full length transporters with an extra transmembrane domain at the N-terminus (TMD0), and (C) half transporters that require dimerization for full function. ABC, ATP-binding cassette; CL, cytoplasmic loops.

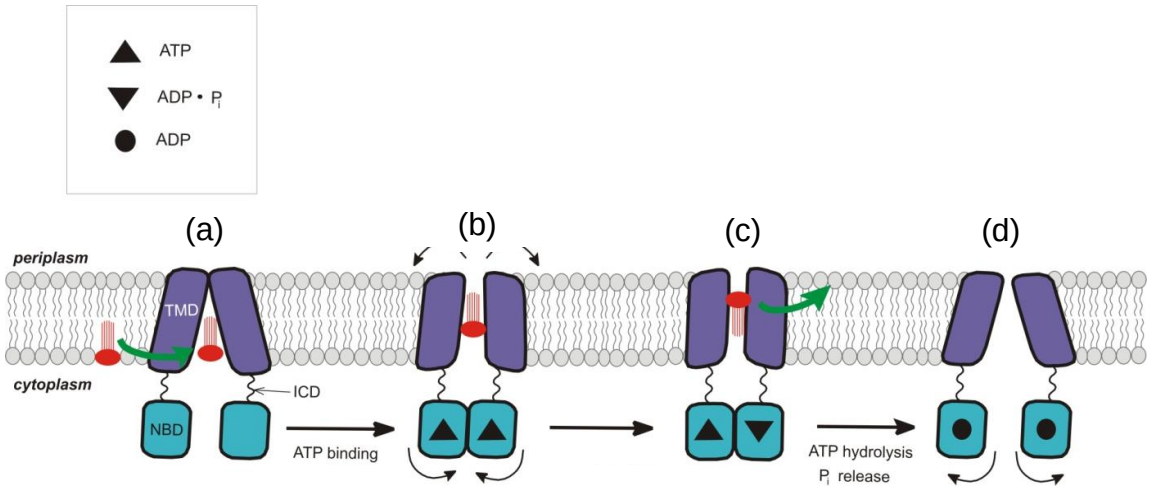

Figure 1.3. Proposed transport mechanism of ABC transporters. (a) Substrates interact with the TMDs from the intracellular face of the membrane. (b) TMDs undergo a conformational change and 2 molecules of ATP bind to the NBDs. (c) ATP binding induces further conformational changes of TMDs, resulting in substrate translocation. (d) ATP hydrolysis and transporter is reset for substrate binding. TMD, transmembrane domain; NBD, nucleotide-binding domains. (Dong et al., 2005)

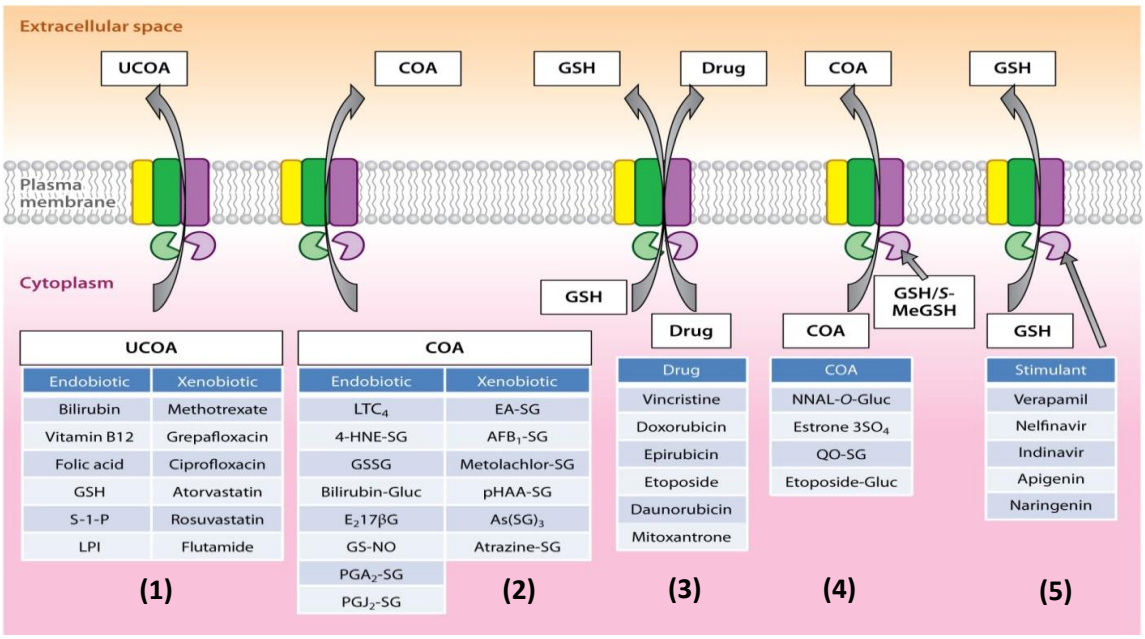

Figure 1.4. Substrates of MRP1. Shown are representative examples of the endo- and xenobiotics (and organic anion metabolites) effluxed from cells by MRP1 in either a glutathione (GSH)-independent or GSH-dependent manner. MRP1 can transport glutathione, glucuronide or sulfate conjugated organic anions (COA) (2) and unconjugated organic anions (UCOA) (1). (3) MRP1 also co-transports GSH and substrates. (4) Some MRP1-mediated COA transport is dependent upon the presence of GSH or its nonreducing derivative, S-methylGSH. (5) In addition, GSH transport is stimulated by the presence of drugs that are not themselves transported by MRP1. 4-HNE-SG, GSH conjugate of 4-Hydroyx-2-nonenal (GS-HNE); AFB1-SG, GSH conjugate of aflatoxin B1-epoxide; COA, conjugated organic anion; E217βG, 17β-estradiol 17-(β-D-glucuronide); EA-SG, GSH conjugate of ethacrynic acid; GS-NO, S-nitrosoglutathione; GSSG, glutathione disulfide; LPI, lysophosphatidylinositol;

LTC4, leukotriene C4; NNAL-OGluc, β-O-glucuronide conjugate of 4-(methylnitrosamino)-1-(3-pyridyl)-1-butanol; PGA2-SG, GSH conjugate of prostaglandin A2; PGJ2-SG, GSH conjugate of 15-deoxy-12,14-prostaglandin J2; pHAA-SG, GSH conjugate of acetaminophen; QO-SG, GSH conjugate of 4-nitroquinoline 1-oxide; S-1-P, sphingosine 1-phosphate; S-MeGSH, S-methyl GSH; UCOA, unconjugated organic anion. (Cole, 2014b)

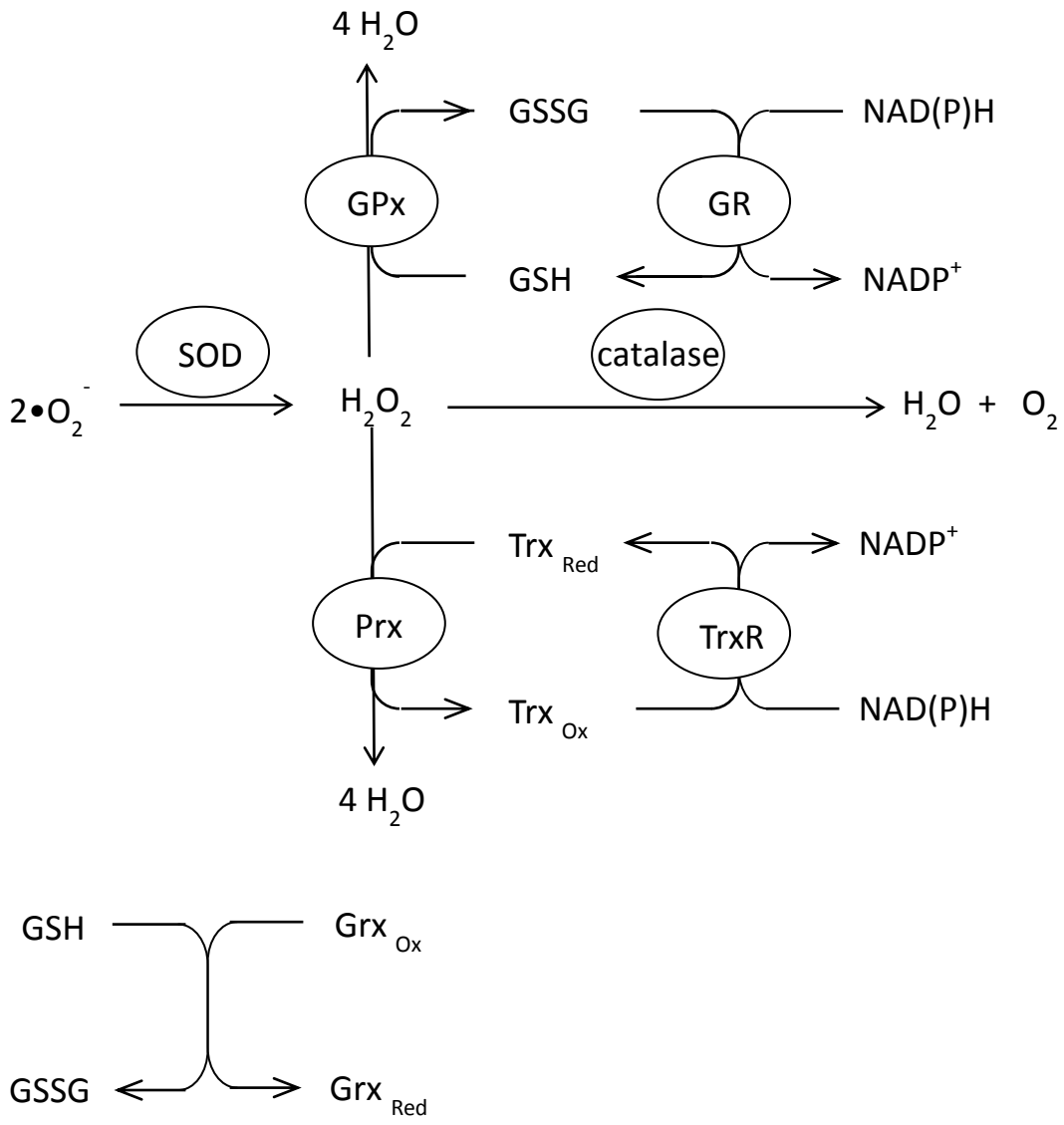

Figure 1.5. Redox signaling. When $\bullet O_2^-$ is formed, SOD converts two $\bullet O_2^-$ into one molecule of H_2O_2 and one molecule of O_2. Catalase catalyzes the decomposition of H_2O_2 into H_2O and O_2. GPx and Prx reduce H_2O_2 to H_2O by consumption of reduced GSH or reduced thioredoxin (Trx). Grx are oxidized by substrates, and reduced non-enzymatically by GSH. Gpx, glutathione peroxidase; GR, glutathione reductase; Grx, glutaredoxin; Prx, peroxiredoxin; SOD, superoxide dismutase; Trx, thioredixin; TrxR, thioredoxin reductase.

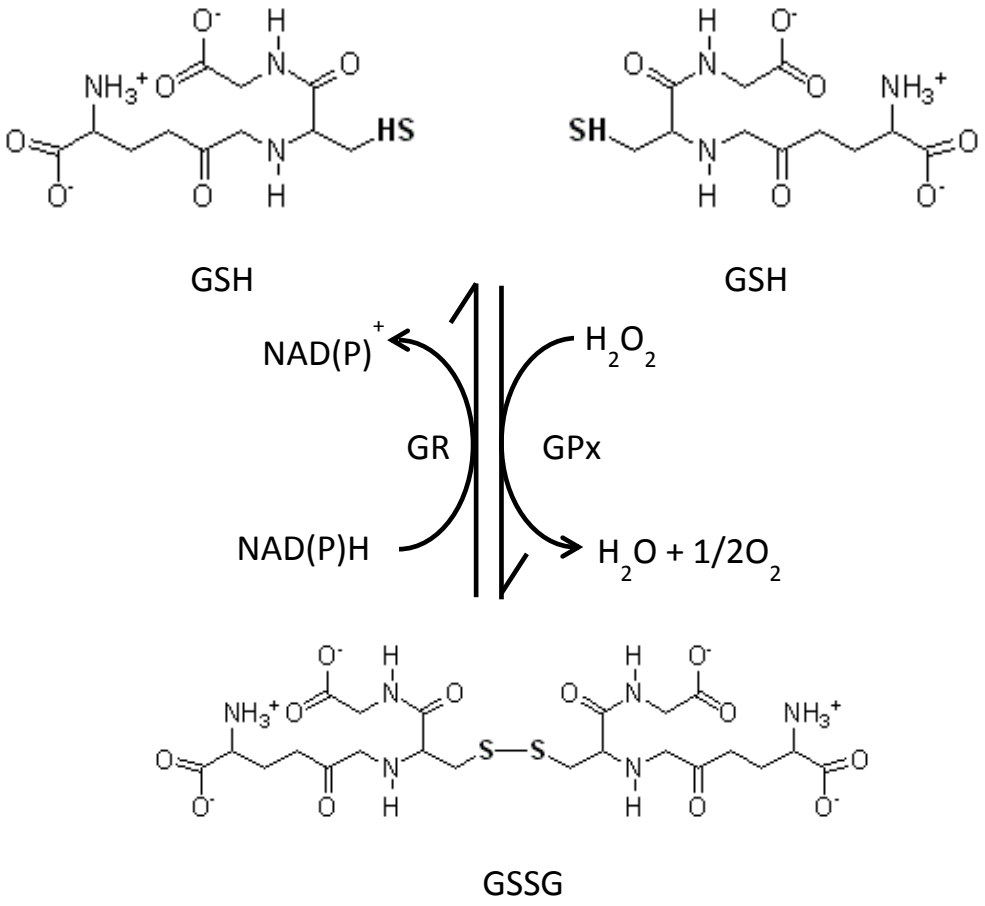

Figure 1.6. Redox cycling maintains cellular GSH/GSSG homeostasis during oxidative challenge. Under oxidative stress, GSH detoxifies ROS to form GSSG. The regeneration of GSH from GSSG is maintained by the GSSG reductase system in a NAD(P)H dependent manner. GR: glutathione reductase; GPx: glutathione peroxidase.

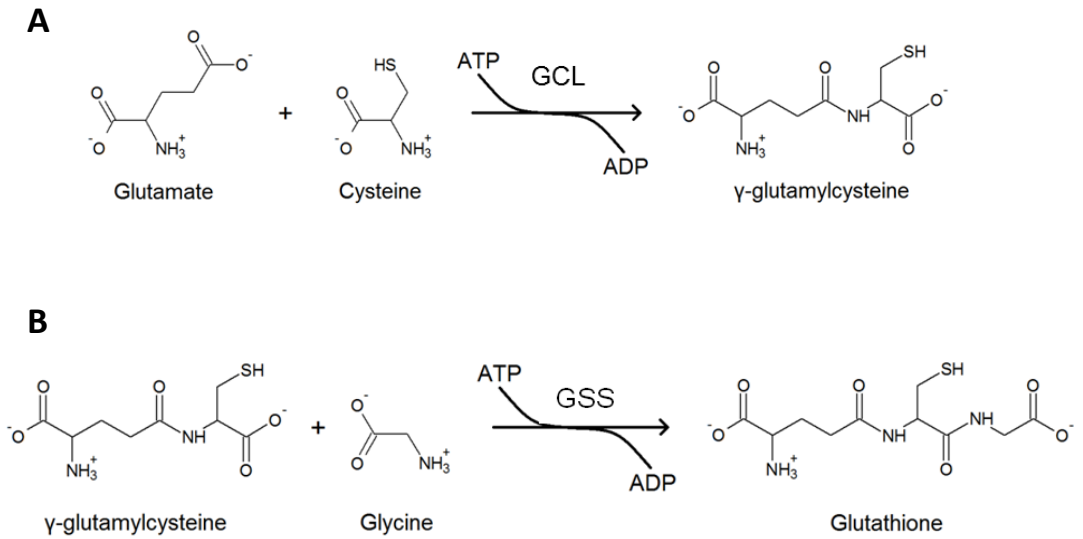

Figure 1.7. Process of GSH synthesis. (A) In the first step of GSH synthesis, an amide linkage is formed between cysteine and glutamate catalyzed by the GCL. (B) Then, GSS catalyzes the reaction between glycine and the cysteine carboxyl of γ-glutamylcysteine dipeptide to form GSH. GCL, γ-glutamate-cysteine ligase; GSS, glutathione synthetase.

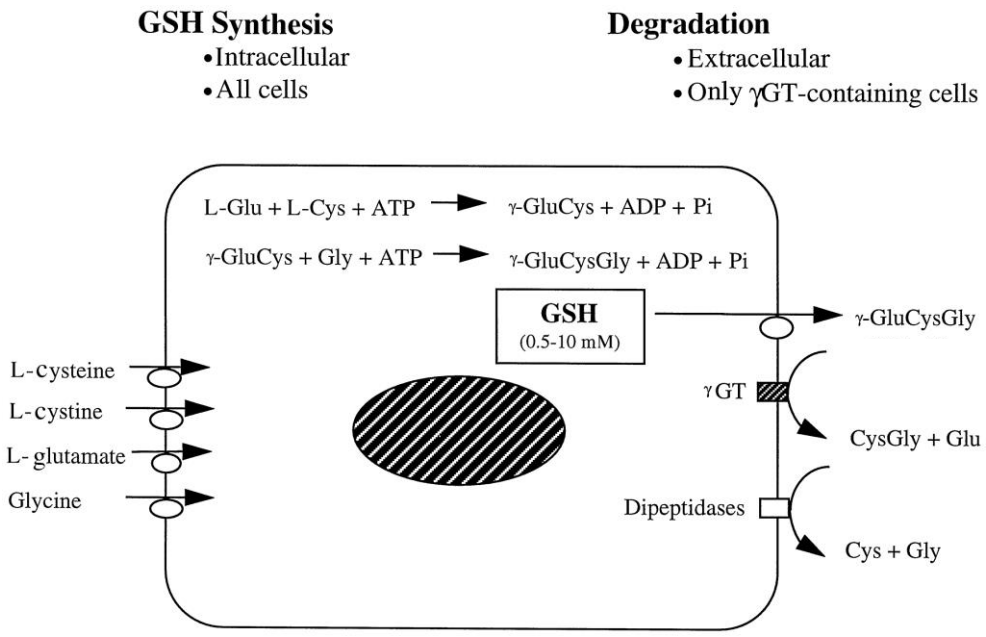

Figure 1.8. GSH degradation. GSH is transported out of the cell and broken down by the membrane-bound ectoenzyme γGT, which removes the γ-glutamyl moiety, and then by dipeptidases, which remove the glycine moiety. The resulting amino acids can be taken up by the cell and used for additional GSH synthesis. ATP, adenosine triphosphate; ADP, adenosine diphosphate; Cys, cysteine; Glu, glutamate; Gly, glycine; Pi, inorganic phosphate; γGT, γ glutamyl transpeptidase. (Wang and Ballatori, 1998)

A

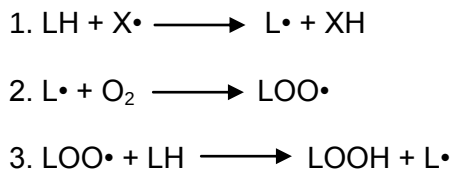

B

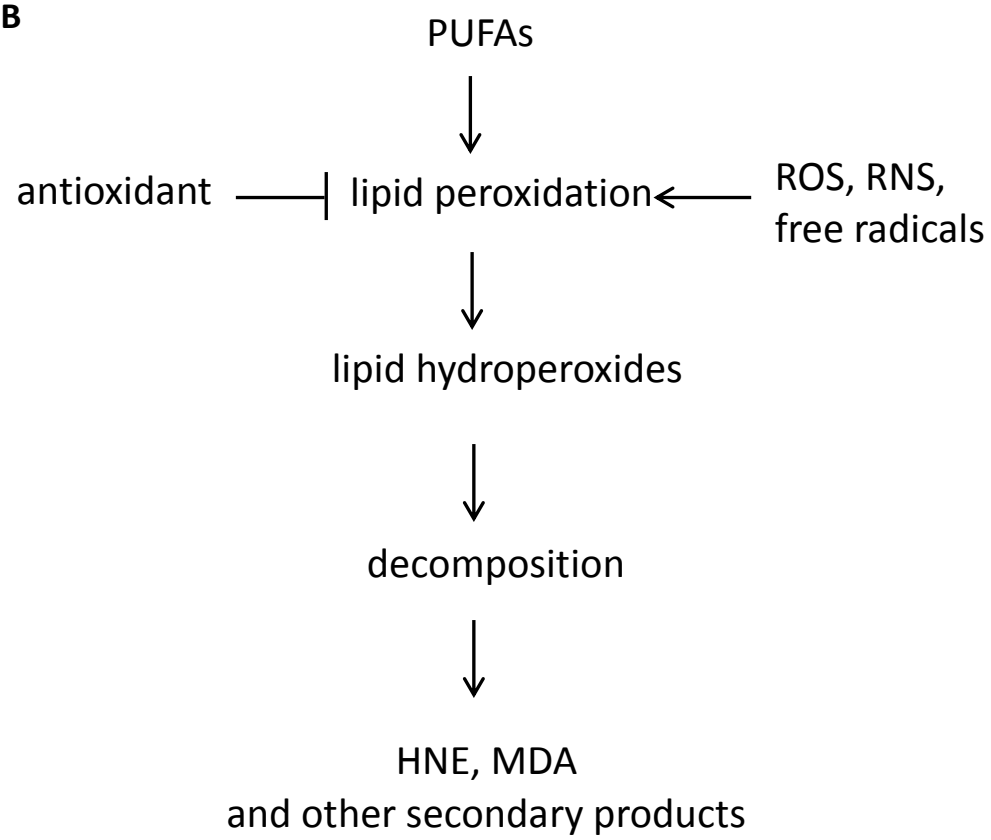

Figure 1.9. Oxidative stress causes lipid peroxidation and HNE formation. (A) Chain reaction of lipid peroxidation; (B) HNE is generated as a secondary product of lipid peroxidation. HNE, 4-Hydroyx-2-nonenal; MDA, malondialdehyde; PUFA, polyunsaturated fatty acids; RNS, reactive nitrogen species; ROS, reactive oxygen species.

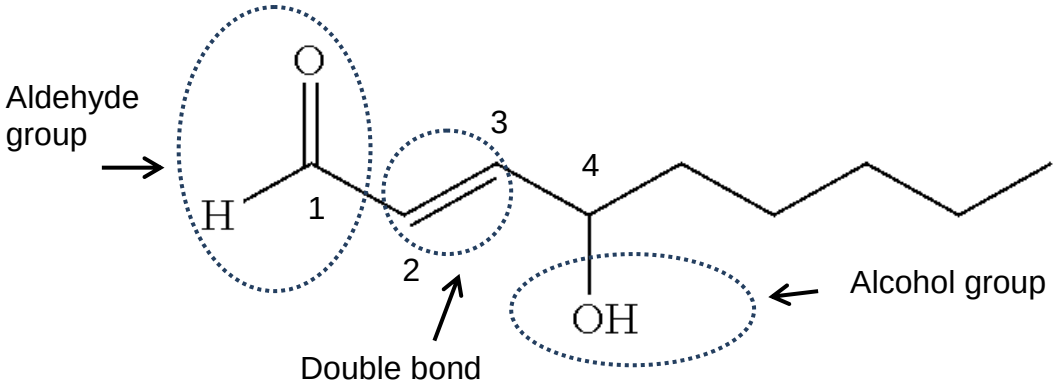

Figure 1.10. Three main functional groups of HNE: an aldehyde, a double bond (alkene) between carbon C2 and C3, and a secondary alcohol at carbon C4.

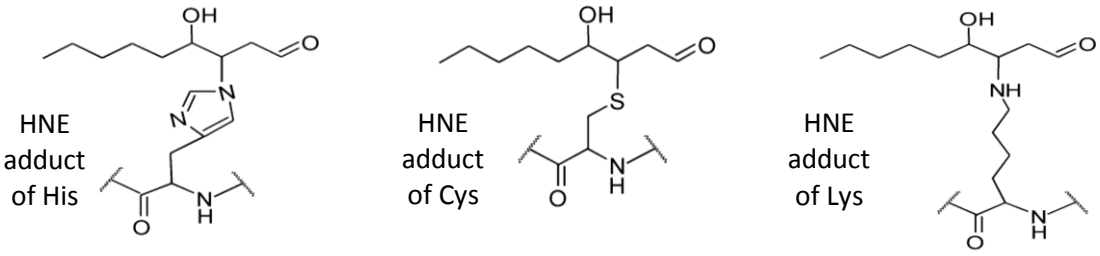

Figure 1.11. A linear depiction of HNE adducts with amino acids. HNE adduction can take place by the 1,4-addition (Michael addition) of the nucleophilic groups in cysteine (Cys), histidine (His) or lysine (Lys) residues of the protein, respectively, onto the electrophilic double bond of HNE, giving an increase in the protein's molecular mass by 156 Da with each molecule of HNE being added.

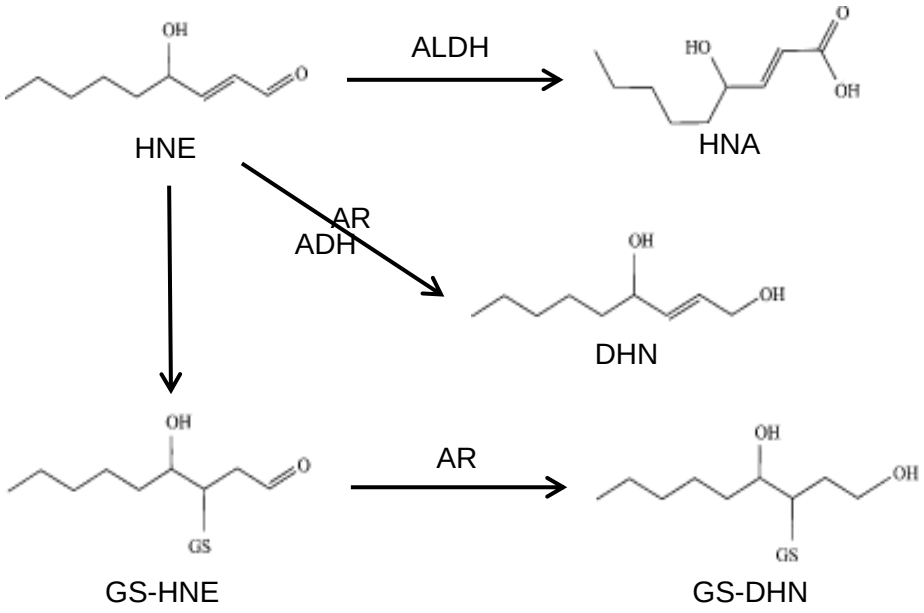

Figure 1.12. Metabolism pathways of HNE. ADH, alcohol dehydrogenase; ALDH, Aldehyde dehydrogenase; AR, alcohol reductase; DHN, 1,4-dihydroxy-2-nonene; GS-HNE, glutathione conjugate of 4-Hydroyx-2-nonenal; GS-DHN, glutathione conjugate of 1,4-dihydroxy-2-nonene; HNA, 4-hydroxy-2-nonenoic acid; HNE, 4-Hydroyx-2-nonenal. (Pappa et al., 2003)

Table 1.1: Human ABC transporters subfamilies

Family	Members	Functions
ABCA	ABCA1 to ABCA12	Cholesterol efflux, phosphatidyl choline efflux, N-retinylidiene-PE efflux
ABCB	ABCB1 to ABCB11	Peptide transport, iron transport, Fe/S cluster transport, bile salt transport, xenobiotics transport
ABCC	ABCC1 to ABCA13	Organic anion efflux, nucleoside transport, chloride ion channel, sulfonylurea receptor, potassium channel regulation, xenobiotic transport
ABCD	ABCD1 to ABCD 4	Very long chain fatty acids transport regulation
ABCE	ABCE 1	Elongation factor complex
ABCF	ABCF1 to ABCF3	Unknown function
ABCG	ABCG1 to ABCG 5	Cholesterol transport, sterol transport, toxin transport

Table 1.2: SNPs of Mrp1 correlated with anthracycline induced cardiotoxicity

Rs#	Mutation (position)	Location Type	Disease Treated	Drug	Effect	Ref
rs45511401	2012 G>T (nsSNP)	Gly671Val Exon 16 (NBD1)	Non-Hodgkins lymphoma	Doxorubicin	cardiotoxicity	Wojnowski et al., 2005
rs3743527	C>T	3'-UTR	ALL (childhood)	Doxorubicin	cardiotoxicity	Semsei et al., 2012
rs246221	825 T>C	Val275Val Exon 8	ALL (childhood)	Doxorubicin	cardiotoxicity	Semsei et al., 2012
rs4148350	G>T	intron 15	Pediatric cancer	Anthracycline	cardiotoxicity	Visscher et al., 2012

ALL, Acute lymphoblastic leukemia; Rs#, reference SNP ID number.

Chapter Two

Loss of Mrp1 potentiates DOX-induced cardiotoxicity in mice

Overview of Study

Cardiotoxicity is one of the most severe side effects caused by anti-cancer chemotherapy, including DOX. Previously our laboratory reported that expression of Mrp1 in cardiac sarcolemma increases in response to a single injection of DOX in mice (Jungsuwadee et al., 2006). Our laboratory also reported that a single intravenous administration of DOX caused significantly higher nuclear injury in Mrp1-/- mice heart compared to their WT littermates. In this chapter, experiments were conducted to investigate the effects of chronic DOX-induced cardiotoxicity in WT and Mrp1-/- mice and confirmed our prior finding in mice treated acutely with DOX, and more importantly, demonstrated the role of Mrp1 in protecting against DOX-induced cardiac dysfunction. The health condition of these mice was monitored. Chronic DOX caused body weight loss and hemotoxicity, and these adverse effects were significantly exacerbated in Mrp1-/- vs WT mice. Using transthoracic echocardiography techniques, it was found that DOX caused more severe left ventricle dysfunction in Mrp1-/- mice, shown as significantly lower fractional shortening (FS) and ejection fraction (EF). This pathological dysfunction was consistent with the measurements of heart apoptosis and BNP expression in heart ventricle. This study is the first to demonstrate the protective effects of Mrp1 against chronic DOX-induced cardiac dysfunction.

Introduction

Doxorubicin (DOX) is an effective chemotherapeutic anthracycline used for a variety of solid tumors and hematologic malignancies; however, its clinical use is significantly limited by its dose-dependent cardiotoxicity (Minotti et al., 2004; Octavia et al., 2012). The incidence of cardiomyopathy is 2.5 times higher in cancer patients treated with DOX than that in untreated patients (Dolye et al., 2005). It is well-established that the reactive oxygen species (ROS) generated by DOX, which cycles between the quinone and semiquinone in cardiac mitochondria, contribute significantly to cardiac pathology (Yen et al., 1996; Gewirtz, 1999; Minotti et al., 2004). However, the self-regulation and defense mechanisms of heart tissue in this process are still unclear.

Multidrug resistance-associated protein 1 (MRP1/ABCC1), a member of the ATP-binding cassette (ABC) transporter protein superfamily, is ubiquitously expressed in multiple tissues, including heart (Flens et al., 1996; Nies et al., 2004). Mrp1 mediates the efflux of glutathione (GSH) and glutathione disulfide (GSSG) as well as GSH, glucuronate and sulfate conjugated organic anions, including leukotriene C4 (LTC4) and the GSH conjugate of 4-Hydroxy-2-nonenal (GS-HNE) (Leier et al., 1994; Cole and Deeley, 1998; Renes et al., 2000; Leslie et al., 2001; Jungsuwadee et al., 2012). Although Mrp1-/- mice have normal fertility and viability, their ability to transport key endo- and xenobiotics is compromised (Wijnholds et al., 1997, Yoshioka et al., 2009).

Accumulating case-control clinical studies have shown that several single-nucleotide polymorphisms (SNPs) of *MRP1* gene are related to susceptibility to

cardiotoxicity observed in cancer patients treated with anthracyclines, including DOX (Wojnowski et al., 2005; Semsei et al., 2012; Visscher et al., 2012). These SNPs may affect efflux of DOX itself, but also may modulate efflux of other important endobiotics (Jungsuwadee et al., 2012). Thus, MRP1 could play an important role in regulation of oxidative stress by effluxing GSH and GSSG as well as GS-HNE (Cole, 2014a; Cole, 2014b; Jungsuwadee et al., 2012).

In the present study, we explored the effects of Mrp1 on DOX-induced cardiotoxicity in mice. Although Mrp1 is highly conserved between human and rodents with 88% sequence homology, the human isoform (MRP1) is able to transport DOX, whereas murine Mrp1 has only a negligible ability to transport this anthracycline (Stride et al., 1997). More specifically, a glutamic acid, which has a negative charge, on TM14 in human MRP1 is critical to accomplish the transport of DOX. This glutamic acid is substituted by a glutamine in murine Mrp1, with loss of the negative charge, and also loss of the ability to transport DOX (Figure 2.1) (Zhang et al., 2001). Therefore, the Mrp1-/- mouse provides a good model to study the role of Mrp1 in DOX cardiotoxicity separately from the effects of DOX retention. Here evidence is presented for the first time that chronic DOX treatment caused more severe cardiac dysfunction in Mrp1-/- mice. These results provide novel insights into the role of Mrp1 in cardiac protection beyond the ability to transport DOX.

Materials and methods

Animals and treatment

C57BL/6 (WT) mice and Mrp1-disrupted C57BL/6 (Mrp1-/-) mice, initially a

gift from Dr. Gary Kruh, were backcrossed for more than ten generations, littermates bred in-house and maintained in the Division of Laboratory Animal Resources. All experiments complied with the requirements of the Institutional Animal Care and Use Committee of the University of Kentucky (Lexington, KY). The animal treatment protocols were based on studies demonstrating decreased cardiac function following chronic treatment with DOX (Zhang et al., 2009). All experiments used male mice 10 to 12-weeks old and weighing 25–35 g. DOX (Pfizer, NY) was administered intraperitoneally at a dose of 3 mg/kg (Figure 2.2 protocol A) or 2 mg/kg (Figure 2.2 protocol B) body weight, or an equivalent volume of saline, twice a week for 3 or 5 weeks, resulting in a cumulative DOX dose of 18 (Protocol A) or 20 mg/kg (Protocol B). Hydration and nutritional gel (72-07-5022, ClearH2O, Portland, ME) were provided to mice as supplements, 1 oz per 5 mice, and replaced every 2 days, in addition to pelleted food and water throughout the treatment period. Animal body weight was recorded throughout the experimental period. Animals were euthanized and examined 48 h or 2 weeks after the last DOX treatment.

Complete blood count

Peripheral blood (~20 µL) was collected from WT and Mrp1-/- mice 48 h and 2 weeks after the last DOX treatment (Protocol B) by sub-mandibular bleeding. Blood cell parameters were obtained on the Hemavet 950FS automated hematology analyzer (Drew Scientific, Dallas, TX).

Transthoracic Echocardiography

Transthoracic echocardiography was performed with a Vevo 2100 High-Resolution In Vivo Imaging System (Visual Sonics Inc., Toronto, Canada). The mice were lightly anesthetized by isoflurane (0.5-1.5%) until the heart rate stabilized at ~500 beats/min. With the use of the M-mode from parasternal short-axis images, left ventricular end-diastolic dimension (LVIDs) and left ventricular end-systolic dimension (LVIDs) were measured. The percentage of left ventricular fractional shortening (LVFS) was calculated as 100 X ((LVIDd-LVIDs)/LVIDd). LV volume at end-diastole (LVEDV) was estimated as [7.0/(2.4 + LVIDd)] X $LVIDd^3$ and at end-systole (LVESV) as [7.0/(2.4 + LVIDs)] X $LVIDs^3$. Left ventricular ejection fraction (LVEF) was determined by using [(LVEDV - LVESV)/ LVEDV] X 100%. Echocardiography was conducted by investigators who were blinded to treatment group assignments and genotype.

Terminal Deoxynucleotidyl Transferase dUTP Nick End Labeling (TUNEL) assay

The tip of the mouse heart ventricle was fixed in 10% formalin, embedded in paraffin, 4 μm sections cut and stained using the ApopTag® Peroxidase In Situ Apoptosis Detection Kit (S7100, Millipore) according to the manufacturer's instructions. Counterstaining with Mayer's hematoxylin aided in the morphologic evaluation of normal and apoptotic nuclei, in which normal nuclei were stained as blue and apoptotic nuclei as brown. The number of TUNEL-positive cells was quantitated using Aperio scanning image analysis of sections. DNase I treatment

was carried out as the positive control.

Hydroxyproline Analysis

Heart ventricle tissue was ground with liquid nitrogen, and 10 mg tissue powder, 100 µL of distilled water and 100 µL of concentrated HCl (10 N) added to a glass vial with Teflon cap and hydrolyzed at 120°C for 24 h. Hydrolyzed samples were transferred to a microcentrifuge tube and spun at 10,000 rpm for 3 min to remove hydrolyzed residue from the sample, and supernatants used for the assay. Briefly, according to manufacturer's instructions (#6017, Chondrex, Inc., Redmond, WA), samples were distributed to a 96-well plate, incubated with chloramine-T solution at room temperature for 20 minutes and incubated with dimethylaminobenzaldehyde (DMAB) solution for 30 minutes at 60°C. Absorbance was measured at 530 nm on a spectrophotometer (Molecular Devices, CA). Hydroxyproline levels were calculated according to standards provided. The results were expressed as total collagen (µg) /heart tissue (mg), assuming that collagen contains an average of 13.5% hydroxyproline.

RNA extraction and real-time quantitative PCR (qRT-PCR)

Total RNA was isolated from heart ventricles using Trizol Reagent (Sigma) according to the manufacturer’s instructions, except that DNase I treatment was incorporated. RNA concentrations were determined using NanoPhotometer (Implen GmbH, München, DE). Total RNA (2 µg) was converted into cDNA with SuperScript III First-Strand Synthesis System for RT-PCR (Invitrogen, USA) and

the mixture diluted without purification in sterile water and used for qRT-PCR analysis. mRNA expression of specific genes was quantified using the LightCycler® 480 Real-Time PCR System (Roche Applied Science, Mannheim, Germany). Forward and reverse primers used are as follows: brain natriuretic peptide (BNP) 5'-GTCAGTCGTTTGGGCTGTAAC-3' (forward) and 5'-AGACCCAGGCAGAGTCAGA-3' (reverse); 18S rRNA 5'-GCAATTATTCCCCATGAACG-3' (forward) and 5'-GGGACTTAATCAACGCAAGC-3' (reverse). These primers were ordered from Integrated DNA Technologies (Coralville, IA, USA); Universal probe library (UPL) probes #71 (BNP), #48 (18S rRNA) were obtained from Roche Applied Science. The qRT-PCR reactions were performed in duplicate in 15 µL reaction volume containing 2 µL 1:10 diluted cDNA and 1× LightCycler 480 Probes Master Mix. 18S rRNA was selected as reference gene, for which cDNA samples were diluted 1:4000. Data were evaluated by calibrator-normalized relative quantification with efficiency correction using the Light Cycler® 480 software version 1.5 (Roche Applied Science, Mannheim, DE). The software calculated the relative amount of the target gene to the reference gene based on the crossing points.

Statistical analysis

All data are expressed as the mean ± SE for n = 5 to 12 mice per group, as detailed in the Figure Legends. For body weight data, a linear mixed model was considered with fixed effects of treatment group, day and their interaction and

random effects of both the intercept and slope. The slope of weight loss and the weight change at the end of the treatment were compared between two treatment groups based on the linear mixed model. For data from other experiments, firstly a Bartlett's test is used to test homogeneity of variance across all groups. If the Bartlett's test result was not significant, further statistical analysis was performed using a one-way ANOVA with post hoc analysis by the Newman-Keuls method. If the Bartlett's test result was significant, further statistical analysis was performed using Welch's t-tests for pairwise comparisons between groups of interest with the Bonferroni correction for multiple comparison adjustment.

Results

Chronic DOX administration decreased mouse body weight and heart weight

Mrp1-/- mice and their WT littermates were treated with either 3 mg/kg body weight, twice a week for 3 weeks (Figure 2.3 protocol A), or 2 mg/kg body weight, twice a week for 5 weeks (Figure 2.3 protocol B). DOX markedly decreased body weight of WT and Mrp1-/- mice; after DOX treatment was discontinued and during the 2-week recovery period, body weight stabilized and began to recover in all DOX treated animals. Comparison of the slope of weight loss for DOX-treated Mrp1-/- vs WT mice and the weight change in the two groups at the end of the treatment (day 21 and 35 for the 3 and 2 mg/kg DOX treatment groups, respectively) showed that the magnitude of the decrease was significantly larger

in Mrp1-/- compared to WT mice ($p < 0.001$ for both comparisons). With the 3 mg/kg DOX treatment, 4 of 13 Mrp1-/- mice were euthanized due to severe body weight loss (22-25% of initial body weight) before the last day of the experimental period. Thus, for subsequent experiments, except for the TUNEL assay, data were acquired using the lower DOX dose (2 mg/kg) treatment (Protocol B). DOX treatment also significantly decreased heart weight in both genotypes (Figure 2.4).

Effects of chronic DOX administration on blood counts

Chronic DOX treatment (2 mg/kg) significantly decreased white blood cell (WBC) and lymphocyte (LY) counts in both genotypes 48 h after the last DOX treatment (Figure 2.5A and 2.5B). Two weeks later, the WBC, including LY counts, had recovered in WT mice, but remained significantly decreased in Mrp1-/- mice ($p < 0.05$) (Figure 2.5C and 2.5D).

Cardiac function after chronic DOX administration

To determine whether cardiac contractile function was affected by chronic DOX administration, LVIDd and LVIDs were assessed by *in vivo* echocardiography 2 weeks after the last DOX treatment (2 mg/kg), and LVFS and LVEF calculated. Figure 2.6A shows representative echocardiograms of WT and Mrp1-/- mice after saline or DOX administration. There were no significant differences in LVFS and LVEF between WT and Mrp1-/- saline treated mice (Figure 2.6B), indicating that Mrp1-/- mice had normal basal contractile function.

DOX treatment increased both LVIDd and LVIDs and decrease LVPWd and LVPWs in WT and Mrp1-/- mice (Figure 2.6 B - E). Importantly, DOX significantly reduced LVFS and LVEF in Mrp1-/- mice, while there were no significant changes in these values in WT mice (Figure 2.6F and 2.6G).

B-type Natriuretic Peptide (BNP) is a cardiac hormone secrected from the ventricles of the heart in response to ventricular volume and pressure overload. Thus, elevated BNP expression was used as a heart failure marker. Here, BNP mRNA expression was found to be significantly higher in DOX treated Mrp1-/- mouse heart compared to WT mouse heart (Figure 2.6H). This was consistent with the cardiac dysfunction observed in DOX treated Mrp1-/- mice. These data clearly demonstrate that loss of Mrp1 exacerbated DOX-induced cardiac dysfunction.

DOX-induced apoptosis in mouse heart

The effects of Mrp1 on DOX-induced cell apoptosis in the heart was investigated using TUNEL staining to evaluate heart sections. Cells containing intensive TdT-positive staining in the nuclei were considered apoptotic. As a result, DOX treatment (3 mg/kg) increased apoptosis in mouse hearts of both genotypes, however, Mrp1-/- hearts showed significantly more extensive (~3.5 fold higher) TUNEL staining nuclei compared to WT mice hearts ($p < 0.05$) (Figure 2.7), consistent with the more severe cardiotoxicity seen with measurements of ventricular systolic function.

Chronic DOX administration increased heart ventricular fibrosis

Since DOX has been reported to induce cardiac fibrosis (Zhu et al., 2008; Li et al., 2006), the mouse ventricular fibrosis was examined by quantitating the collagen level. As shown in Figure 2.8, saline treated WT and Mrp1-/- mice heart had similar collagen levels, while DOX treatment significantly increased ventricular collagen level in both WT and Mrp1-/- mice. However, no significant difference in the collagen level was found between genotypes.

Discussion

The key finding in the present study is that global deletion of Mrp1 potentiates DOX-induced cardiac toxicity in mice as measured by echocardiography, apoptosis and the ventricular dysfunction marker BNP. DOX is an anti-tumor anthracycline that is effective in treating a wide variety of cancers, but produces dose-limiting cardiac toxicity. Although all of the factors contributing to the mechanism for DOX-induced cardiotoxicity are not known, it is well accepted that oxidative stress contributes significantly to DOX-induced heart failure (Yen et al., 1996; Minotti et al., 2004; Kang et al., 2007). Our group and others have shown that adduction of cardiac proteins with HNE, a toxic product of lipid peroxidation induced by oxidative stress, is increased in DOX treated mice (Renes et al., 2000; Jungsuwadee et al., 2006). Additionally, sarcolemmal membrane vesicles from WT mouse heart transport GS-HNE, but this activity is absent in such vesicles from Mrp1-/- mice (Jungsuwadee et al., 2009). In addition, 72 h after a single dose of DOX (15 mg/kg body weight, iv) there is

significantly more nuclear injury in Mrp1-/- compared to WT hearts (Deng et al., submitted). Based on these findings, we hypothesized that Mrp1 protects against DOX-induced cardiac dysfunction.

Here the previous findings were extended to assess whether loss of Mrp1 affects cardiac function following DOX treatment. The data show that chronic DOX treatment caused a more severe left ventricle dysfunction in Mrp1-/- mice, presenting as decreased LVFS and decreased LVEF. These pathological changes were also consistent with the higher BNP expression and more apoptotic nuclei observed in Mrp1-/- mouse heart. These data further demonstrated that loss of Mrp1 potentiated DOX-induced cardiac dysfunction in addition to the nuclear damage in heart, even though Mrp1-/- mice heart have higher GSH levels due to the loss GSH efflux via Mrp1 (Deng et al., submitted). Together, these data strongly support the hypothesis that Mrp1 protects the heart against DOX toxicity *in vivo*.

Several ABC transport mRNA/proteins have been reported to be present to various degrees in heart (Couture et al., 2006), and could contribute to efflux of DOX. Pgp (Abcb1a, Abcb1b), BCRP (Abcg2) and Mrp2 (Abcc2) were demonstrated to contribute to DOX resistance by mediating its efflux (Couture et al., 2006; Vlaming et al., 2006; Natarajan et al., 2012). In addition, Mrp4 (Abcc4) is able to efflux GSH and GSSG (Ballatori et al., 2005). It has been reported that there is no/very low expression level of Abcc2 in heart (Couture et al., 2006). Also we did not detect the protein expression of Abcg2 in heart tissue. To rule out potentially altered, compensatory expression of other transporters in the heart of

Mrp1-/- mice, we measured the protein expression of Abcb1 and Abcc4 2 weeks after the last dose of DOX or saline. These data show that none of these transporters showed a significant difference between WT and Mrp1-/- mice heart following treatment with saline or DOX (Figure 2.9).

Finally, decreased recovery from hematopoietic toxicity was seen in Mrp1-/- mice following DOX treatment. This transient myelosuppression, shown as decreased WBC counts and LY counts in DOX treated mice, is probably caused by the suppression or apoptosis of hematopoietic progenitor cells. But how Mrp1 affects the replenishment of these blood cells is not clear. Another key finding was that DOX treatment caused a more severe body weight loss in Mrp1-/- mice. This is likely associated with reduced food consumption, since DOX causes a loss of appetite in DOX-treated cancer patients. It is also well-known that DOX causes dose-limiting gastrointestinal injury due to its toxic effect on intestinal epithelium, including the rapidly dividing stem cells located at the base of the intestinal crypts. The apoptosis in intestinal epithelium and the loss of villi throughout the small intestine could compromise digestive and absorptive capacities, finally causing severe body weight loss in mice (Ijiri and Potten, 1987). However, since these Mrp1-/- mice are constitutive knockout animals, we could not determine whether the intestine or other organs were primarily responsible for this differential extent of body weight loss between WT and Mrp1-/- mice.

In summary, loss of Mrp1 potentiates DOX-induced cardiotoxicity, showing a severe ventricular dysfunction and cellular apoptosis in heart tissue. These studies are the first to document a protective role of Mrp1 in DOX-induced

cardiotoxicity and may provide critical information regarding the potential adverse sequelae of introduction of MRP1 inhibitors as adjuncts to clinical chemotherapy of multidrug resistant tumors.

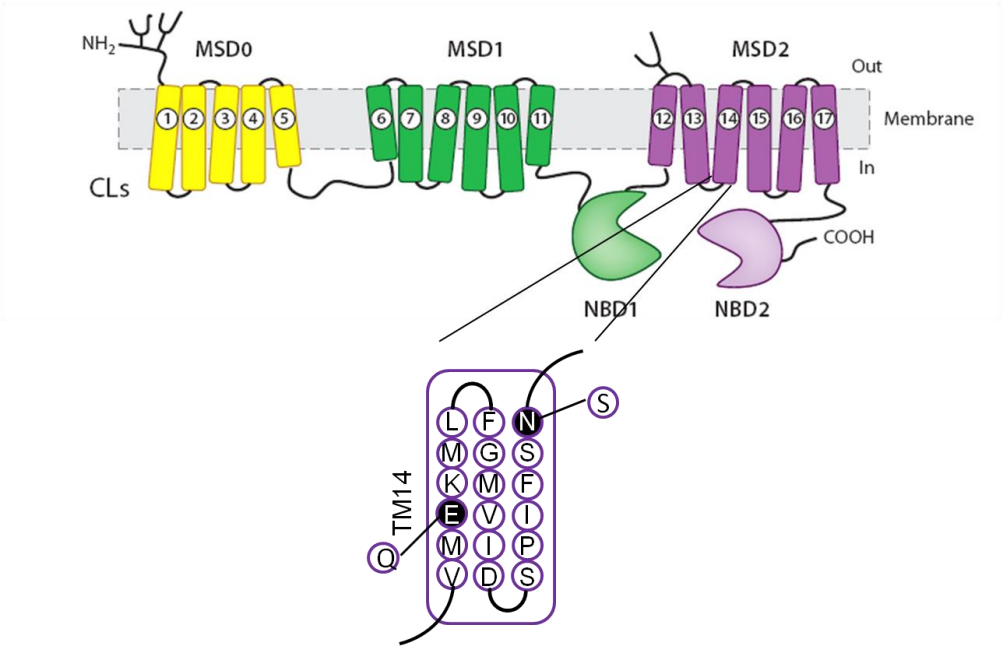

Figure 2.1. Murine Mrp1 does not transport DOX due to critical amino acid differences with human MRP1. The figure shows the predicted topology of human and murine MRP1/Mrp1 with 17 TM helices. An expanded view of the region encompassing TM helix 14 is illustrated in the bottom half of the figure. The amino acids shown in the expanded view are those found in human MRP1. Residues in open circles are identical in the murine and human proteins. Residues that are different between the two proteins are indicated by shaded circles, and the amino acids present in murine Mrp1 at the equivalent positions are shown to the side. L, leucine; M, methionione; K, lysine; E, glutamic acid; V, valine; F, phenylaline; G, glycine; I, isoleucine; D, aspartic acid; N, asparagin; S, Serine; P, proline; Q, glutamine; CL: cytoplasmic loops.

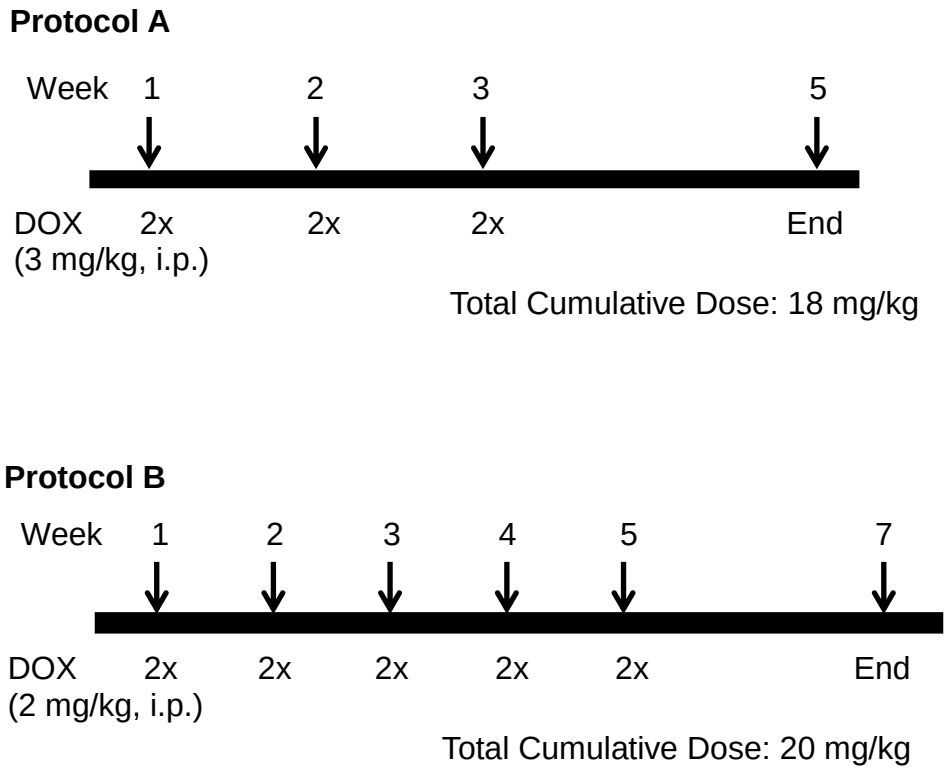

Figure 2.2. Chronic DOX treatment protocols. Protocol A: WT and Mrp1-/- mice were administrated intraperitoneal DOX, 3 mg/kg body weight, or an equivalent volume of saline, twice a week for 3 weeks, resulting in a cumulative dose of 18 mg/kg DOX. Protocol B: WT and Mrp1-/- mice were administrated intraperitoneal DOX, 2 mg/kg body weight, or an equivalent volume of saline, twice a week for 5 weeks, resulting in a cumulative dose of 20 mg/kg DOX.

A

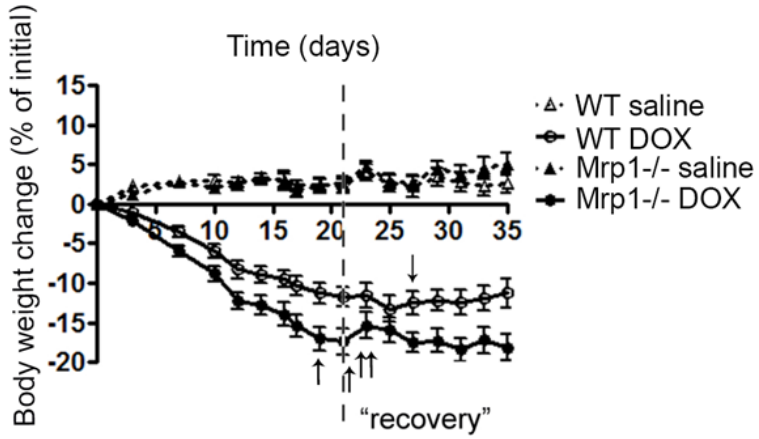

B

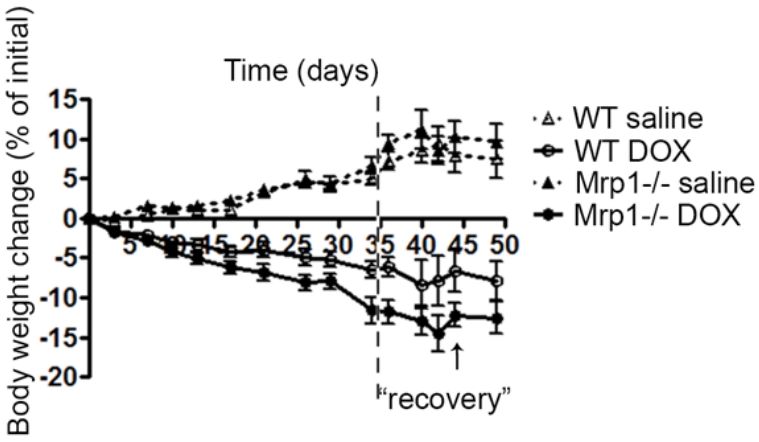

Figure 2.3. Body weight change during chronic DOX treatment. WT and Mrp1-/- mice were administrated intraperitoneal DOX with protocol A (A) or protocol B (B), and maintained for an additional two weeks ("recovery"); animal weight was monitored throughout. Arrow: one mouse was sacrificed on each of the indicated days due to body weight loss (loss of 22 - 25% of initial body weight). Values are mean ± SE. (Panel A, n = 12; Panel B, n = 12 before day 35 and n = 6 after day 35)

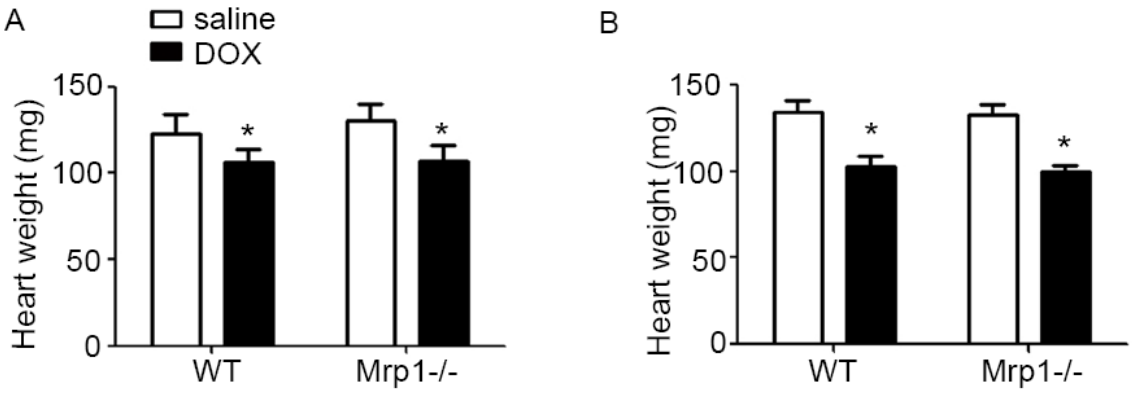

Figure 2.4. Heart weight change after chronic DOX treatment. WT and Mrp1-/- mice were administered intraperitoneal DOX with protocols A (A) or B (B). Two weeks later, the hearts were removed immediately and weighed. Each bar represents the mean ± SE. (In figure A, n= 12 for saline treated group; n=12 for DOX treated WT mice; n=10 for DOX treated Mrp1-/- mice; in figure B, n=6 for each group, *, $p < 0.05$ DOX vs. saline of the same genotype by Newman-Keuls multiple comparison test after one-way ANOVA)

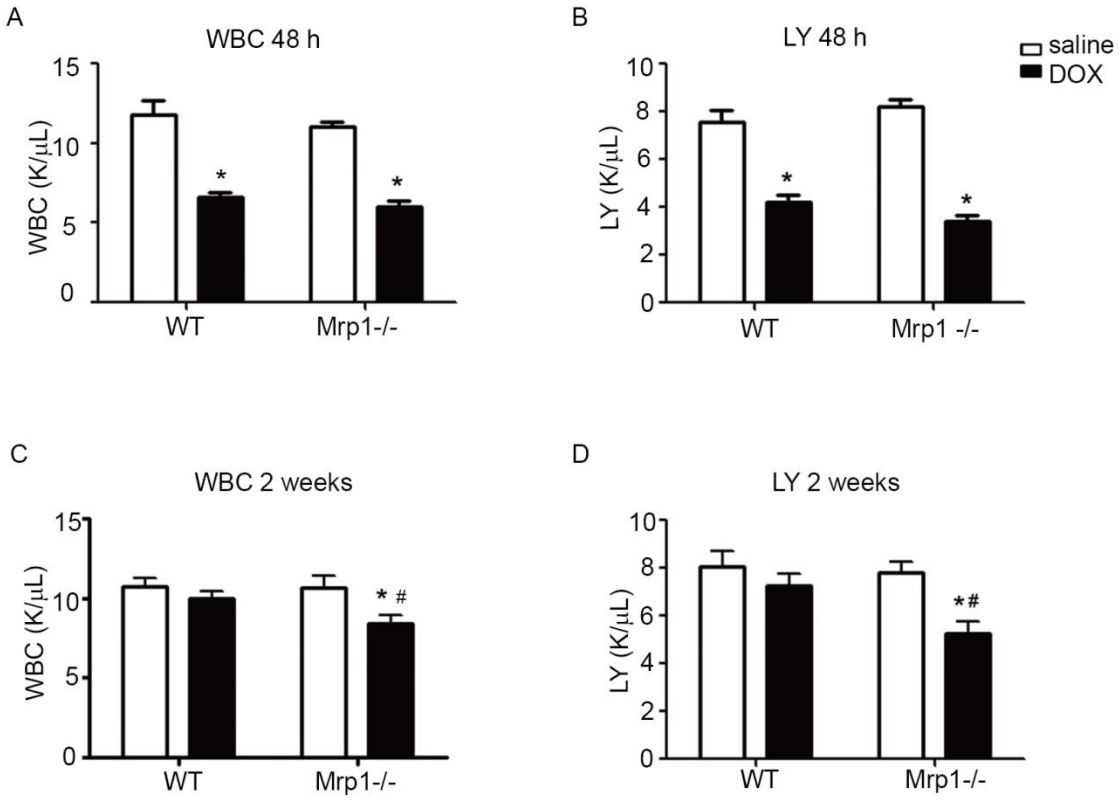

Figure 2.5. The effects of DOX on white blood cell (WBC) and lymphocyte (LY) counts. Mice were treated with protocol B, and WBC and LY counts measured 48 h (A and B) and 2 weeks (C and D) after the last DOX dose. Decreased WBC and LY counts were observed in both WT and Mrp1-/- mice at 48 h after the last DOX dose, and had recovered two weeks later in WT mice, but remained depressed in Mrp1-/- mice. K/μL, 1000 cells per microliter. Each bar represents the mean $\pm$ SE. (n=8 for saline treated group; n=12 for DOX treated group, *, $p < 0.05$ DOX vs. saline of the same genotype; #, $p < 0.05$ Mrp1-/- vs. respective WT mice by Newman-Keuls multiple comparison test after one-way ANOVA).

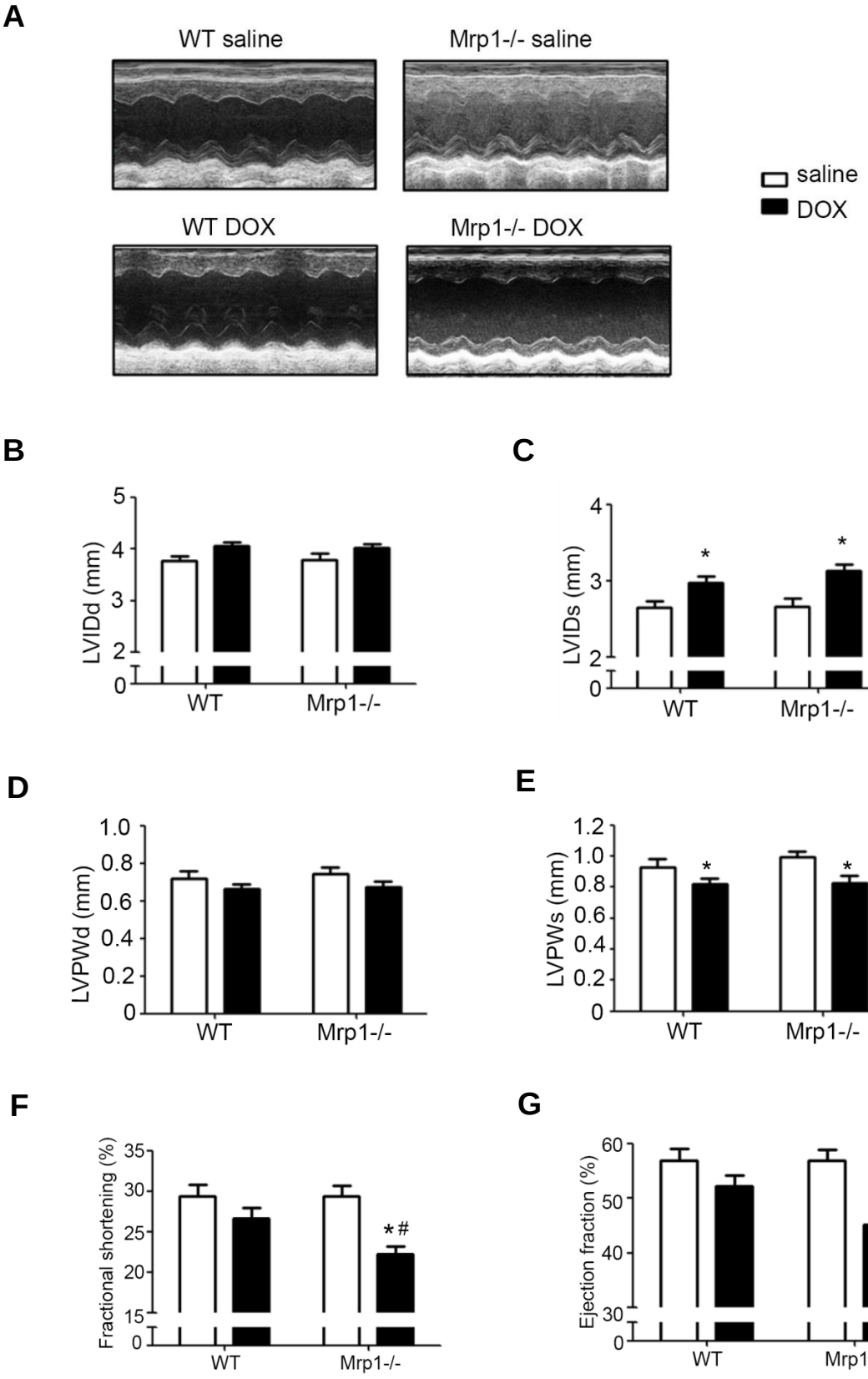
A
WT saline
Mrp1-/- saline
WT DOX
Mrp1-/- DOX
saline
DOX
B
LVIDd (mm)
WT
Mrp1-/-
C
LVIDs (mm)
WT
Mrp1-/-
D
LVPWd (mm)
WT
Mrp1-/-
E
LVPWs (mm)
WT
Mrp1-/-
F
Fractional shortening (%)
WT
Mrp1-/-
G
Ejection fraction (%)
WT
Mrp1-/-

H

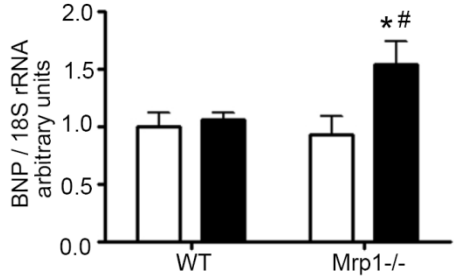

Figure 2.6. Chronic DOX treatment leads to more severe systolic dysfunction in Mrp1-/- mice vs. WT mice. Mice were treated with protocol B, and cardiac function assessed through M-mode transthoracic echocardiography. (A) Representative M-mode echocardiogram of left ventricular (LV) wall motion; (B) LVIDd, (C) LVIDs, (D) LVPWd, (E) LVPWs, (F) Fractional shortening, (G) Ejection fraction and (H) mRNA expression of BNP analyzed by qRT-PCR 2 weeks after chronic saline or DOX treatment. Each bar represents mean ± SE. (n=8 for saline treated group; n=12 for DOX treated group; *, $p < 0.05$ DOX vs. saline of the same genotype; #, $p < 0.05$ Mrp1-/- vs. respective WT mice by Newman-Keuls multiple comparison test after one-way ANOVA). LVIDd: left ventricular end-diastolic dimension; LVIDs: left ventricular end-systolic dimension; LVPWd, left ventricular diastolic posterior wall thickness; LVPWs, left ventricular systolic posterior wall thickness.

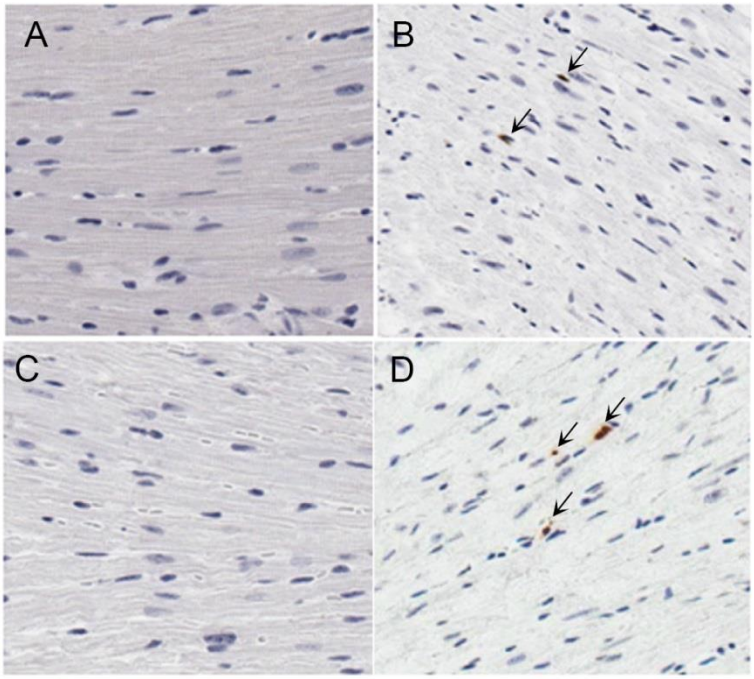

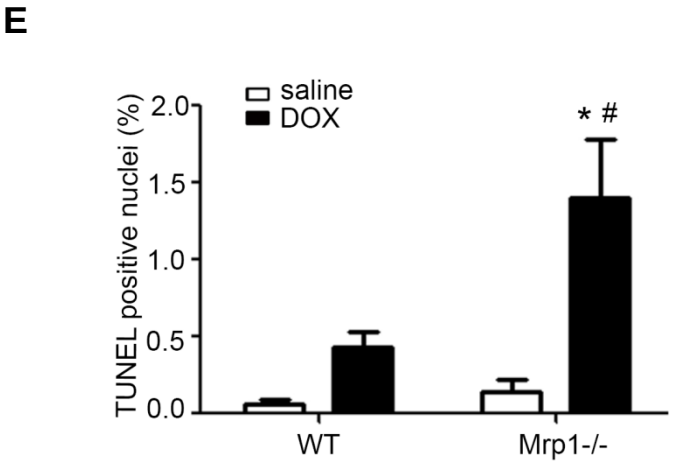

Figure 2.7. Apoptosis in mouse myocardium. Mice were treated using protocol A, and apoptosis from mouse myocardium detected by TUNEL (Terminal deoxynucleotidyl transferase dUTP nick end labeling assay) staining. Representative photomicrographs are shown demonstrating TUNEL staining of heart sections from saline treated WT (A), DOX treated WT (B), saline treated Mrp1-/- (C), and DOX treated Mrp1-/- mice (D). TUNEL-positive cells are indicated by brown staining, and the TUNEL-positive nuclei are indicated by

arrows. (E) Histogram showing the quantitative analysis of TUNEL-positive cells. Each bar represents mean ± SE (n=6 for saline treated group; n= 10 for DOX treated WT mice, n=8 for DOX treated Mrp1-/- mice. *, $p < 0.05$ DOX vs. saline of the same genotype; #, $p < 0.05$ Mrp1-/- vs. respective WT mice by Welch's t-test.)

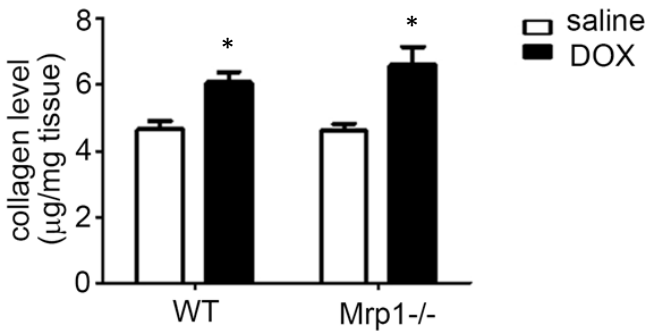

Figure 2.8. DOX increased collagen level in mouse heart. Mice were treated using protocol B, and hydroxyproline levels in mouse heart tissue measured. The results are expressed as total collagen/heart tissue, assuming that collagen contains an average of 13.5% hydroxyproline. Each bar represents the mean ± SE. (n = 8, *, $p < 0.05$ DOX vs. saline of the same genotype by Newman-Keuls multiple comparison test after one-way ANOVA).

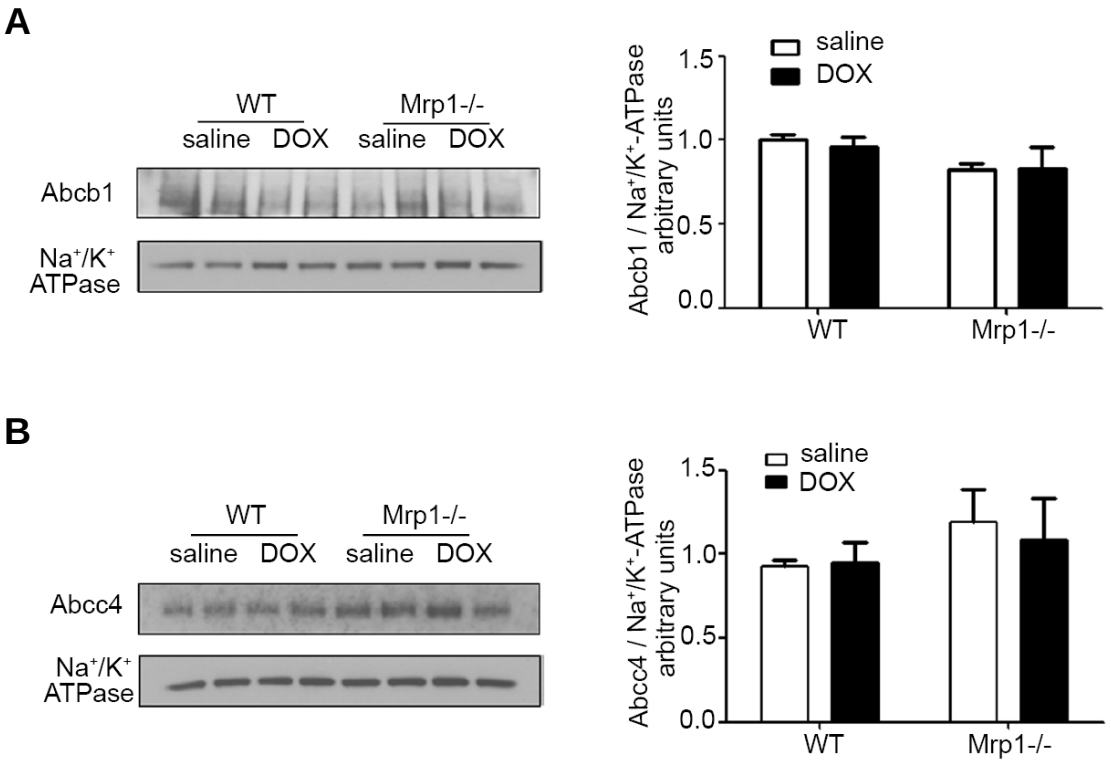

Figure 2.9. Protein expressions of Abcb1 and Abcc4 in mouse heart. Mice were treated with protocol B, and the protein level of Abcb1 and Abcc2 were measured 2 weeks after the last dose of DOX by real time PCR. Each bar represents the mean ± SE. (n = 3)

Chapter Three

Mrp1 protects both cardiomyocytes and cardiac fibroblasts against DOX cytotoxicity

Overview of Study

The studies in chapter 2 demonstrated that loss of Mrp1 potentiates chronic DOX treatment induced cardiotoxicity in mice, presenting more severe left ventricle dysfunction and greater cell apoptosis in Mrp1-/- mouse heart. Here, to extend the findings of Mrp1's cardiac protective role to a cellular level, and identify the specific function of Mrp1 in different cell types in heart, the effects of Mrp1 on DOX cytotoxicity in cardiomyocytes (CM) and cardiac fibroblasts (CF) was further investigated. Neonatal mouse CM and CF, isolated from WT and Mrp1-/- 1-3 days old pups, were treated with DOX (0.3 - 4 μM) for various times. DOX significantly increased Mrp1 mRNA and protein expression level in both CM and CF cultures. The methyl thiazol tetrazolium (MTT) assay showed that CM and CF derived from Mrp1-/- mice demonstrate a greater decrease in cell viability after DOX treatment. Further studies suggested that there was more cell apoptosis and DNA damage in DOX treated Mrp1-/- cells, presenting as higher caspase 3 cleavage, PARP cleavage and γH2.AX expression vs WT cells. Taken together, these results indicate that Mrp1 protects both CM and CF against DOX induced cytotoxicity.

Introduction

Cardiotoxicity is one of the most serious side effects in DOX treated cancer patients. Identifying the gene(s) involved in normal hearts' defense against this toxicity and understanding the mechanisms will be very helpful to find the potential approaches to prevent or alleviate this dose-limiting toxicity. Our *in vivo* studies demonstrate that loss of Mrp1 potentiates chronic DOX treatment induced cardiotoxicity in mice, with Mrp1-/- mice exhibiting more nuclear injury after a single DOX injection and more severe cardiac dysfunction and greater heart apoptosis following chronic DOX treatment. Here, to extend the bases of Mrp1's cardiac protective role to a cellular level, the role of Mrp1 in DOX toxicity in cardiomyocytes (CM) and cardiac fibroblasts (CF) was further evestigated.

CM and CF form the two largest cell populations in heart, while other cell types, such as endothelial or vascular smooth muscle cells, represent comparatively small populations. CMs are the major cells that make up the atria and ventricles of the heart, and account for more than 50% of total cell number in heart. During fetal life, cardiomyocyte DNA synthesis is associated with cell proliferation, and after birth (up to approximately neonatal day 3) a second DNA synthesis phase is associated with binucleation. After that, cardiac growth involves increasing the size of the myocytes without substantial increases in cell number (Woodcock et al., 2005). The low proliferative capacity of adult CMs means that loss of working CMs in adult heart cannot be replaced and must be compensated by increased work load of the remaining myocytes; otherwise, cardiac dysfunction will develop. This also partially explains why the heart is so

susceptible to DOX toxicity compared to other tissues with better self-regeneration capacity. The CMs are able to shorten through the interaction between myofilament proteins actin and myosin, and these cells must be able to shorten and lengthen properly to maintain normal cardiac structure and function. A rapidly expanding body of evidence indicates that CM death by apoptosis and necrosis is an important mechanism of DOX-induced cardiomyopathy (Zhang et al., 2009; Octavia et al., 2012).

CFs are the most abundant non-cardiomyocytes within the heart. They are found throughout cardiac tissue surrounding CM and bridging 'the voids' between myocardial tissue layers. Compared to CM, the understanding of CF function is much less. CFs provide a supporting structure to the healthy heart, contribute to myocardial structure, cell signaling, and electro-mechanical function in healthy myocardium (Camelliti et al., 2005). Beyond their very important roles in maintaining myocardial function under normal condition, CFs also contribute to adverse cardiac remodeling during pathological conditions, such as hypertension, myocardial infarction, and heart failure (Souders et al., 2009; Shi et al., 2011). Upon cardiac injury, CFs may proliferate and secret extracellular matrix and growth factor, leading to scar formation, cardiac fibrosis, myocardial stiffening and finally, cause cardiac dysfunction. Emerging research indicates that CFs are involved in arrhythmia initiation and maintenance by affecting electrical propagation (Kamkin et al., 2005).

The previous study in our laboratory and the data in Chapter 2 showed the cardiac protective function of Mrp1 in DOX treated mice (Deng et al., submitted).

Here, to further extend our findings to a cellular level, the effects of Mrp1 on DOX cytotoxicity was further investigated in the two major cell populations in heart: CM and CF. The results showed that in neonatal CM and CF cultures, DOX increased Mrp1 expression at both mRNA level and protein levels. CM and CF derived from Mrp1-/- mice were more sensitive to DOX toxicity, presenting lower cell survival, more cell apoptosis and more DNA damage. These data demonstrated that Mrp1 protects both CM and CF against DOX toxicity.

Materials and methods

Neonatal mouse CM/CF isolation and culture

C57BL/6 (WT) mice and Mrp1-disrupted C57BL/6 (Mrp1-/-) mice were backcrossed for more than ten generations. Experiments complied with the requirements of the Institutional Animal Care and Use Committee of the University of Kentucky (Lexington, KY). Primary CM and CF were obtained from Mrp1-/- neonatal mice and their WT littermates at 1–3 days of age. Mice were sacrificed by cervical dislocation, hearts were removed aseptically with the ventricles only retained and maintained in cold Hanks' balanced salt solution (HBSS) without Ca^{2+} and Mg^{2+}. The ventricles were washed with the same HBSS and minced into small fragments that were subjected to enzymatic digestion in the HBSS with collagenase type 2 (Worthington Biochemical Corp., Lakewood, NJ). Serial cycles of agitation were performed. After each cycle, the supernatant (containing the isolated cells) was removed and FBS added to a final concentration of 10%, the resulting mixture centrifuged for 10 min at 100 g, and

then the cells resuspended in DMEM with 10% FBS (v/v), 100 units/ml penicillin, and 100 µg/ml streptomycin (GIBCO, Grand Island, NY). Cells were preplated for 2 h at 37°C, to obtain CM and non-myocyte cells, predominantly CF. For CM culture, 100 µmol/L Bromodeoxyuridine (Sigma Chemical Co.) was added during the first 48 h to prevent proliferation of nonmyocytes. CM purity was tested by staining with antibody to cardiac-sarcomeric actin according to the manufacturer's instructions (Sigma Chemical Co). CM purity averaged >95% when examined after 48 h of culture. CF cultures were examined for positivity of expression of vimentin by immunofluorescence (Figure 3.1). Mouse anti-vimentin mAb (sc73259) was purchased from Santa Cruz Biotechnology (Santa Cruz, CA). CF cultures were used for experiments after two passages to eliminate other nonmyocytes

Methyl thiazol tetrazolium (MTT) assay

The cytotoxicity of DOX was determined by the MTT test. WT and Mrp1-/- CM or CF cells were seeded and grown in a 96-well plate at 37°C in a 5% CO_2 saturated atmosphere overnight. To develop a dose-response curve, DOX stock solution (2 mg/ml, Pfizer, NY) was dissolved in culture medium to final concentrations of 0 - 4 µM, and was incubated with cells in culture for 3 h, after which the media containing DOX was removed. Cells were rinsed once with 1× PBS, and finally incubated with fresh media for an additional 48 h. The MTT assay was performed according to the manufacturer's instructions (CellTiter 96 Aqueous One Solution Cell Proliferation Assay, Promega, Madison, WI). The

absorbance at 480 nm was measured for each well by SpectraMax M5 multi-detection reader (Molecular Devices, CA). The absorbance of untreated control cells was taken as 100% viability and the values of treated cells were calculated as a percentage of control. The data are represented as mean ± SE from 3 independent experiments.

Measurement of DOX concentration in cells

WT and Mrp1-/- CM or CF cells (10^6) were seeded and grown in a 12-well plate at 37°C in a 5% CO_2 saturated atmosphere overnight. Cells were treated with 30 μM DOX. Following 1 h of incubation, cells were washed three times with PBS and incubated with fresh DMEM medium for the indicated time. Finally, the cells were washed three times with PBS and incubated in 75% acidified (0.75 N HCl) isopropanol with 1% Triton X-100 and shaken for 30 min at room temperature. The absorbance of the supernatant was read using a fluorescence spectrofluorometer at wavelengths of Ex=470 nm and Em=590 nm. The value of DOX accumulation within the cells was calculated according to the standard curve.

RNA extraction and real-time quantitative PCR (qRT-PCR)

Total RNA extraction, cDNA preparation and qRT-PCR were conducted as the method description in Chapter 2. PCR primers for Mrp1 are as follows: Mrp1 5'-tgtgggaaaacacatctttga-3' (forward) and 5'-ctgtgcgtgaccaagatcc-3' (reverse); 18S rRNA 5'-gcaattattccccatgaacg-3' (forward) and 5'-gggacttaatcaacgcaagc-3'

(reverse). Universal ProbeLibrary probes #105 (Mrp1), (18S rRNA) were obtained from Roche Applied Science.

Immunoblot Assay

Protein concentrations were determined with the bicinchoninic acid protein assay (Pierce, Rockford, IL). Protein samples were fractionated on a 4% to 12% SDS-PAGE gel (EC6038BOX, Life Technologies) and transferred to nitrocellulose (Whatman, Stanford, ME). The blots were incubated with the primary antibody diluted in TBS/5% nonfat milk/0.1% Tween 20 at 4^0C overnight, then washed in TBS/0.1% Tween 20, and subsequently incubated with horseradish peroxidase (HRP)-labeled secondary antibody in TBS/5% nonfat milk/0.1% Tween 20. Chemiluminescence detection was done using Enhanced Chemiluminescence Plus (RPN2236, GE Healthcare, UK). Antibodies were obtained as follows: rat anti-Mrp1 mAb (801-007-c250; Alexis, San Diego, CA), rabbit anti-GAPDH pAb (sc-25778) and rabbit anti-actin pAb (sc-1616-R Santa Cruz Biotechnology, Santa Cruz, CA), rabbit anti-PARP pAb (#9542), rabbit anti-cleaved caspase3 pAb (#9661) and rabbit anti–phospho-histone H2A.X (γH2A.X) pAb (Ser139) (#9718) from Cell Signaling (Beverly, MA, USA), anti-rat Ig-HRP, anti-rabbit Ig-HRP and anti-mouse Ig-HRP from Amersham Biosciences (Piscataway, NJ).

Statistical analysis

All data are expressed as the mean ± SD for n = 3 to 6 per group, as detailed

in the Figure Legends. In studies comparing two groups, statistical analysis was performed with the Student's t-test. In studies comparing multiple groups to the same control group, statistical analysis was performed with one-way ANOVA followed by Dunnett's post-test. In studies comparing more than two groups, statistical analysis was performed with one-way ANOVA followed by Newman-Keuls multiple comparison test.

Results

DOX upregulates Mrp1 expression in CM and CF

To examine the effect of DOX on expression of Mrp1, CM and CF were isolated from WT neonatal mouse heart tissue and treated with DOX for 24 h, then expression of Mrp1 analyzed by Real-time PCR and Western blotting. As shown in Figure 3.2, Mrp1 was constitutively present in CM and CF. Moreover, DOX treatment significantly increased both Mrp1 mRNA (Figure 3.2A) and protein expression (Figure 3.2C) in CM in a concentration-dependent manner. A similar pattern was also observed in CF cultures (Figure 3.2B and Figure 3.2D). GAPDH was used as a protein loading control, as the expression of GAPDH did not change with DOX treatment. These results showed that DOX enhanced Mrp1 expression in cultured neonatal mouse CM and CF, implying that this protein could be involved in the cellular response to DOX.

Effect of Mrp1 on DOX-induced caytotoxicity

To characterize the role of Mrp1 in DOX resistance in a cell type specific manner, cytotoxicity of DOX in WT and Mrp1-/- CM and CF was measured by

MTT assay. As shown in Figure 3.3A, after 3 h of DOX treatment following incubation with DOX-free media for another 48 h, 0.3, 1 and 3 μM DOX decreased viability, shown as mean ± SD, to 64±3%, 35±3% and 11±2%, respectively, in Mrp1-/- CM, compared to 75±2%, 52±6% and 25±5% viability in WT ($p < 0.05$). Similar experiments in CF cultures demonstrated again that CF isolated from Mrp1-/- mice showed enhanced DOX toxicity (Figure 3.3B). The expression of Mrp1 was only detected in WT cells but not Mrp1-/ cells. These results indicated that Mrp1 protects both CM and CF against DOX cytotoxicity.

Effect of Mrp1 on DOX-induced cell apoptosis and DNA damage

In order to understand the mechanism of cell death, apoptosis-related proteins were chracterized in WT and Mrp1-/- CM and CF. DOX treatment increased PARP cleavage, caspase3 cleavage, and these increases were significantly greater in Mrp1-/- CM compared to WT CM (Figure 3.4A). Similar results were observed in CF cultures (Figure 3.4B).

The DNA damage was further assessed by quantitating expression of γH2AX. The increased expression of γH2AX was observed at early time points and continuously increased over time (0, 3, 6 and 9 h after treatment with DOX) (Figure 3.5A). Consistent with the results obtained by measure of PARP cleavage and caspase 3 cleavage, γH2AX expression was statistically significantly higher in Mrp1-/- CM compared to WT CM at 24 h after DOX treatment (Figure 3.5B). Similar results were observed in CF cultures (Figure 3.5C and D). These results indicated greater apoptosis and DNA damage in

Mrp1-/- CM and CF following DOX treatment compared with WT cells.

Although no evidence has shown that murine Mrp1 is able to transport DOX, and in our previous study in mouse model, there is no significant difference of DOX concentration between WT and Mrp1-/- mouse heart tissue at 3, 6 12 h after a single intravenous administration of 15 mg/kg DOX (Deng et al, submitted), the intracellular DOX accumulation in WT and Mrp1-/- cells was further examined. As shown in Figure 3.6, there is no significant difference in DOX intracellular retention between genotypes. These data ruled out the possibility of different intracellular DOX accumulation as the cause of the different susceptibility to DOX in WT and Mrp1-/- cells. Because fluorescence was used as the method of detection, fluorescent DOX metabolites may be contributing to the total DOX concentration.

Discussion

DOX is effective in treating a wide variety of cancers, but produces dose-dependent cardiac toxicity. Our group has shown that loss of Mrp1 in C57BL mice potentiates acute DOX treatment induced heart nuclear injuries and chronic DOX treatment-induced cardiac toxicity, including impaired left ventricular systolic function and increased heart apoptosis (Deng et al., submitted; Chapter 2). The key finding in the present study is that deletion of Mrp1 potentiates DOX-induced toxicity in both CM and CF in a dose-dependent manner.

It is well known that the heart is comprised of a syncytium of CM and surrounding nonmyocytes, the majority of which are CF. These two types of cells

are highly interspersed in the myocardium and more and more evidence shows that bidirectional cross talk between CM and CF plays important roles in determining cardiac mechanical and electrical function in both normal and diseased hearts. Therefore, this current study investigated how Mrp1 affects DOX toxicity in these two different cells types.

Mrp1 was consistently expressed in cultured neonatal mice CM and CF, and DOX treatment increased Mrp1 expression in a dose-dependent manner. More importantly, Mrp1-/- cells were more sensitive to DOX-induced cytotoxicity, showing a lower cell survival, higher caspase 3 cleavage, PARP cleavage and higher γH2AX expression. These data clearly demonstrated that Mrp1 protects both CM and CF against DOX toxicity, and also agreed with the results in Chapter 2 showing a cardiac protective function of Mrp1 in the chronic DOX-treated mouse model. However, beyond the apoptosis and DNA damage, it is possible that other mechanisms are involved in the protective effects provided by Mrp1, based on the physiologic function of CM and CF. For example, a large body of evidence shows that beyond the maintenance of normal structure and function of the heart (Souders et al., 2009), CF serve as a source of mitogens, extracellular matrix proteins, growth factors, and cytokines that could affect the phenotype of CM. In addition, crosstalk between CF and CM is important for both cardiac development and remodeling in response to injury (Ottaviano et al., 2011). How Mrp1 could attribute to this communication between CM and CF needs to be further studied.

Transcriptional regulation of Mrp1 upon treatment with DOX has been shown

to involve many transcription factors, including Sp1, antioxidant response element (ARE), and the JNK pathway. Oxidative stress induces nuclear factor-like 2 (Nrf2) translocation from the cytosol to the nucleus and binding with ARE, and finally induce the transcription of Mrp1 and antioxidative genes (Hayashi et al., 2003; Itoh et al., 2003; Nguyen et al., 2005). Our laboratory have shown that upon DOX treatment of mice, Mrp1 expression in sarcolemma increases within 6 h and remains elevated for 24 h (Jungsuwadee et al., 2006). In this study, DOX treatment significantly induced Mrp1 mRNA and protein expression in both CM and CF in a dose-dependent manner. Induction of Nqo1 and HO-1, two typical downstream genes of the Nrf2 pathway, was also observed in CM and CF after DOX treatment (data shown in Chapter 4). These data imply that in CM and CF, Mrp1 expression is increased by the activation of the Nrf2 pathway under DOX-induced oxidative stress.

In summary, the key finding of this *in vitro* study is that loss of Mrp1 potentiates DOX cytotoxicity in CM and CF culture, presenting as more severe apoptosis and DNA damage. It confirms the cardiac protective function of Mrp1 in vivo as shown in Chapter 2. Taken together, these data provide strong evidence indicating that Mrp1 provides protection in CM and CF in the face of DOX cytotoxicity.

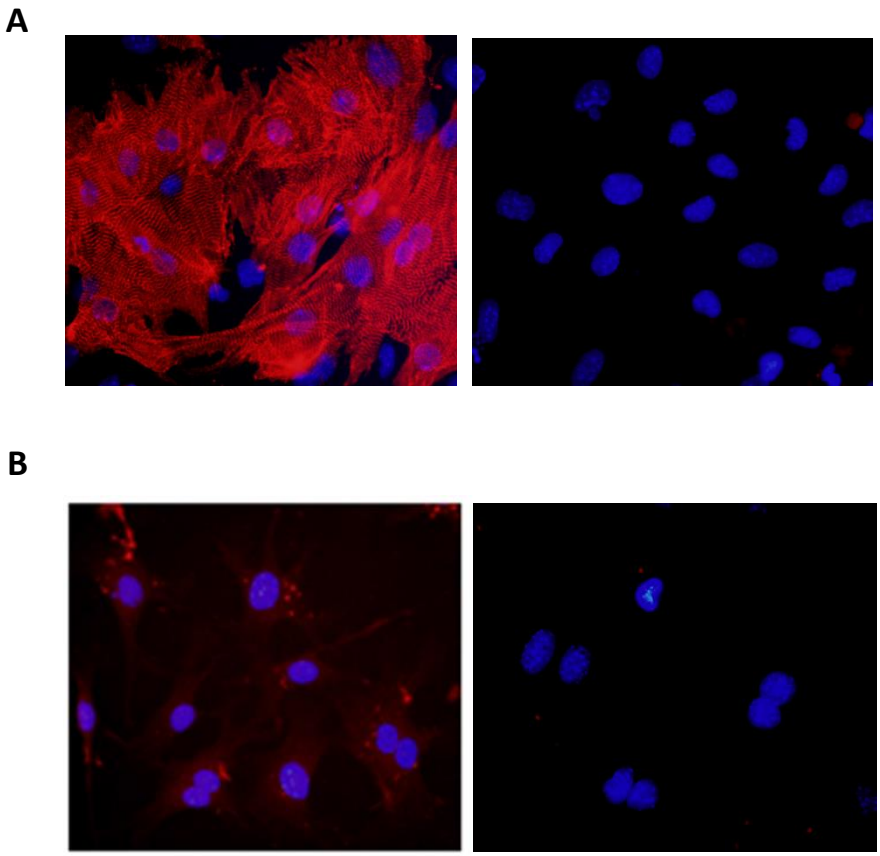

Figure 3.1. Identification of neonatal mouse cardiomyocytes (CM) and neonatal mouse cardiac fibroblasts (CF). (A) Representative immunofluorescent staining for α-actinin (red fluorescence) in CM (A, left). A, right: negative control (use of mouse IgG instead of α-actinin antibody) in CF culture. (B) Representative immunofluorescent staining for anti-vimentin (red fluorescence) in CF (B, left). B, right: negative control (use mouse IgG instead of anti-vimentin antibody) in CF culture. DAPI (4',6-diamidino-2-phenylindole) staining was used to identify individual nuclei.

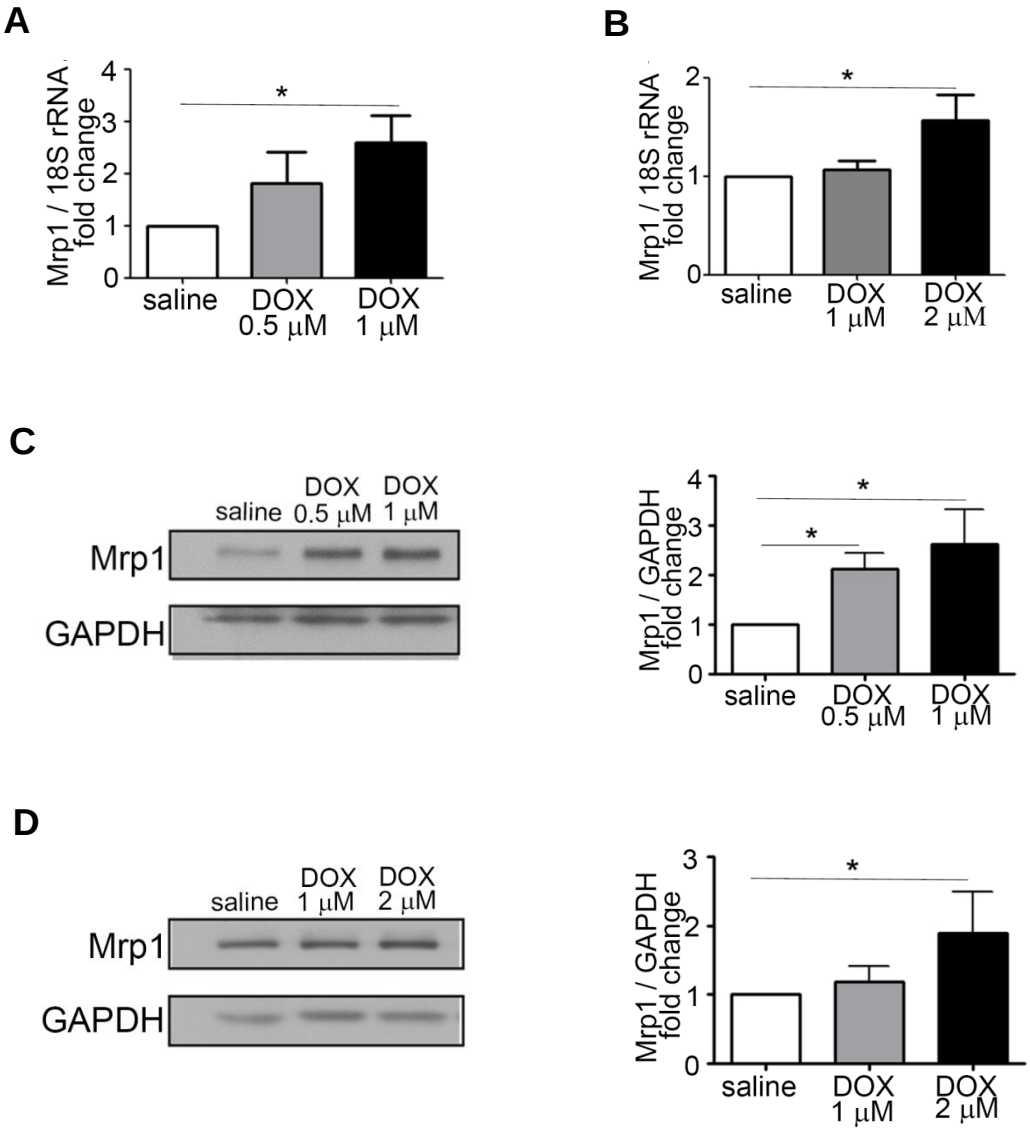

Figure 3.2. DOX increased Mrp1 expression in CM and CF culture. Quantitative analysis of Mrp1 mRNA expression (detected by Real - Time PCR) in CM (A) and CF (B) 24 h after treatment with saline or varying concentrations of DOX. Quantitative analysis of Mrp1 protein expression (detected by Western blot) in CM (C) and CF (D) 24 h after treatment with saline or DOX. The blots are representative of one of 3 independent experiments. Each bar represents the mean ± SD. (*, $p < 0.05$ by Dunnett's post-test after one-way ANOVA)

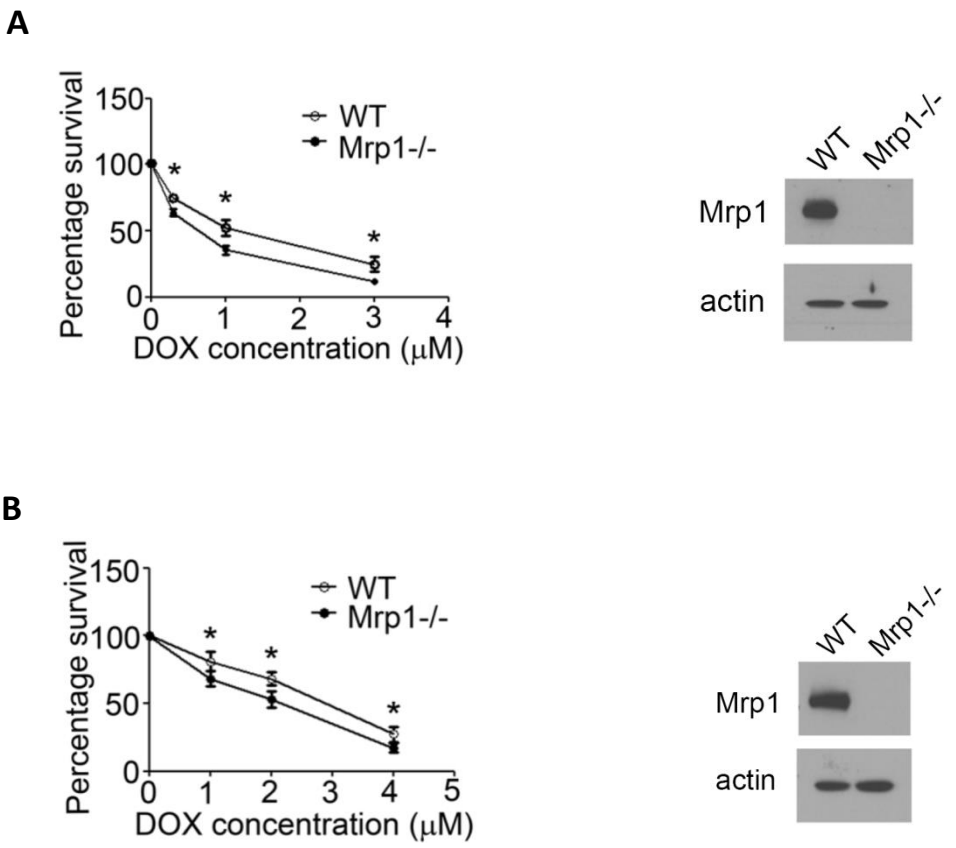

Figure 3.3. Effects of DOX on cell viability in WT and Mrp1-/- cells. CM (A) and CF (B) were cultured on a 96-well plate for 48 h before treatment with varying concentrations of DOX for 3 h, followed by incubation in fresh medium. Tetrazolium reduction was measured 48 h after DOX removal. Each point represents the mean ± SD from 3 independent experiments. Expression of Mrp1 was detected by Western blot in WT and Mrp1-/- CM (A) and CF (B) (*, $p < 0.05$ by Student's t-test)

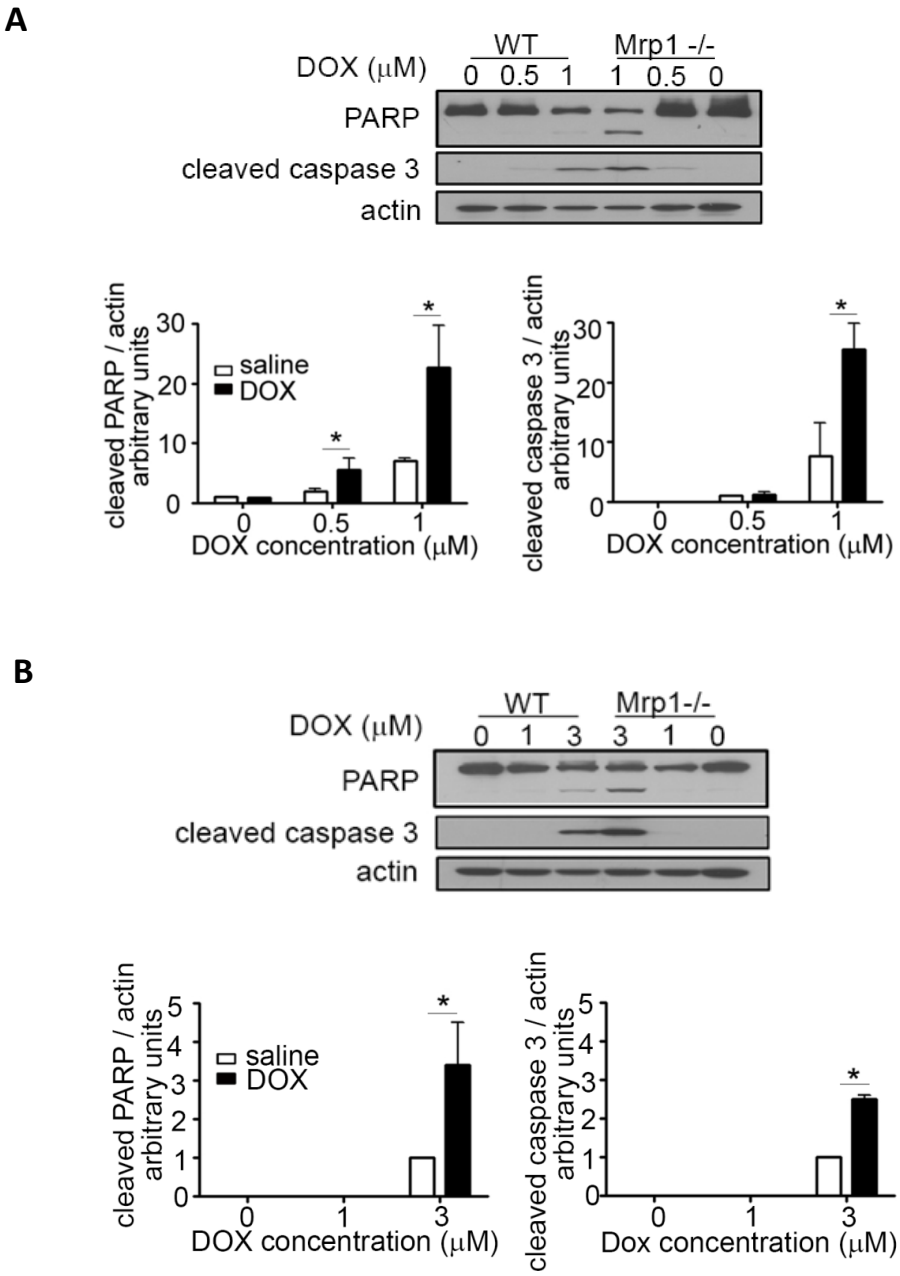

Figure 3.4. Effects of DOX on cell apoptosis in WT and Mrp1-/- cells. The greater increase of cleaved PARP, and cleaved caspase-3 in CM (A) and CF (B) derived from Mrp1-/- mice was detected by Western blot 24 h after DOX removal. The blots are representative of one of 3 independent experiments. Each bar represents the mean ± SD. (*, $p < 0.05$ by Newman-Keuls multiple comparison test after one-way ANOVA)

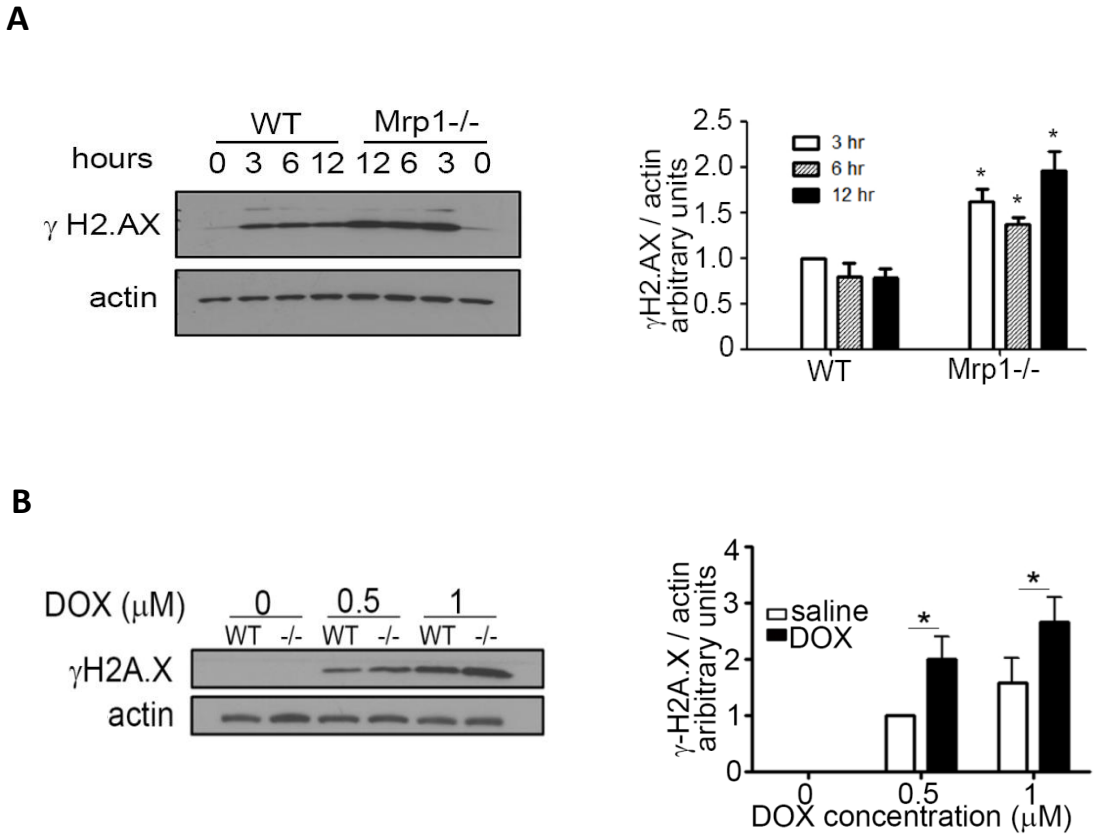

Figure 3.5 A and B. Effects of DOX on DNA damage in WT and Mrp1-/- CM. The greater increase of γH2A.X in CM derived from Mrp1-/- mice was detected by Western blot 0 h, 3 h, 6 h, 12 h (A) and 24 h (B) after DOX removal. The blots are representative of one of 3 independent experiments. Each bar represents the mean ± SD. (*, $p < 0.05$ by Newman-Keuls multiple comparison test after one-way ANOVA).

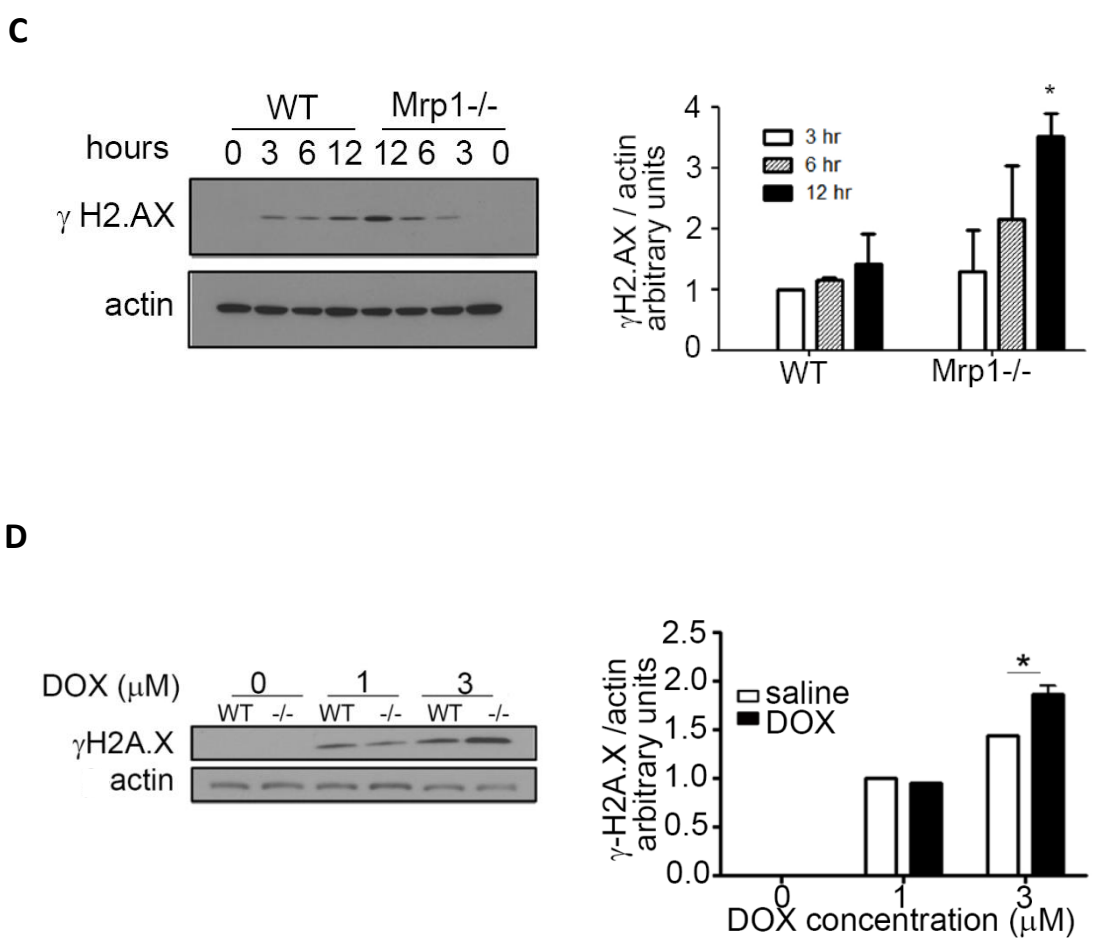

Figure 3.5 C and D. Effects of DOX on DNA damage in WT and Mrp1-/- CF. The greater increase of γH2A.X in CF derived from Mrp1-/- mice was detected by Western blot 0 h, 3 h, 6 h, 12 h (C) and 24 h (D) after DOX removal. The blots are representative of one of 3 independent experiments. Each bar represents the mean ± SD. (*, $p < 0.05$ by Newman-Keuls multiple comparison test after one-way ANOVA).

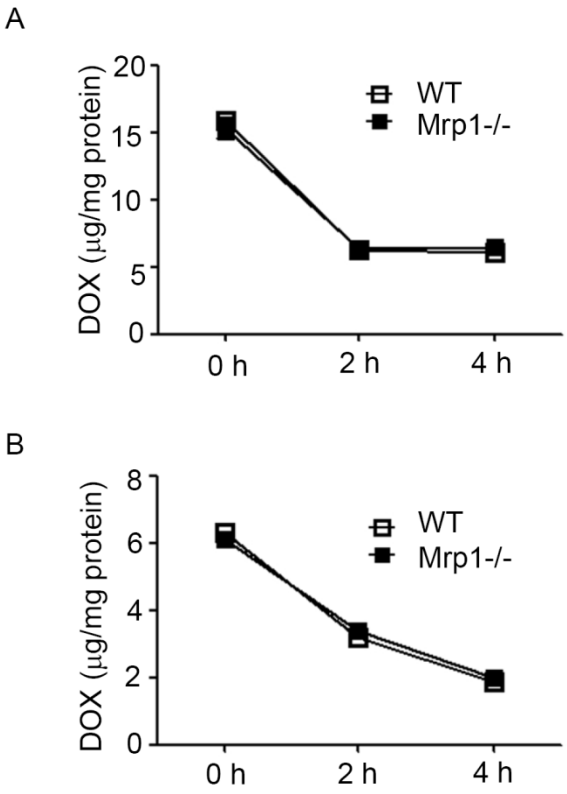

Figure 3.6. Accumulation of DOX in WT and Mrp1-/- CM and CF. Cells were treated with 30 μM DOX. Following 1 h of incubation, cells were washed three times with PBS and incubated with fresh DMEM medium for the indicated times. Finally, the cells were washed three times with PBS and incubated in acidified (0.75 N HCl) isopropanol with 1% Triton X-100 and shaken for 30 min at room temperature. The absorbance of the supernatant was read using a fluorescence spectrofluorometer at wavelengths of Ex=470 nm and Em=590 nm. The value of DOX accumulation within the cells was calculated according to the standard curve. Each point represents the mean ± SD (n = 3).

Chapter Four

Mechanisms of Mrp1's cardiac protective function

Overview of Study

The data presented in Chapter 2 demonstrated that the loss of Mrp1 potentiates DOX-induced cardiac dysfunction in mice. Chapter 3 further revealed the protective role of Mrp1 against DOX toxicity in two major cell components of heart tissue: cardiomyocytes and cardiac fibroblasts. This chapter explores the mechanisms involved in Mrp1's protection against DOX toxicity.

In the present study, GSH and GSSG levels were measured to evaluate the redox status in chronic DOX-treated mouse heart and CM/CF culture. Expression of GSH synthesis enzymes was measured to examine the possible mechanisms responsible for the changes in GSH levels. The GS-HNE levels in mouse heart were also assessed by LC/MS/MS. The protein oxidative damage in CM and CF culture were also measured, including protein carbonyl, HNE-protein adducts and 3 nitrotyrosine-protein adducts. Multiple antioxidant enzymes expression levels were also examined. The results showed that loss of Mrp1 caused increased GSH and GSSG levels in untreated or saline treated mouse heart and in CM/CF culture. Following 0.5 μM DOX treatment, Mrp1-/- CM showed increased GSH (1.7±0.3-fold) and GSSG (1.8±0.2-fold) levels relative to WT CM ($p < 0.05$), however the redox potential (*Eh*) of the GSH/GSSG pool was not changed. Similar effects were observed in CF. The increased GSH

pool after DOX treatment in Mrp1-/- cells is at least partially due to the increased GSH synthesis since DOX increased mRNA and protein expression of the rate-limiting GSH synthesis enzymes glutamate-cysteine ligase catalytic (GCLc) and glutamate-cysteine ligase regulatory subunits (GCLm) in Mrp1-/- but not WT cells. DOX treatment increased GS-HNE levels in mouse heart, but without an obvious difference between genotypes. Finally, expression of extracellular superoxide dismutase (ECSOD/SOD3) was lower in Mrp1-/- CM vs. WT CM treated with either saline (62±8% of WT) or DOX (43±12% of WT) ($p < 0.05$). Taken together, these data clearly showed that Mrp1 affected the intracellular GSH and GSSG levels in mouse heart tissue as well as in the CM and CF culture. In treatment-naïve Mrp1-/- mouse heart and cells, the higher GSH level is likely due to the loss of efflux mediated by Mrp1. But with DOX treatment, the further increase of the GSH pool in Mrp1-/- CM and CF involves the activation of the Nfr2 pathway and increased GSH synthesis. Unlike our hypothesis, loss of Mrp1 does not affect the intracellular level of GS-HNE in DOX treated mouse heart, implying that complex compensatory effects occur.

Introduction

GSH is the most abundant cellular non-protein thiol and is a critical factor responsible for the maintenance of cellular redox balance under oxidative stress. In the presence of ROS, GSH is rapidly oxidized to GSSG, resulting in a decreased intracellular GSH/GSSG ratio, an indicator of oxidative stress. Maintenance of GSH homeostasis plays a vital role in a multitude of cellular

processes, including drug and free radical detoxification, cell differentiation, proliferation and apoptosis (Jones, 2008). Mrp1-/- mice have increased basal levels of GSH due to the decreased Mrp1-mediated efflux, while overexpression of Mrp1 decreases intracellular levels of GSH (Cole et al., 1990; Rappa et al., 1997). Our previous study showed that the treatment-naïve Mrp1-/- mouse heart has a significantly higher GSH level compared to WT mice. In addition, Mrp1 also mediates the efflux of GSSG so that loss of Mrp1 could potentially disrupt the balance of the GSH/GSSG redox couple, impairing a normal tissue's ability to protect itself against oxidative stress-induced injury.

HNE is an α, β-unsaturated aldehyde derived from peroxidation of ω-6 polyunsaturated fatty acids, and a toxic product of lipid peroxidation (Esterbauer et al. 1991; Butterfield and Stadtman 1997). It is partially detoxified by conjugation with GSH, either spontaneously or through GSH-S-transferase (GST) to form GS-HNE, which must be effluxed to alleviate intracellular toxicity (Volkel et al., 2005). Our laboratory had previously reported that mutant MRP1 Gly671Val impairs MRP1's ability to efflux GS-HNE by more than 80% (Jungsuwadee et al., 2012). Also, the HEK cells that overexpress this mutant MRP1 (Gly671Val) are more sensitive to DOX toxicity relative to cells expressing wild-type MRP1. Furthermore, HNE adducted protein is increased in mouse heart after DOX treatment and sarcolemmal membrane vesicles from Mrp1-/- mouse are unable to transport GS-HNE, indicating that Mrp1 is the only ATP dependent efflux transporter present in the mouse heart (Jungsuwadee et al., 2006).

Aerobic organisms possess antioxidant defense systems to protect cells from the damage caused by ROS. Superoxide dismutase (SOD) and catalase are two important antioxidant enzymes which remove $\bullet O_2^-$ and H_2O_2, respectively and maintain the normal redox status in cells. Thus, the regulations of these genes at both expression and activity levels play pivotal roles in balancing the concentration of ROS. SOD converts two $\bullet O_2^-$ into one molecule of H_2O_2 and one molecule of O_2, while catalase further catalyzes the decomposition of H_2O_2 into H_2O and O_2. In mammals, three distinct isoforms of SOD have been identified and characterized: copper-zinc superoxide dismutase (Cu,ZnSOD/SOD1), manganese superoxide dismutase (MnSOD/SOD2) and extracellular superoxide dismutase (ECSOD/SOD3). Three forms of SOD convert $\bullet O_2^-$ into H_2O_2, but have distinct protein structures, metal cofactor requirements, and intracellular localizations (Miao and St Clair, 2009). Cu,ZnSOD is localized mainly in cytoplasm and nucleus, while MnSOD resides in the mitochondrial matrix. The physiological role of MnSOD has been demonstrated in that MnSOD knockout mice died shortly after birth with dilated cardiomyopathy and neurodegeneration (Li et al., 1995; Lebovitz et al., 1996). Further, overexpression of MnSOD in mice protects heart against DOX-induced cardiotoxicity (Yen at el., 1996; Yen at el., 1999). ECSOD is a copper- and zinc-containing dismutase and it is the only isoform of SOD responsible for scavenging $\bullet O_2^-$ in the extracellular environment. It is a glycosylated homotetrameric enzyme (155 kDa) that is secreted from cells to bind heparin sulfate proteoglycans on the cell surface and in the extracellular matrix. There,

ECSOD converts $\bullet O_2^-$ into less toxic H_2O_2. In addition, ECSOD plays a key role in preserving the bioavailability of nitric oxide by protecting it against destruction by $\bullet O_2^-$ and formation of highly toxic peroxynitrite. Despite their effects on maintaining the normal redox status, antioxidant enzymes are also regulated by oxidative stress at both the expression level and activity level (Li and Singal, 2000; Franco et al., 1999).

GSH, GSSG and GS-HNE are substrates of Mrp1, and they are either related to redox status regulation or are toxic oxidative stress products themselves. Thus, we expected that Mrp1 plays an important role in oxidative stress regulation. In this chapter, experiments were conducted to explore how Mrp1 affects GSH, GSSG, and GS-HNE intracellular levels as well as expression of other antioxidant enzymes.

Materials and methods

Measurement of GS-HNE in mouse heart by LC-MS/MS

Heart ventricle (50 mg tissue), prepared by removal of the atrium and attached fat tissue and vessels, was homogenized in 400 µL of distilled water followed by addition of 50 µL of 1 µM d^3-GS-HNE. The chemical purity of d^3-GS-HNE was determined by LC-MS. Proteins were precipitated from heart homogenate by adding 1600 µL of ice-cold acetonitrile followed by vortexing for 5 min and centrifugation at 4000 rpm for 10 min. The supernatant was transferred to a 4 mL glass vial and dried under N_2. The dried samples were reconstituted in 100 µL of acetonitrile:H_2O (50:50), vortexed and let stand at room temperature

for 10 min, and centrifuged at 15000 rpm for 5 min. The supernatants were then transferred to autosampler vials. Analysis of GS-HNE was carried out using a Shimadzu High performance Liquid Chromatograph coupled with an AB Sciex 4000-Qtrap hybrid linear ion trap triple quadrupole mass spectrometer (MS) operated in multiple reaction monitoring (MRM) mode. The samples were separated on a Machery-Nagel Nucleodur C8 Gravity column (2.0 mm×125 mm, 5 µm) by gradient elution with 0.05% formic acid in water (solvent A) and acetonitrile: water (95:5) containing 0.05% formic acid (solvent B) according to the following program: 100% solvent A for the first 1 min, then linear to 100% solvent B over the next 3 min, and maintained at 100% B for the last 2 min. The column was equilibrated back to the initial conditions within 3 min. The flow rate was 0.5 mL/min with a column temperature of 30°C. The sample injection volume was 10 µL. The MS was operated in the positive electrospray ionization mode with optimal ion source settings with a declustering potential of 71 V, entrance potential of 10 V, collision energy of 21 V, collision cell exit potential of 8 V, curtain gas of 20 psi, ion spray voltage of 5500 V, ion source gas1/gas2 of 40 psi and temperature of 550°C. MRM transitions monitored were as follows: 464.2/308 and 464.2/446. d^3-GS-HNE was used as an internal standard for quantitation of GS-HNE with the following MRM ion transitions: 467.2/308.1 and 467.2/449. Both pairs of fragments gave very similar quantitative results and data presented in this dissertation are based on the fragments 464.2/446.

Heart ventricle homogenate

The heart ventricle was prepared by removal of the atrium and attached fat tissue and vessels, and then homogenized in 10 volumes of ice-cold buffer consisting of 0.225 M mannitol, 0.075 M sucrose, 1 mM EGTA, and protease inhibitors (1 mM phenylmethyl sulfonyl fluoride, 1 μg/mL leupeptin, 1μg/mL aprotinin, and 1 μg/mL pepstatin). The protein concentrations of heart ventricle homogenates were determined with the bicinchoninic acid (BCA) protein assay.

HPLC assay of GSH and GSSG

For animal study, heart ventricle homogenate prepared as above was used for GSH derivatization and quantification of GSH and GSSG. For cell culture study, CM (10^6 cells) or CF (3 X 10^5 cells) were plated and cultured on 6 well plates overnight and treated with 0.5 μM or 1 μM DOX for 3 h, and 24 h later, cells were scraped off and lysed with RIPA buffer. The cell lysate was used for GSH derivatization and quantification of GSH and GSSG. For GSH measurement, the supernatant was added to redox quenching buffer (20 mM HCl, 5 mM diethylenetriaminepentaacetic acid, and 10 mM ascorbic acid) and then mixed with monobromobimane (MBB; prepared in HPLC-grade acetonitrile) derivatization buffer to yield final concentrations of 30 mM NaOH, 250 mM diethylenetriaminepenta acetic acid, and 2.5 mM MBB (Senft et al, 2000). Derivatization of GSH with MBB was carried out at 45°C for 15 min and the reaction stopped by addition of 0.6 N HCl. GSSG was derivatized by the same method following pretreatment of the heart homogenate with 0.5 mM N-

ethylmaleimide to conjugate free GSH and reduction of GSSG to GSH by addition of 5 mM dithiothreitol. The MBB-derivatized samples were centrifuged and the supernatants assayed for thiol-bimane fluorescence by HPLC using a linear gradient from 0-100% solvent B (50% methanol and 0.25% acetic acid in water) in solvent A (10% methanol and 0.25% acetic acid in water) within 28 min at a flow rate of 0.8 mL/min with fluorescence detection at Ex_{370}/Em_{485}, detected with the Waters 2475 Multi λ fluorescence detector as described (Senft et al., 2000). Fluorescence intensities versus time of elution were quantified using Waters Breeze chromatography software v.3.2 (Waters Corporation, Milford, USA) and peak areas were integrated and converted to nmol equivalents according to the GSH standard curve.

The redox potential (*Eh*) of the GSH/GSSG pool was determined in CM and CF culture. It was calculated using the estimated cellular GSH and GSSG concentrations and the Nernst equation: $Eh = Eo + (RT/nF)\ \ln([GSSG]/[GSH]^2)$. To estimate cellular concentrations, 1 mg of cell protein was assumed to be associated with 5 µl of cell volume (Mannery et al., 2010). R is the gas constant, T is temperature, n is the number of electrons transferred, F is the faraday constant, and *Eo* = - 264 mV at a pH of 7.4.

Immunoblot Assay

Immunoblot assays were conducted as described in Chapter 3. Antibodies were obtained as follows: rabbit anti-GCLc pAb (ab80841), rabbit anti-GCLm pAb (ab8144), and Rabbit anti-Nqo1 pAb(ab34173) from Abcam (Cambridge, MA),

mouse anti-catalase mAb (sc-271803), rabbit anti-Cu,Zn superoxide dismutase (Cu,ZnSOD) pAb (sc-11407) from Santa Cruz Biotechnology (Santa Cruz, CA), rabbit anti-Mn superoxide dismutase (MnSOD) pAb from Upstate (Lake Placid, NY). Rabbit anti-ECSOD pAb was a generous gift from Dr. Ladislav Dory, University of North Texas.

Slot blot assay

CM and CF cell pellets were sonicated in a lysis buffer (0.32 Sucrose, 2mM EDTA, 2mM EGTA; 20mM HEPES) containing the protease inhibitors leupeptin (4 µg/mL), pepstatin (4 µg/mL), aprotinin (5 µg/mL), and PMSF (0.2 mM) with pH 7.4 (measured at room temperature). Small amounts of homogenates (3 uL) were used to determine the total protein concentration by the BCA method (Pierce, Rockford, IL). For protein carbonyl determination, samples were derivatized with 2,4- dinitrophenylhydrazine (DNPH). For protein-bound HNE and 3-NT, 3 uL of the homogenized sample was mixed and diluted with an equal volume of 12% SDS. Samples were further denatured with 10 µL of modified Laemmli buffer (0.125 M Trizma base, 4% SDS, and 20% glycerol) for 20 min at room temperature. Next, 250 ng of the derivatized protein was loaded in each slot (48-well slot format Bio-Dot SF apparatus with nitrocellulose membranes, pore size 0.45 µm, Bio-Rad, Hercules, CA, USA). The membranes were incubated with primary antibodies anti-3-NT pAb (from Life Technologies, Carlsbad, USA; dilution 1:2500), anti-protein-bound HNE pAb (from Alpha Diagnostic International, San Antonio, TX, USA; dilution 1: 500) or polyclonal

RbxDNP (from OxyBlot Protein Oxidation Detection Kit, Chemicon-Millipore, Billerica, MA, USA, dilution1:200) and goat 1:7500 anti-rabbit IgG (Sigma–Aldrich) antibody for the secondary detection. The antibody reaction was developed using 5-bromo-4-chloro-3-indolyl phosphate in conjunction with nitroblue tetrazolium. The nitrocellulose membranes were dried overnight and scanned by photo scanner (Epson Perfection V600, Long Beach, CA, USA), and slot-blot line densities were quantified by the ImageQuant TL software package (GE Healthcare Bio-Sciences, Piscataway, NJ, USA).

RNA extraction and real-time quantitative PCR (qRT-PCR)

Total RNA extraction, cDNA preparation and qRT-PCR were conducted as described in Chapter 2. The sequence of primers and Universal ProbeLibrary probe for specific genes are shown in Table 4.1.

Statistical analysis

All data are expressed as the mean ± SD or mean ± SE for n = 3 to 6 per group, as detailed in the Figure Legends. In studies comparing two groups, statistical analysis was performed with the Student's t-test. In studies comparing multiple groups to the same control group, statistical analysis was performed with one-way ANOVA followed by Dunnett's post-test. In studies comparing more than two groups, statistical analysis was performed with one-way ANOVA followed by Newman-Keuls multiple comparison test.

Results

DOX treatment increases GS-HNE level in mouse heart tissue

DOX initiates ROS and causes lipid peroxidation, while HNE is the one of the major toxic lipid metabolites. The highly electrophilic HNE reacts rapidly with nucleophiles, particularly GSH, to form GS-HNE, which is a substrate of Mrp1. Here, the retention of GS-HNE was characterized in WT and Mrp1-/- mouse heart tissue following chronic DOX treatment (2 mg/kg). As shown in Figure 4.1, chronic DOX treatment increased GS-HNE levels in WT and Mrp1-/- mouse heart at 48 h (Figure 4.1A) and 2 weeks (Figure 4.1B) after the last DOX treatment. The increase was statistically significant only at 2 weeks, but not 48 h after the last DOX treatment. However, in contrast to our expectations, there was no significant difference in GS-HNE levels between genotypes.

GSH and GSSG levels in mouse heart tissue

As GSH and GSSG are known substrates for Mrp1, we investigated whether loss of Mrp1 would alter GSH and GSSG levels in the cell, and therefore disrupt the balance of the GSH/GSSG redox couple. In the *in vivo* study, GSH and GSSG level were examined in mouse heart 48 h and 2 weeks after the last dose of DOX in the chronic treatment. DOX treatment significantly decreased both GSH and the GSH/GSSG ratio at 48 h, indicating DOX-induced oxidative stress (Figure 4.2A). GSH and GSH/GSSG returned to control levels two weeks later, at the end of the recovery period (Figure 4.2B). Although there was no significant difference in the GSH/GSSG ratio between WT and Mrp1-/- mice at

either time point, it is interesting to note the significantly higher basal (saline treatment) levels of GSH and GSSG in Mrp1-/- compared to WT mouse heart. GSSG levels were also significantly increased in Mrp1-/- vs WT mice following DOX treatment at both time points. This observation is consistent with the function of Mrp1 to efflux GSH and GSSG.

GSH and GSSG measurement in CM and CF

The intracellular GSH and GSSG levels in CM and CF culture were also assessed. Consistent with our findings in treatment-naïve and saline-treated mice, untreated CM and CF derived from Mrp1-/- mice had significantly higher GSH and GSSG levels compared to WT cells (Figure 4.3). However, no difference in the GSH/GSSG ratio was observed between genotypes. This question was further investigated in DOX treated cells. In preliminary studies, the time course of the changes in GSH and GSSG in cells following DOX treatment was examined. CM were treated with saline or DOX, and intracellular GSH and GSSG examined at various times over 24 h. As shown in Figure 4.4, the GSH level decreased and the GSSG level increased rapidly in both WT and Mrp1-/- CM within 15 min after addition of DOX. Over the next 24 h, GSH and GSSG levels gradually returned to basal levels in WT CM. However, GSH and GSSG levels continuously increased and remained at a higher level in Mrp1-/- cells. Subsequent studies characterized GSH and GSSG levels at the 15 min, 30 min and 24 h time points after treatment with DOX. At 15 min and 30 min after DOX treatment, GSH levels decreased and GSSG levels increased in both

WT and Mrp1-/- CMs. Thus, the GSH/GSSG ratio (Figure 4.5A) of the GSH/GSSG pool decreased and the redox potential (*Eh*) (Table 4.2) became less negative in DOX treated cells. However, GSH and GSSG levels in Mrp1-/- cells were significantly increased 24 h after DOX treatment, but were not different in WT cells (Figure 4.6A). As a consequence, the GSH/GSSG ratio and the redox potential (*Eh*) of the GSH/GSSG pool did not change in either genotype with either treatment (Table 4.3). Similar effects were observed in CF cultures (Figure 4.5B and 4.6B).

Expression of GSH biosynthesis enzymes

The increase in GSH levels after DOX treatment in Mrp1-/- cells could be due to decreased GSH efflux, increased GSH biosynthesis or increased recycling from GSSG. Thus, the mRNA and protein expression levels of GSH biosynthesis enzymes and GSH reductase (GR) were examined. As shown in Figure 4.7A, DOX treatment significantly increased both mRNA and protein expression of GCLc, GCLm, and glutathione synthetase (GSS) at 24 h in Mrp1-/- CM, but had no effects in WT CM. DOX treatment had no effect on GR protein expression in either genotype (data not shown). Similar results were observed in CF (Figure 4.7B). These data indicate that the higher level of GSH in DOX treated Mrp1-/- cells could be at least partly due to the increased expression of GSH biosynthesis enzymes, and a subsequent higher rate of GSH synthesis.

Protein expression of antioxidant enzymes

The expression of important antioxidant enzymes were exmined, and showed that in both CM and CF, DOX slightly increased protein expression of catalase, Cu,ZnSOD and MnSOD in both genotypes, but these changes were not statistically significant (Figure 4.8). However, the mRNA and protein expression of SOD3 was decreased in Mrp1-/- CM compared to WT CM after saline treatment (64 ± 2% of WT mRNA level, $p < 0.05$, 62 ± 8% of WT protein level, $p < 0.05$) (Figure 4.9A). DOX treatment significantly decreased the expression of SOD3 in both WT and Mrp1-/- CM, such that SOD3 expression was still lower in Mrp1-/- CM (46 ± 5% of WT mRNA level, $p < 0.05$, 43 ± 12 % of WT protein level, $p < 0.05$). Interestingly, this difference in SOD3 between genotypes was not observed in CF (Figure 4.9B). The mRNA expression of glutathione peroxidase (Gpx), glutathione S-transferase (GST) and NAD(P)H dehydrogenase, quinone 1 (NQO1), heme oxygenase 1 (HO-1) were also detected and DOX increased expression of GPx1, GPx3, GSTM1 and GSTM2 in both WT and Mrp1-/- CM and CF, but there was no difference between genotypes (Figure 4.10). However, mRNA and protein expression of Nqo1 was higher and HO-1 mRNA expression was significantly elevated in Mrp1-/- vs WT CM and CF after DOX treatment (Figure 4.11).

Protein oxidative damage in DOX treated CM and CF

Protein oxidative damages in CM and CF were also detected culture including HNE-protein adducts, 3 nitrotyrosine-protein adducts and protein carbonyl levels.

Although we expected that the oxidative stress induced by DOX would increase these measures of protein oxidative damages, within 30 min after the DOX treatment, these protein oxidative damage markers just slightly increased in DOX treated cell culture in both genotype. However, these increases were not statistically significant. There was no obvious difference observed between WT and Mrp1-/- cells (Figure 4.12). Similar results were obtained in samples collected 24 h after DOX treatment.

Discussion

Changes in HNE formation and GSH/GSSG homeostasis are two important consequences of oxidative stress. Since GS-HNE, GSH and GSSG are all substrates of Mrp1, we hypothesized that loss of Mrp1 would change the efflux of these molecules and potentially cause abnormal cellular responses to oxidative stress. This chapter explores the effects of Mrp1 on redox status in mouse heart as well as in CM and CF culture. Measurements conducted included levels of intracellular GS-HNE, GSH and GSSG as well as expression of antioxidant enzymes and protein oxidative damage.

An increase in HNE and HNE adducted protein are detected in heart tissues as early as 3 hr following DOX administration (Luo et al., 1997; Liu and Tan, 2003; Chaiswing et al., 2004). Further, sarcolemmal membrane vesicles from Mrp1-/- mouse are unable to transport GS-HNE, indicating that Mrp1 is the only ATP dependent efflux transporter of GS-HNE in the mouse heart (Jungsuwadee et al., 2006; Jungsuwadee et al., 2012). Here, chronic DOX treatment increased

GS-HNE in the mouse heart, indicating that DOX-induced oxidative stress. It was anticipated that the loss of Mrp1 would eliminate the efflux of GS-HNE and cause its intracellular accumulation. However, there was no significant difference in the GS-HNE concentration between WT and Mrp1-/- mice heart. These data imply a complex adaptation in Mrp1-/- mice. To protect macromolecules from modification or adduction by HNE, mammalian cells metabolize HNE rapidly. In addition to conjugation with GSH to yield GS-HNE, HNE metabolism includes reduction to the corresponding alcohol, 1,4-dihydroxy-2-nonene (DHN) or oxidation to the corresponding acid, 4-hydroxy-2-nonenoic acid (HNA) (Alary et al., 2003; Volkel et al, 2005). The loss of GS-HNE efflux may saturate these metabolic pathways, but can also lead to metabolism of GS-HNE via an NADH-dependent alcohol dehydrogenase (ADH)-catalyzed reduction to GS-DHN and/or aldehyde dehydrogenase-catalyzed oxidation to GS-HNA. The biological activities of these GSH conjugates are not yet well characterized nor has their cellular efflux by Mrp1 been described (Dalleau et al., 2013; Frohnert and Bernlohr, 2014). We did not measure these additional HNE metabolic products, thus we cannot conclude whether loss of Mrp1 alters HNE metabolism in mouse heart.

One of the mechanisms whereby cells maintain their redox status is by maintaining the GSH/GSSG ratio. Since Mrp1 can transport both GSH and GSSG, we hypothesized that loss of Mrp1 would disrupt the GSH/GSSG balance. In our chronic treatment mouse model, GSH and the GSH/GSSG ratio decreased at 48 h after the last dose of DOX. In CM and CF culture, GSH and the

GSH/GSSG ratio decreased very quickly, within 15 min of DOX addition. Although as an indicator of intracellular oxidative stress, the GSH/GSSG ratio was similar between WT and Mrp1-/- mice heart and cell culture, the GSH and GSSH levels were always higher in Mrp1-/- mice hearts and Mrp1-/- cells compared to WT. This is consistent with our previous finding that treatment-naïve Mrp1-/- mice heart had significantly higher GSH compared to WT mice, as well as to other group's finding regarding the effects of Mrp1 on the intracellular GSH level.

A major determinant of cellular GSH homeostasis is GCL, which catalyzes the first and rate-limiting step in de novo synthesis of GSH from glutamate and cysteine. Its activity is controlled by a complex regulation at several levels, including transcriptional activation by oxidative stress, reversible formation of a disulfide bond between its two subunits (GCLc and GCLm), and the feedback inhibition by GSH (Richman et al., 1975; Huang et al., 1993; Fraser et al., 2003; Franklin et al., 2009). in this study, even in the absence of a significant difference in GCLc and GCLm expression, the treatment-naïve Mrp1-/- mice heart and saline treated Mrp1-/- cells exhibited higher GSH compared to WT mice heart and cells. These data indicate the important role of Mrp1-mediated efflux in intracellular GSH regulation. Although it is known that GCL activity is feedback-inhibited by GSH, we did not measure GCL activity so do not know the extent of feedback inhibition in treatment-naïve Mrp1-/- cells. We also found that DOX increased concentrations of GSH and GSSG in Mrp1-/- cells but not WT cells; however, the redox potential (*Eh*) of the GSH/GSSG pool was similar

between genotypes. To test whether this increased GSH pool was due to increased GSH synthesis, the expression of GSH synthesis enzymes GCLc, GCLm and GSS were examined. After DOX treatment, Mrp1-/- cells have significantly higher expression of GCLc and GCLm at both mRNA and protein levels compared to WT cells. The expression of GCLc, GCLm and GSS are all known to respond to oxidative stress and all three genes are upregulated by Nrf2 pathway activation at the transcription level. In this study, the expression of NQO1 and HO-1, two typical downstream genes of the Nrf2 pathway, were significantly higher in DOX treated Mrp1-/- cells vs WT cells. These data indicated that the greater Nrf2 pathway activation caused increased expression of GCLc and GCLm in Mrp1-/- cells. We did not measure GCL activity in DOX treated cells, and we do not know whether enzyme activity was inhibited by the high level of GSH in Mrp1-/- cells. We speculate that such feedback inhibition occurred, but was not sufficient to decrease the overall GSH synthesis rate because of the enhanced expression of the GCL enzymes which were upregulated at the transcription level. Thus, the feedback inhibition of GCL activity by GSH is not the major determinant of GSH levels in DOX treated Mrp1-/- cells. Taken together, these results suggest that despite comparable *Eh* for GSH/GSSG in WT and Mrp-/- cells, the oxidative stress Mrp1-/- cells suffer stimulates the Nrf2 signaling pathway, causing the upregulation of the GSH synthesis enzymes at the transcriptional level. Importantly, the higher intracellular GSH level and the increase of GCLc and GCLm expression still cannot protect the Mrp1-/- cell from DOX-induced cytotoxicity.

Recently, an emerging concept, reductive stress, may provide some clue regarding why the higher GSH level could not rescue Mrp1-/- cells from DOX toxicity (Narasimhan et al., 2015). There are increasing examples of excessive amounts of reducing equivalents, in the forms of NAD(P)H and/or GSH, resulting in cellular dysfunction and cardiac disease (Narasimhan et al., 2015, Brewer et al., 2012). Zhang et al. (2010) reported that overexpression of heat shock protein HSP2 leads to an increased ratio of GSH/GSSG, and a decrease of ROS, yet resulted in cardiomyopathy. The human mutant αB-crystallin overexpression mouse model characterized by Rajasekaran et al. (2007; 2011) shows sustained activation of the Nrf2 signaling pathway, increases in GSH and the GSH/GSSG ratio, and hypertrophic cardiomyopathy. Involvement of reductive stress is further demonstrated by the fact that quenching of reducing power rescued the mice from heart failure (Rajasekaran et al., 2007; Rajasekaran et al., 2011). The more recent study indicates that GSH-induced reductive stress is causally linked to mitochondrial oxidation and cytotoxicity, with the mechanism not fully understood (Zhang et al., 2012). In our study, compared to WT cells, Mrp1-/- cells had significantly higher GSH and GSSG after saline treatment and even higher after DOX treatment. This is a little surprising since we expected the change of GSH and GSSG level elicited by DOX would return to pretreatment levels after the appropriate antioxidant cellular response had taken effect. However, we saw sustained activation of Nrf2 signaling and upregulation of GSH synthesis enzymes in DOX treated Mrp1-/- cells. We postulate that in DOX-treated Mrp1-/- cells, the normal redox signaling activation and compensatory

responsiveness are disrupted and lead to cytotoxic consequences. However, we did not observe any structural or functional tissue injury in saline treated Mrp1-/- mice heart (Deng et al., submitted). Thus, it is unlikely that reductive stress is a major contributor to the observed cardiac injury after DOX. Other measurements, including NADPH/NADP, a battery of antioxidant enzymes and oxidative stress markers, need to be assessed before making any conclusions regarding the role of reductive stress in Mrp1-/- mice heart.

In this study, we did not measure the extracellular GSH concentration, which may serve to protect the interstitium from oxidants. If the loss of Mrp1 impairs GSH efflux, loss of extracellular GSH may also accelerate oxidative damage in the extracellular environment. In addition, the extracellular GSH can be broken down in the extracellular space by γGT and dipeptidase, thus producing cysteine. The lower extracellular GSH concentration could affect the cysteine/cystine balance, which is also critical for maintaining extracellular redox status (Levonen et al., 2004). For example, extracellular GSH has been shown to offer neuroprotection against methyl mercury toxicity in a manner dependent on MRP1-mediated efflux (Rush et al. 2012). To test the importance of extracellular GSH in CM and CF culture, exogenous non-cell penetrable GSH was added in the medium and compared the cell survival following DOX treatment. The exogenous GSH reduced the cell death in WT and Mrp1-/- cells, with 10 mM GSH eliminating the difference of cell viability between WT and Mrp1-/- cells (Figure 4.10). This means that the lower GSH in the extracellular environment could contribute to the DOX sensitivity in Mrp1-/- cells.

Furthermore, the significance of GSSG, which is also transported by MRP1, cannot be overlooked, given its cytotoxicity. The increased intracellular GSSG concentration by microinjection or inhibition of the efflux through Mrp1 has been shown to cause glutathionylation of cysteine-containing proteins, resulting in damaged protein function, finally causing cell death (Park et al., 2009). Whether this could happen in Mrp1-/- mouse heart is not known. All these possibilities need to be confirmed by more studies.

Numerous studies have shown that GSH depletion is a common feature of apoptosis induced by a variety of stress. GSH depletion has been associated with apoptosis either by predisposing cells to apoptosis or by modulating mitochondrial membrane potential and subsequent activation of caspases (Armstrong et al., 2002). GSH depletion could be mediated through its oxidation to GSSG by ROS, the efflux through GSH transporters or the loss of membrane integrity (Circu et al., 2008; Franco et.al, 2007; Ghibelli et al., 1998; Hammond et al., 2004). Several studies have shown that prevention of GSH efflux could attenuate or prevent apoptosis (Ghibelli et al., 1998; He et al., 2003; Circu et al., 2009). However, conflicting results exist regarding the identity of the specific transporter involved in GSH depletion. Several studies have suggested a role for MRP1 in GSH depletion (Mueller et al., 2005; Hammond et al., 2007; Laberge et al., 2007; Sreekumar et al., 2012). In contrast to those studies, other groups demonstrated that inhibition of MRP1-mediated transport accelerates apoptosis and GSH loss (Franco et al., 2007; Franco et al., 2014). The discrepancy among these studies could be due to differences in cell types, cell culture conditions,

levels of MRP1 expression, duration of the stress, the stimulus used to induce apoptosis and GSH levels maintained during experimentation among various studies. In our experiment, in the absence of Mrp1-mediated GSH efflux, the Mrp1-/- cells were still more sensitive to DOX toxicity demonstrated as less cell survival and more apoptosis compared to WT cells. Thus, GSH efflux mediated by Mrp1 is not essential and not the major determinant of DOX-induced apoptosis in CM and CF.

Another very important finding is that there was less ECSOD/SOD3 expression in Mrp1-/- CM compared to WT CM with either saline or DOX treatment. Among the three SOD isoforms (Cu,ZnSOD, MnSOD2 and ECSOD), ECSOD is the sole enzyme that is located in the extracellular matrix. It catalyzes the dismutation of $\bullet O_2^-$ to H_2O_2 and O_2, and maintains relatively low levels of $O_2^{\bullet-}$ in the extracellular environment. Overexpression of ECSOD in heart tissue or ECSOD administration in animal models has been shown to attenuate oxidative stress and to mitigate tissue dysfunction in cardiovascular disease mimetics (Li et al., 2001; Li et al., 1998; Wahlund et al., 1992). Cardiac-specific ECSOD overexpression attenuates ROS levels and increases NO bioavailability in response to ischemia/reperfusion, thus protecting against reperfusion injury (Obal et al., 2012). In contrast, lack of ECSOD leads to increases in myocardial apoptosis and significantly more left ventricle fibrosis in mice treated with DOX (Kliment et al, 2009). These data suggest that the lower ECSOD expression in Mrp1-/- CM contributes to the greater sensitivity of CM to DOX. However, the mechanism by which loss of Mrp1 decreases ECSOD expression remains

unclear. An earlier study reported that treatment of two fibroblast lines with a wide concentration range of oxidizing agents uniformly, dose-dependently and continuously reduced ECSOD expression in a manner coordinated by cytokines, rather than as a response of individual cells to oxidants (Strålin and Marklund, 1994). It is thus possible that the loss of Mrp1 places the cells under oxidative stress, which in turn changes the cytokine regulation, and finally impairs the expression of ECSOD. In addition, Reddy et al. (2007) reported that type II alveolar epithelial cells derived from Nrf2-/- mice show significantly higher SOD3 mRNA expression compared to WT cells, while GSH supplementation in Nrf2-/- cells decreases the SOD3 expression down to the level of WT cells. These data are consistent with the Nrf2 activation, higher GSH level and lower SOD3 expression observed in Mrp1-/- CM. However, to further test whether oxidative stress, Nrf2 activation or the high level of GSH caused the lower expression of SOD3 in Mrp1-/- CM, we need to treat the CM with other oxidizing agents to see if they cause similar effects as DOX, or we could deplete the GSH in CM culture to see if it removes the difference of SOD3 expression between genotypes. Taken together, loss of Mrp1 lead to lower expression of SOD3 and it may contribute to the sensitivity of Mrp1-/- CM to DOX toxicity.

It is worth noting that the difference in SOD3 expression between genotypes was only found in CM but not CF. It indicates that distinct regulation of *SOD3* gene exist in these two cell types. The different response of *SOD3* gene expression to DOX treatment in CM and CF are further studied and discussed in the next chapter (Chapter 5). However it is still largely unknown why loss of

Mrp1 only deceases SOD3 expression in CM but not CF, how these ECSOD produced by these two cell types coordinate with each other and how these ECSOD proteins from different sources contribute to the DOX-induced pathological changes in the heart. Studies focusing on these questions will be very helpful to identify the function of SOD3 in specific cell components of heart.

In summary, the key findings of this study are that loss of Mrp1 caused an increase of intracellular GSH and GSSG in both mouse heart and CM/CF culture. Following DOX treatment, the increased GSH pool in Mrp1-/- CM and CF is due to the loss of Mrp1-mediated efflux as well as the increased GSH synthesis. This study shows that retention of intracellular GSH does not inhibit further GSH synthesis in Mrp1-/- cells, thus providing important information regarding the dynamics of Mrp1 in regulating cellular GSH levels. Since the role of GSH in maintaining redox status is well understood, these data highlight the potential role of Mrp1 in oxidative stress regulation. In addition, the effects of Mrp1 on extracellular antioxidant defense systems, such as the extracellular GSH pool and ECSOD, open a new field of study of Mrp1's function that merits further investigation.

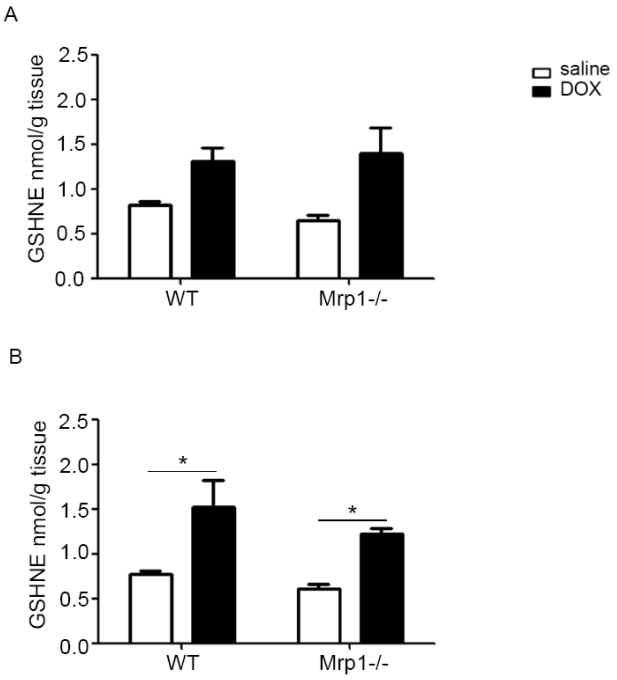

Figure 4.1. Concentration of GS-HNE in heart tissue. Mice were treated with protocol B (2 mg/kg DOX each time, twice a week for 5 weeks), and GS-HNE concentration in heart was measured by LC-MS/MS 48 h (A) or 2 weeks (B) after the last dose of saline or DOX. Each bar represents the mean ± SE. (n = 5 for saline treated group; n = 6 for DOX treated group. *, $p < 0.05$ DOX vs. saline of the same genotype by Newman-Keuls multiple comparison test after one-way ANOVA.)

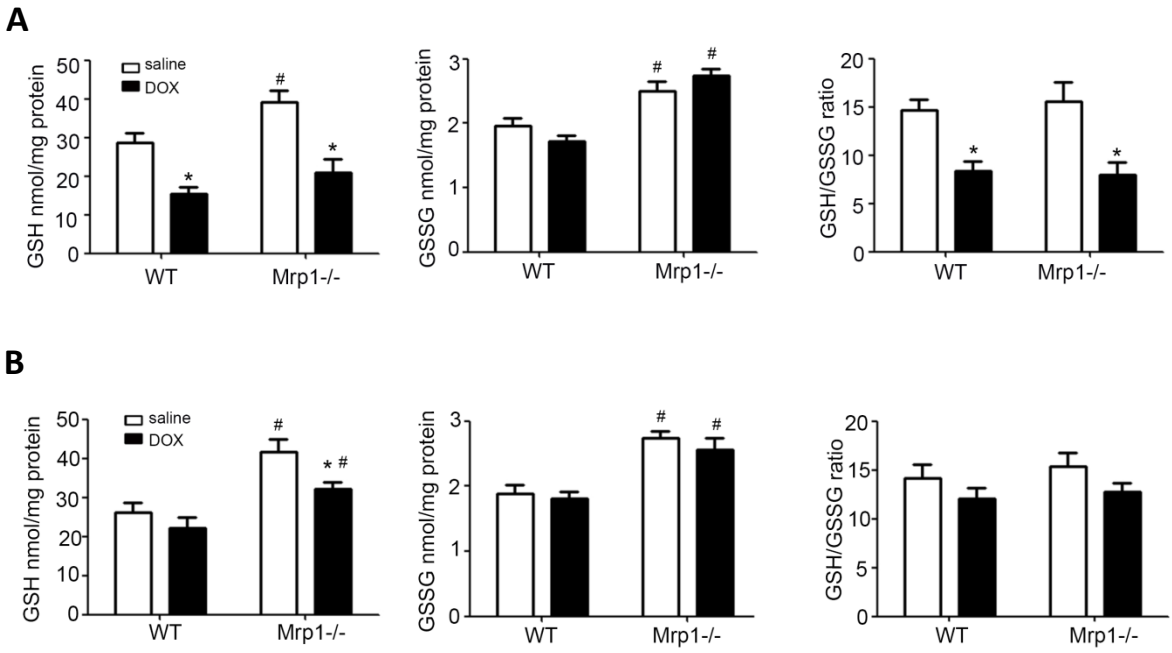

Figure 4.2. Assessment of GSH, GSSG and the GSH/GSSG ratio in mouse heart. Mice were treated with protocol B (2 mg/kg DOX each time, twice a week for 5 weeks), and GSH and GSSG concentrations measured by HPLC at 48 h (A) or 2 weeks (B) after the last dose of DOX. Each bar represents the mean ± SE (n = 6, *, $p < 0.05$ DOX vs. saline of the same genotype; #, $p < 0.05$ vs. respective WT mice by Newman-Keuls multiple comparison test after one-way ANOVA).

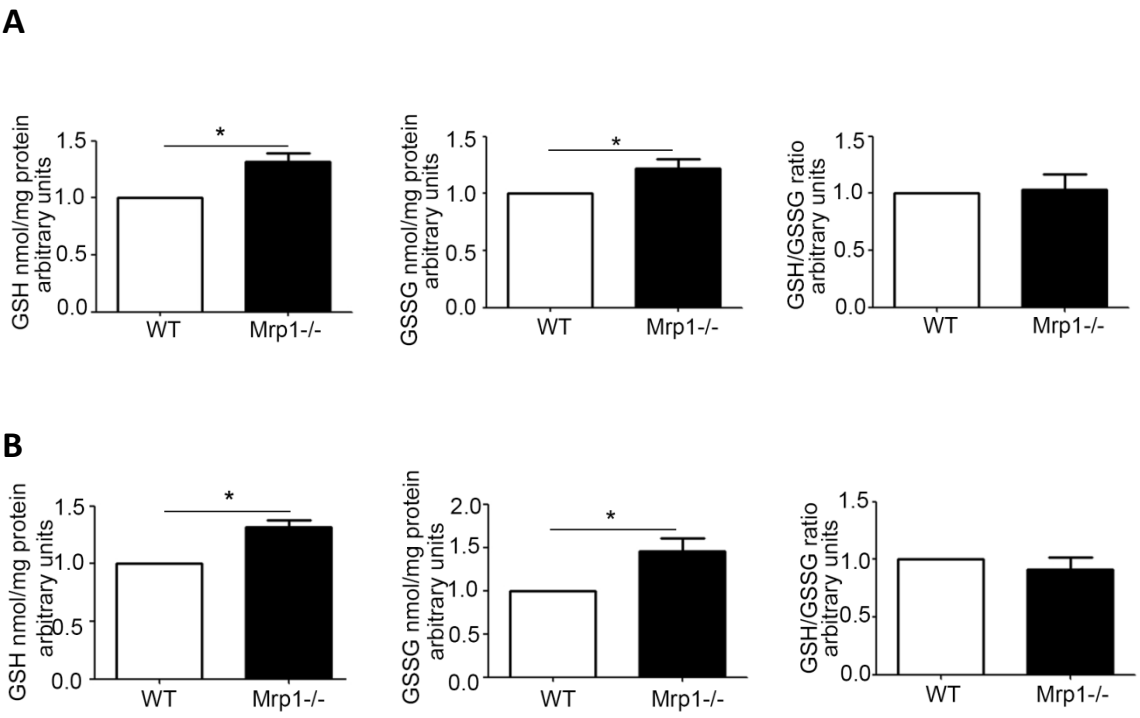

Figure 4.3. Concentration of GSH and GSSG, and the GSH/GSSG ratio in untreated CM (A) and CF (B). GSH and GSSG were measured by HPLC. Significantly higher basal levels of GSH and GSSG were observed in Mrp1-/- cells compared to WT cells so that there was no difference in GSH/GSSG ratio between genotypes. Each bar represents the mean ± SD (n = 3, * $p < 0.01$ by Welch's t- test)

A

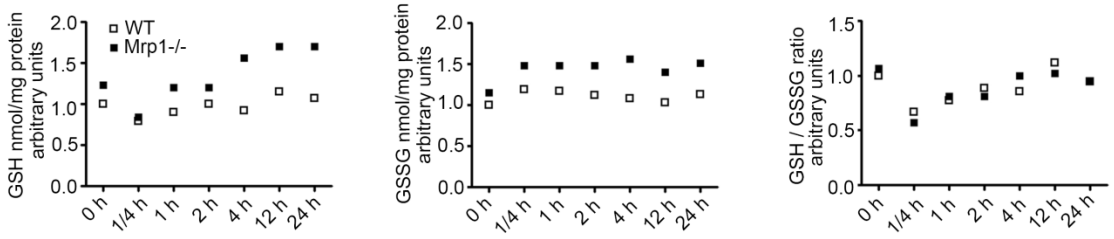

B

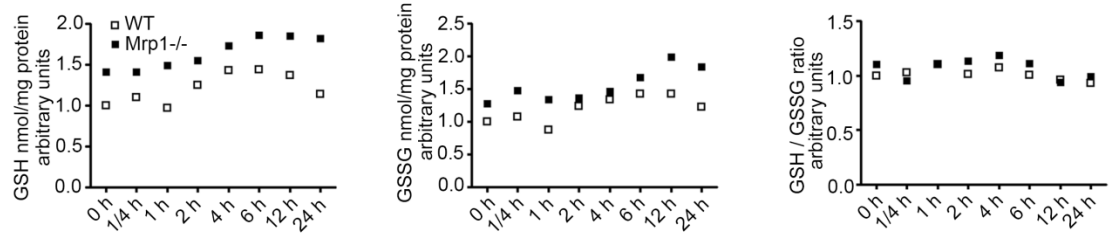

Figure 4.4. Dynamic changes of GSH, GSSG level, and the GSH/GSSG ratio in CM and CF. CM (A) and CF (B) were treated with saline or DOX (0.5 µM in CM and 1 µM in CF) for 3 h, then the saline or DOX containing medium was removed and cells were incubated in fresh medium. GSH and GSSG were measured by HPLC at the indicated times after the addition of DOX. Data represent results from one preparation of cells.

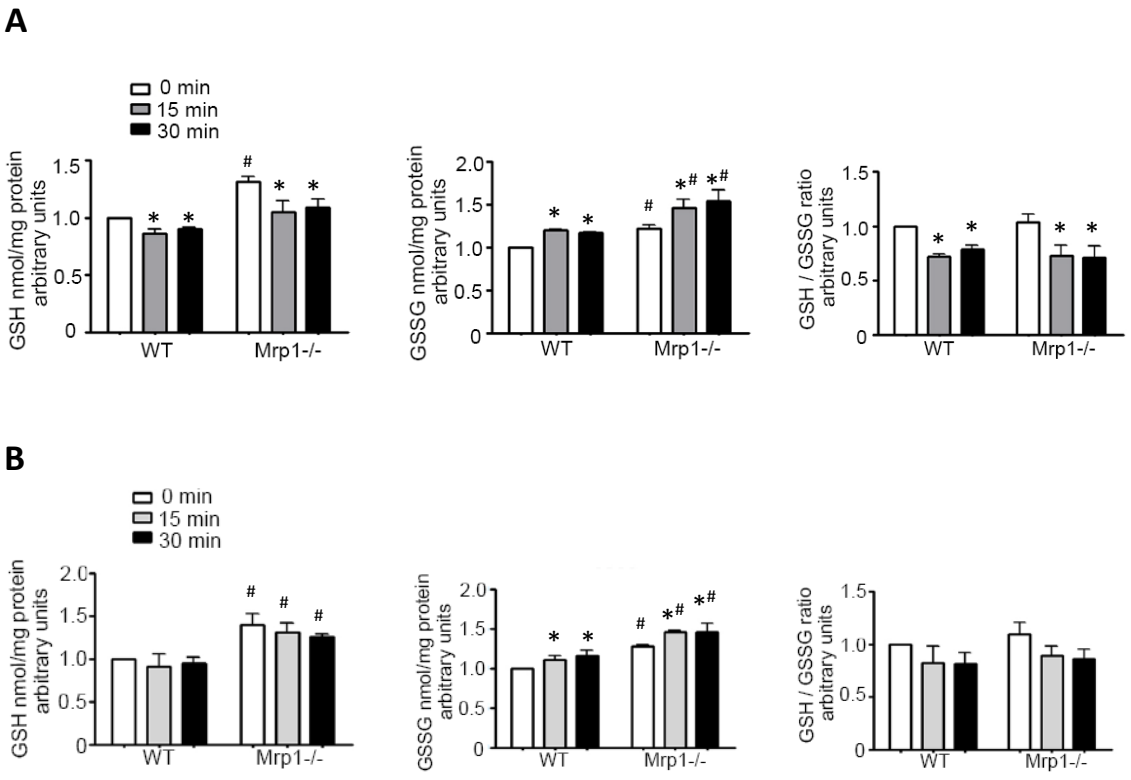

Figure 4.5. Concentration of GSH and GSSG, and the GSH/GSSG ratio at 15 min and 30 min after DOX treatment in CM and CF. CM (A) and CF (B) were treated with saline or DOX (0.5 µM in CM and 1 µM in CF). Fifteen min or thirty min later, cell were harvested and GSH and GSSG were measured by HPLC. Each bar represents the mean ± SD (n = 3; *, $p < 0.05$ DOX vs. 0 min of the same genotype; #, $p < 0.05$ Mrp1-/- vs. respective WT cells by Newman-Keuls multiple comparison test after one-way ANOVA)

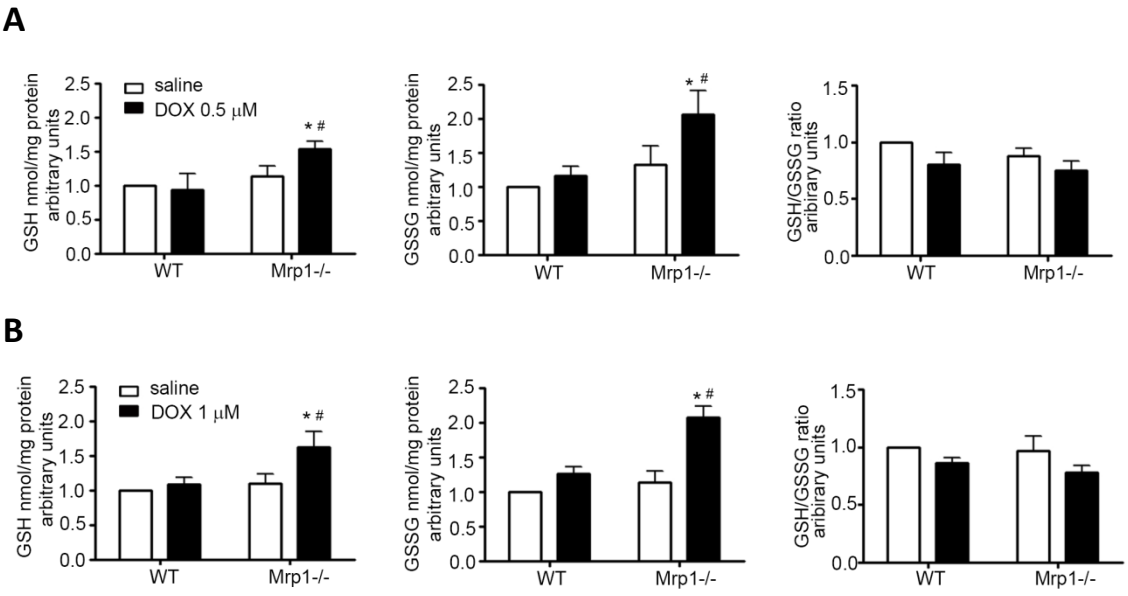

Figure 4.6. Concentration of GSH and GSSG, and the GSH/GSSG ratio at 24 h after saline or DOX treatment in CM and CF. CM (A) and CF (B) were treated with saline or DOX (0.5 μM in CM and 1 μM in CF) for 3 h, then the saline or DOX containing medium was removed and cells were incubated in fresh medium for another 24 h, at which time GSH and GSSG were measured by HPLC. Each bar represents the mean ± SD (n = 3; *, $p < 0.05$ DOX vs. saline of the same genotype; #, $p < 0.05$ Mrp1-/- vs. respective WT cells by Newman-Keuls multiple comparison test after one-way ANOVA)

A

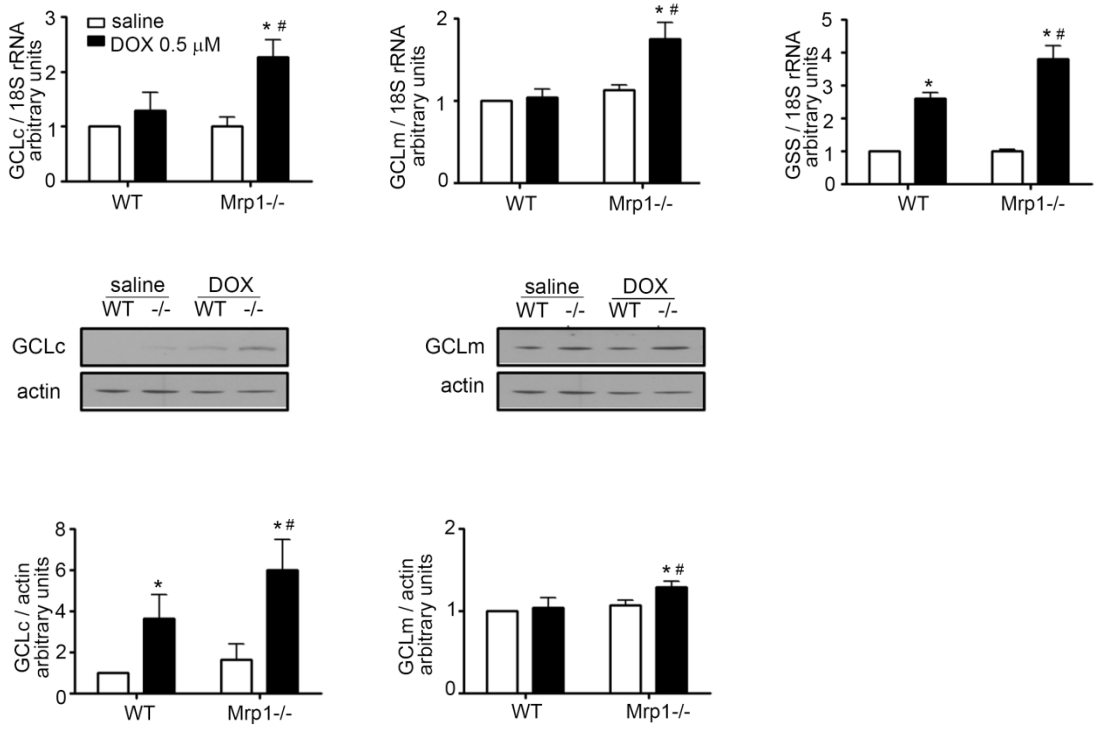

Figure 4.7A. Quantitative analysis of GCLc, GCLm, and GSS expression in CM. CM were treated with saline or 0.5 μM DOX for 3 h, then the saline or DOX containing medium removed and cells incubated in fresh medium for another 24 h. The blots are representative of one of 3 independent experiments. Each bar represents the mean ± SD. (*, $p < 0.05$ DOX vs. saline of the same genotype; #, $p < 0.05$ Mrp1-/- vs. respective WT cells by Newman-Keuls multiple comparison test after one-way ANOVA. GCLc (glutamate-cysteine ligase, catalytic subunit), GCLm (glutamate--cysteine ligase, regulatory subunit), and GSS (glutathione synthetase).

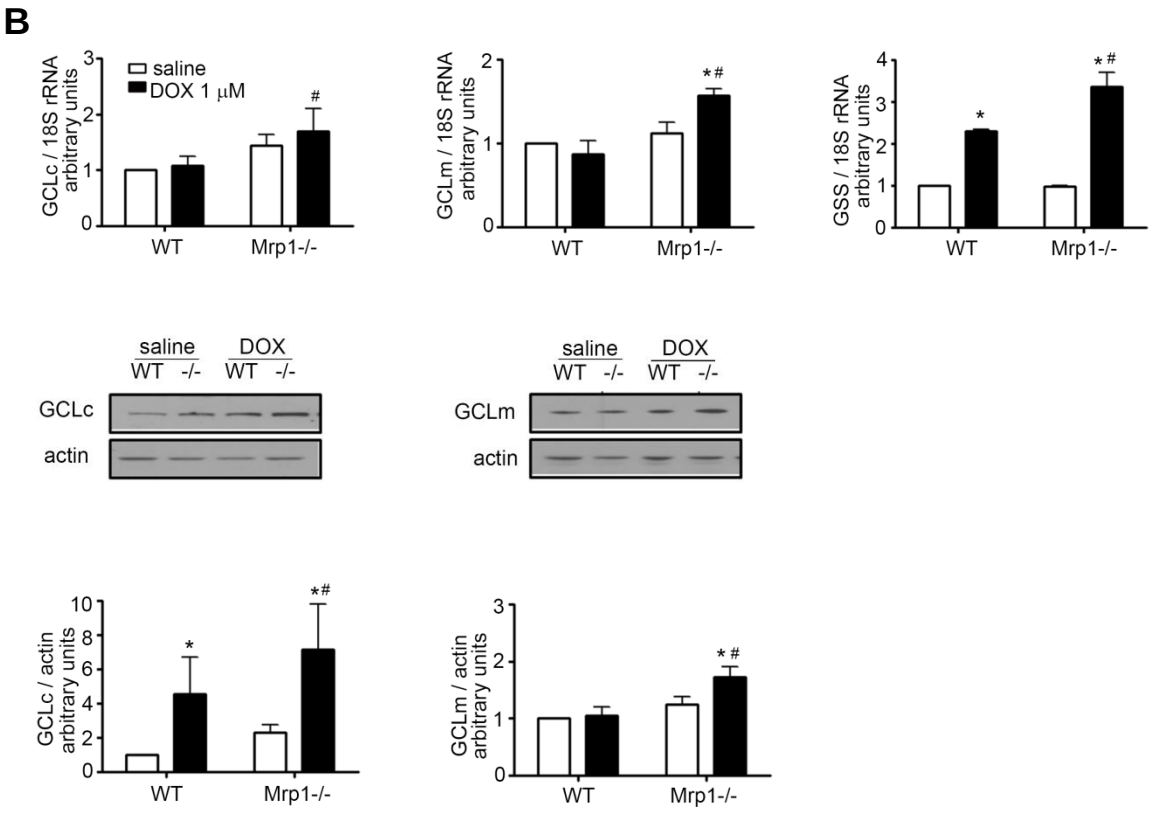

Figure 4.7B Quantitative analysis of GCLc, GCLm, and GSS expression in CF. CF were treated with saline or 1 μM DOX for 3 h, then the saline or DOX containing medium removed and cells incubated in fresh medium for another 24 h. The blots are representative of one of 3 independent experiments. Each bar represents the mean ± SD. (*, $p < 0.05$ DOX vs. saline of the same genotype; #, $p < 0.05$ Mrp1-/- vs. respective WT cells by Newman-Keuls multiple comparison test after one-way ANOVA. GCLc, glutamate-cysteine ligase, catalytic subunit; GCLm, glutamate--cysteine ligase, regulatory subunit; GSS, glutathione synthetase.

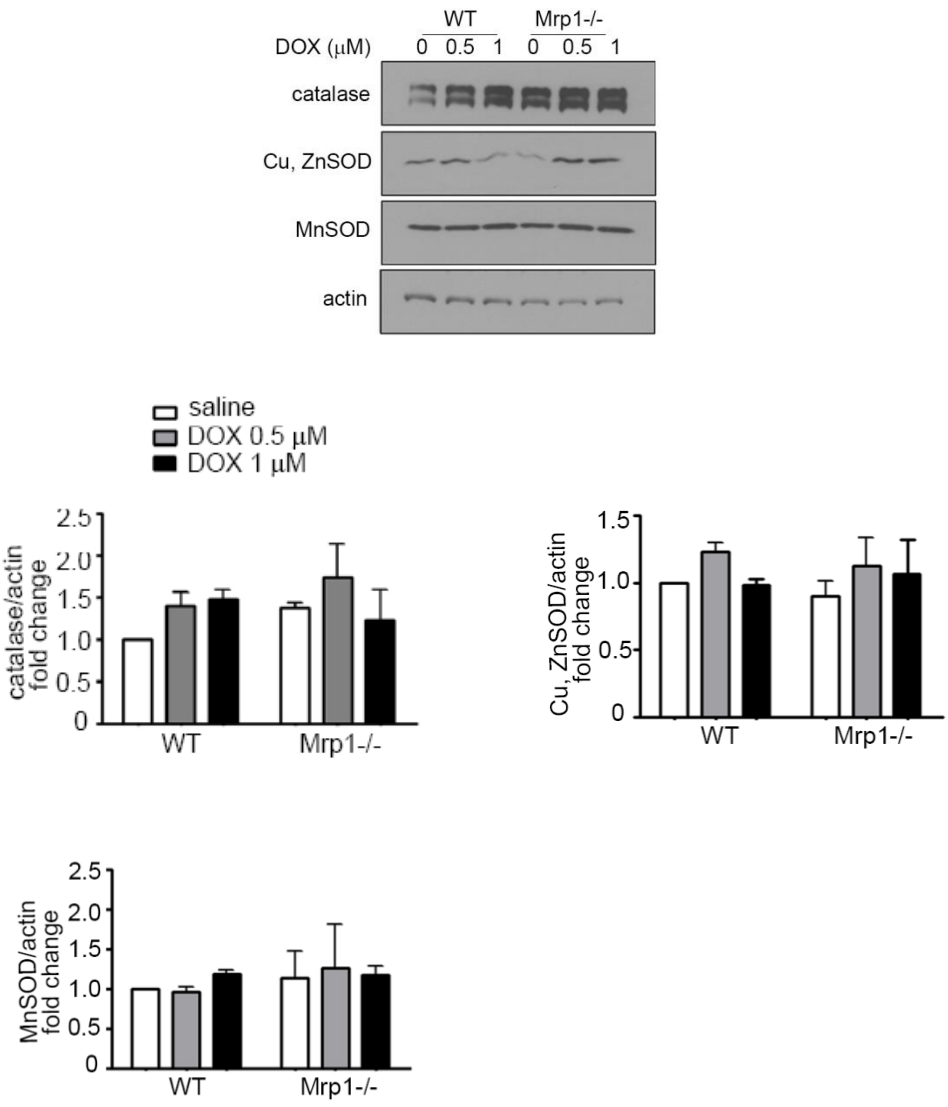

Figure 4.8A. Quantitative analysis of antioxidant enzymes expression in CM. CM were treated with saline or 0.5 μM and 1 μM DOX for 3 h, the saline or DOX containing medium removed and cells incubated in fresh medium for another 24 h. Protein expression was detected by Western blot. The blots are representative of one of 3 independent experiments. Each bar represents the mean ± SD.

B

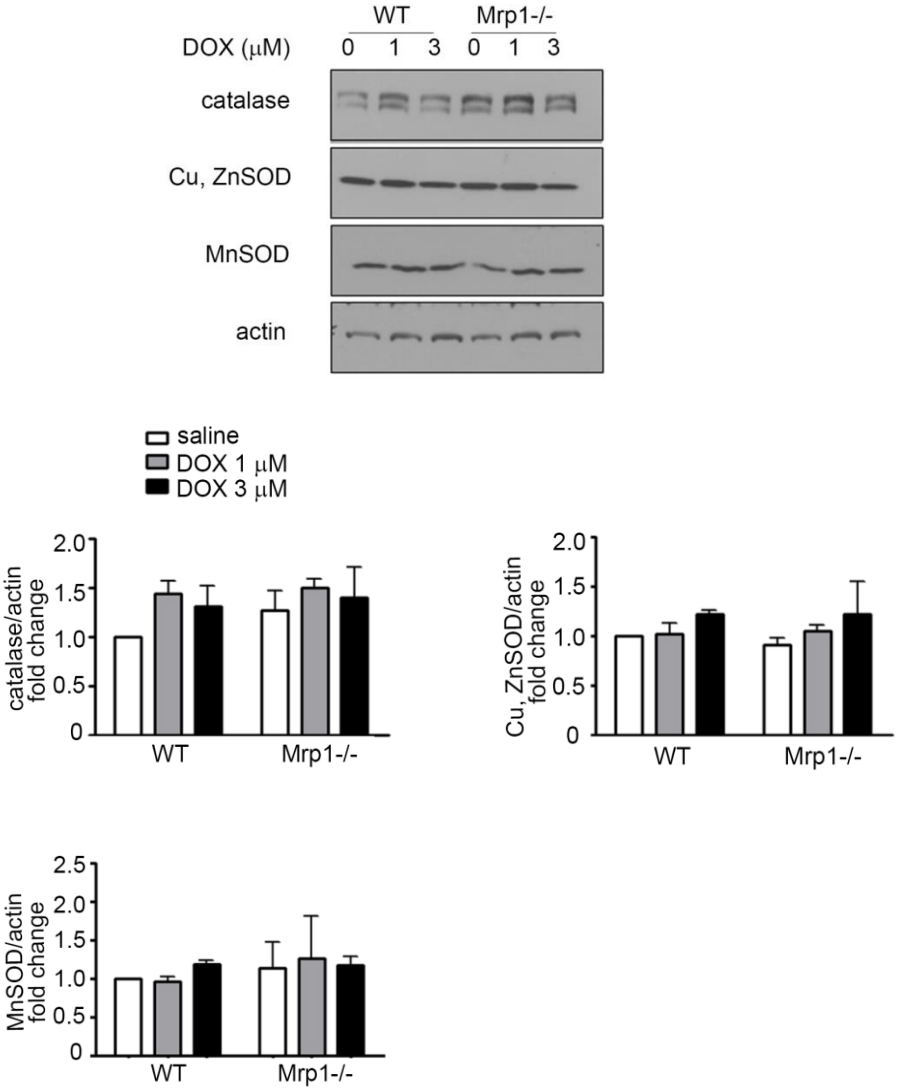

Figure 4.8B. Quantitative analysis of antioxidant enzymes expression in CF. CF were treated with saline or 1 μM and 3 μM DOX for 3 h, the saline or DOX containing medium removed and cells incubated in fresh medium for another 24 h. Protein expression was detected by Western blot. The blots are representative of one of 3 independent experiments. Each bar represents the mean ± SD.

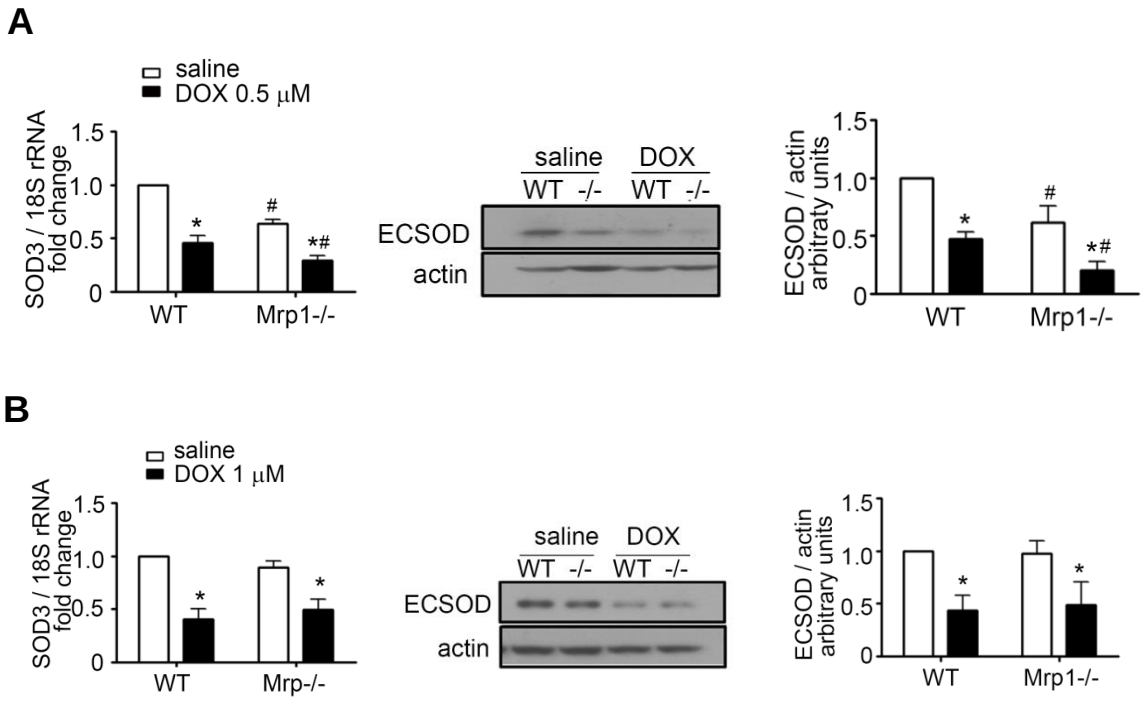

Figure 4.9. Quantitative analysis ECSOD expression in CM and CF. CM (A) and CF (B) were treated with saline or DOX (0.5 μM in CM and 1 μM in CF) for 3 h, the saline or DOX containing medium removed and cells incubated in fresh medium for another 24 h. mRNA expression was detected by Real-Time PCR and protein expression was detected by Western blot. The blots are representative of one of 3 independent experiments. Each bar represents the mean ± SD. (*, $p < 0.05$ DOX vs. saline of the same genotype; #, $p < 0.05$ Mrp1-/- vs. respective WT cells by Newman-Keuls multiple comparison test after one-way ANOVA)

A

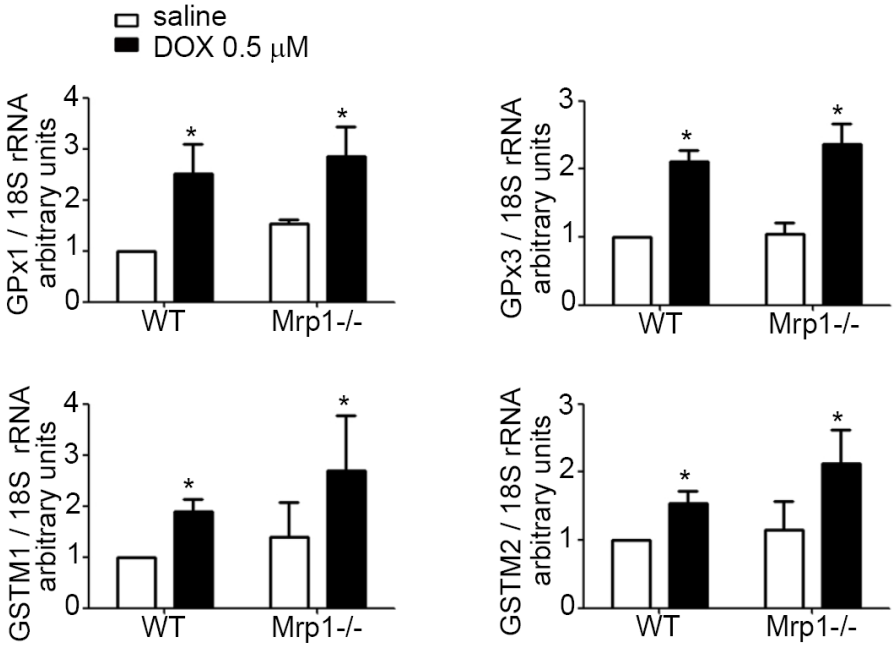

Figure 4.10A. Quantitative analysis of GPx1, GPx3, GSTM1 and GSTM2 mRNA expression in CM. CM were treated with saline or 0.5 μM DOX for 3 h, then the saline (SAL) or DOX containing medium removed and cells incubated in fresh medium for another 24 h. mRNA expression was detected by Real - Time PCR. Each bar represents the mean ± SD. (n = 3; *, $p < 0.05$ DOX vs. saline of the same genotype; #, $p < 0.05$ Mrp1-/- vs. respective WT cells by Newman-Keuls multiple comparison test after One-way ANOVA) GPx, glutathione peroxidase; GST, glutathione S-transferase;

B

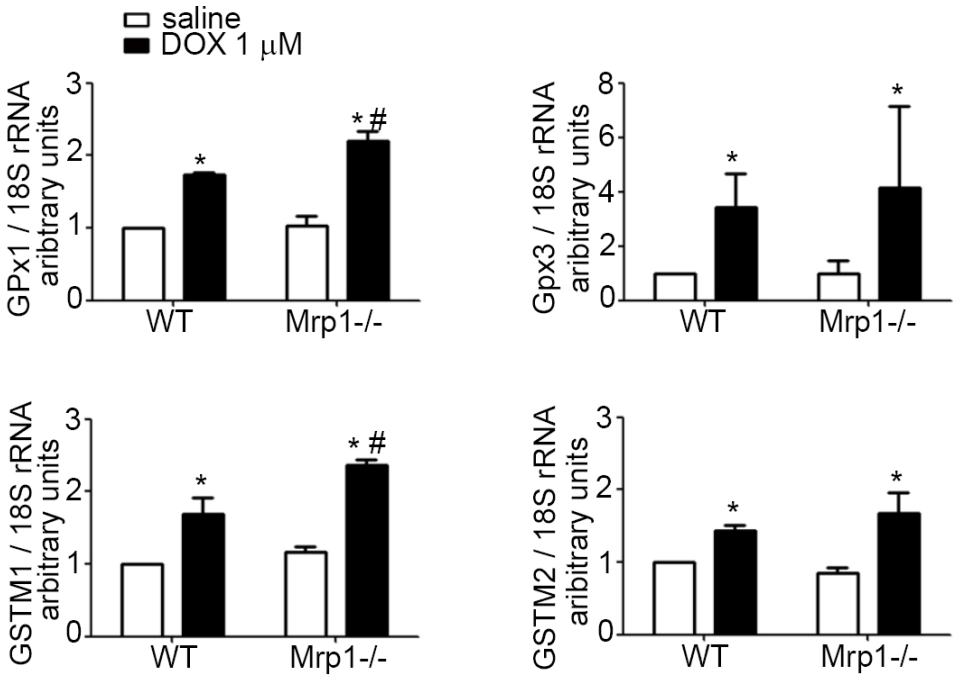

Figure 4.10B. Quantitative analysis of GPx1, GPx3. GSTM1 and GSTM2 mRNA expression in CF. CF were treated with saline or 1 μM DOX for 3 h, then the saline (SAL) or DOX containing medium removed and cells incubated in fresh medium for another 24 h. mRNA expression was detected by Real - Time PCR. Each bar represents the mean ± SD. (n = 3; *, $p < 0.05$ DOX vs. saline of the same genotype; #, $p < 0.05$ Mrp1-/- vs. respective WT cells by Newman-Keuls multiple comparison test after One-way ANOVA) GPx, glutathione peroxidase; GST, glutathione S-transferase;

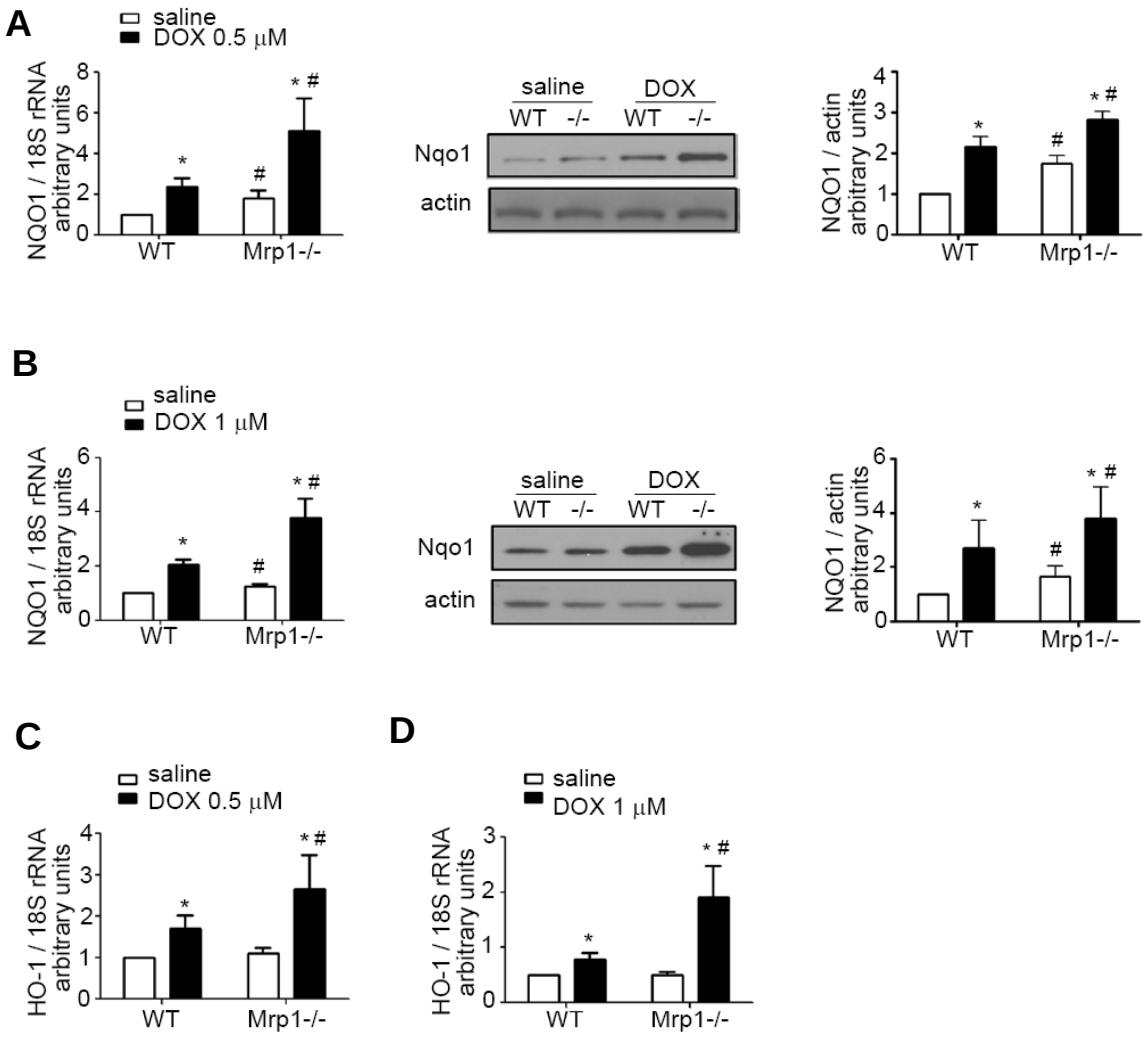

Figure 4.11. Quantitative analysis of Nqo1 and HO-1 mRNA and protein expression in CM and CF. CM (A and C) and CF (B and D) were treated with saline or DOX (0.5 μM in CM and 1 μM in CF) for 3 h, the saline (SAL) or DOX containing medium removed and cells incubated in fresh medium for another 24 h. mRNA expression was detected by Real-Time PCR and protein expression was detected by Western blot. The blots are representative of one of 3 independent experiments. Each bar represents the mean ± SD. (n = 3; *, $p < 0.05$ DOX vs. saline of the same genotype; #, $p < 0.05$ Mrp1-/- vs. respective WT cells by Newman-Keuls multiple comparison test after One-way ANOVA)

A

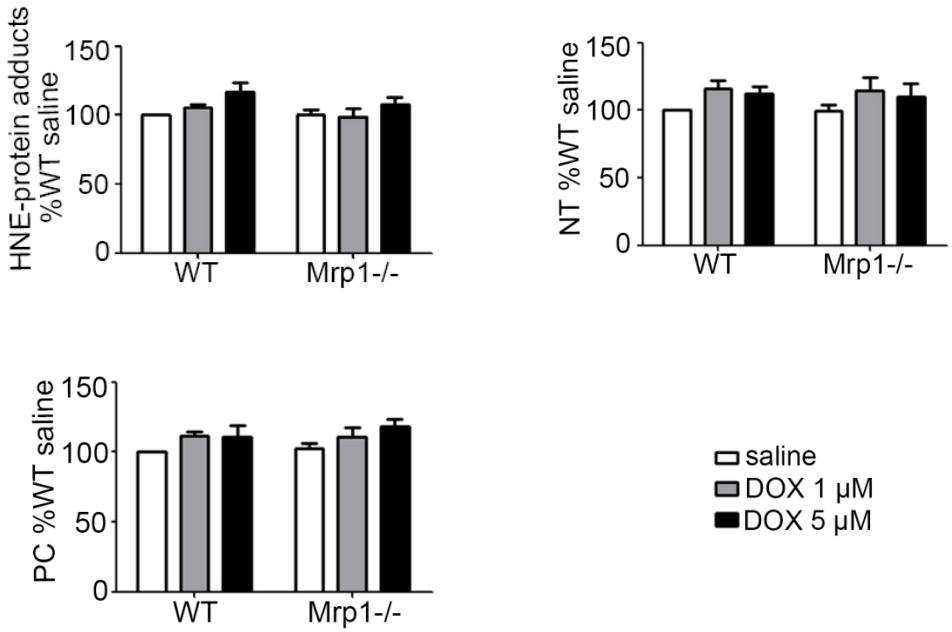

Figure 4.12A. Protein oxidative damage in CM. CM were treated with saline or 1 or 5 µM DOX for 30 min. Then, HNE-protein adducts, 3-nitrotyrosine-protein adducts and protein carbonyl levels were assessed by slot-blot assay. NT, 3-nitrotyrosine-protein adducts; PC, protein carbonyl. Each bar represents the mean ± SE. (n = 3)

B

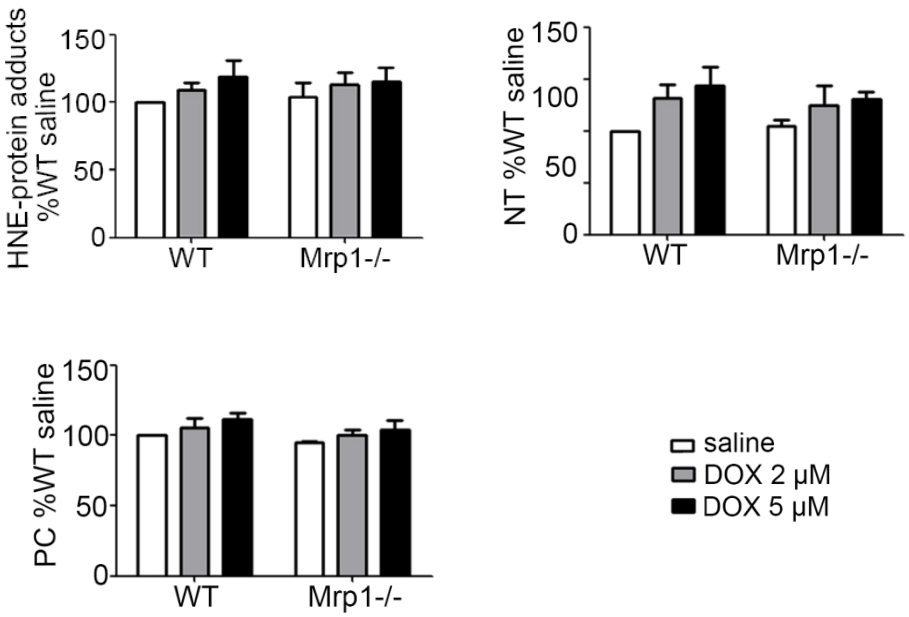

Figure 4.12B. Protein oxidative damage in CF. CF were treated with saline or 2 or 5 μM DOX for 30 min. Then, HNE-protein adducts, 3-nitrotyrosine-protein adducts and protein carbonyl levels were assessed by slot-blot assay. NT, 3 nitrotyrosine-protein adducts; PC, protein carbonyl. Each bar represents the mean ± SE. (n = 3)

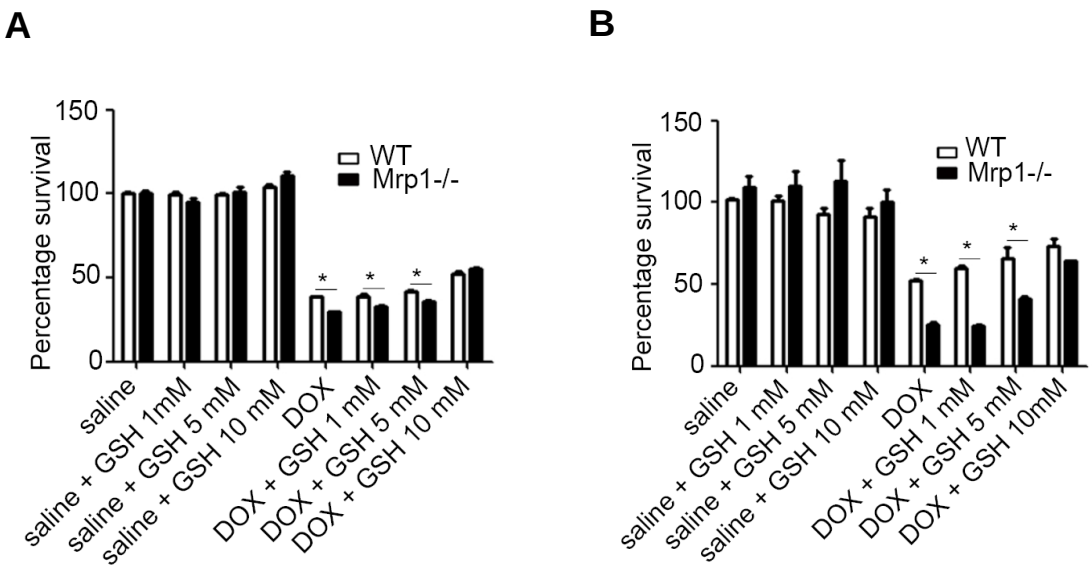

Figure 4.13. Exogenous GSH rescued Mrp1-/- CM and CF. CM (A) and CF (B) were cultured on a 96-well plate for 48 h before treatment with saline or DOX for 3 h. Tetrazolium reduction was measured 48 h after DOX removal. Varying concentrations of GSH were added to the medium during DOX treatment and after removal of DOX. Only addition of 10 mM GSH eliminated the difference in cell viability between WT and Mrp1-/- cells. Each bar represents the mean ± SD. (n = 6, *, $p < 0.05$ by Newman-Keuls multiple comparison test after One-way ANOVA)

Table 4.1. Primers and Universal ProbeLibrary probes used for qRT-PCR

Genes	Forward primer (5′-3′)	Reverse primer (5′-3′)	Universal Probe Library probe
18S rRNA	gcaattattccccatgaacg	gggacttaatcaacgcaagc	#48
GPx1	tttcccgtgcaatcagttc	tcggacgtacttgagggaat	#2
GPx3	ggcttcccttccaaccaa	cccacctggtcgaacatact	#92
GSS	agatggctacatgcccagtc	gcacgagatctctctagcatca	#48
GSTM1	gcagctcatcatgctctgtta	tttctcagggatggtcttcaa	#106
GSTM2	agttggccatggtttgctac	agcttcatcttctcagggagac	#106
GCLc	ctgcacatctaccacgcagt	gaacatcgcctccattcagt	SYBR green
GCLm	tgactcacaatgacccgaaa	tcaatgtcagggatgctttct	#108
HO-1	aggctaagaccgccttcct	tgtgttcctctgtcagcatca	#17
NQO1	agcgttcggtattacgatcc	agtacaatcagggctcttctcg	#50
SOD3	ctcttgggagagcctgaca	gccagtagcaagccgtagaa	#102

GPx, glutathione peroxidase; GSS, glutathione synthetase; GST, glutathione S-transferase; HO-1: heme oxygenase 1; NQO1, NAD(P)H dehydrogenase, quinone 1; GCLc, glutamate-cysteine ligase catalytic subunit; GCLm, glutamate-cysteine ligase regulatory subunit; Mrp1, multidrug resistance-associated protein 1; SOD3, superoxide dismutase 3.

128

Table 4.2: Redox potential (*Eh*) of the GSH/GSSG pool in CM and CF (15 min and 30 min)

		***Eh* of GSH/GSSG (mV) Ave ± SD**		
Cell	**Mice**	**Treatment**		
		0 min	**DOX 15 min**	**DOX 30 min**
CM	WT	-237.7 ±2.3	-231.4± 0.8 *	-232.8± 2.6 *
	Mrp1-/-	-240.6±1.6	-234.8±2.3 *	233.0± 3.0 *
CF	WT	-236.5±1.3	-230.0±5.4	230.5± 3.5
	Mrp1-/-	-239.4 ±2.5	-235.4 ±2.2	234.9± 1.9

The redox potential (*Eh*) of the GSH/GSSG pool in CM and CF at 15min and 30 min after DOX treatment. CM and CF were treated with DOX (0.5 µM in CM and 1 µM in CF) for 0, 15 and 30 min. *Eh* is calculated by the Nernst equation, $Eh = Eo + (RT/nF)\ \ln([GSSG]/[GSH]^2)$. To estimate cellular concentrations, 1 mg of cell protein was assumed to be associated with 5 µl of cell volume (Mannery et al., 2010). R is the gas constant, T is temperature, n is the number of electrons transferred, F is the faraday constant, and *Eo* = - 264 mV at a pH of 7.4. Data are presented as mean ± SD (n = 3; *, $p < 0.05$ DOX vs. 0 min of the same genotype by Dunnett's post-test after one-way ANOVA)

Table 4.3: Redox potential (*Eh*) of the GSH/GSSG pool in CM and CF (24 h)

		***Eh* of GSH/GSSG (mV) Ave ± SD**	
Cell	**Mice**	**Treatment**	
		saline	**DOX**
CM	WT	-234.6 ±1.6	-229.1± 7.0
	Mrp1-/-	-234.8 ±2.7	-236.5 ±1.2
CF	WT	-235.4 ±3.0	-235.0±2.1
	Mrp1-/-	-237.7 ±1.0	-237.2 ±4.5

The redox potential (*Eh*) of the GSH/GSSG pool in CM and CF after saline or DOX treatment. CM and CF were treated with saline or DOX (0.5 µM in CM and 1 µM in CF) for 3 h, the saline or DOX containing medium removed and cells incubated in fresh medium for another 24 h. *Eh* is calculated by the Nernst equation, $Eh = Eo + (RT/nF)\ \ln([GSSG]\ /[GSH]^2)$. To estimate cellular concentrations, 1 mg of cell protein was assumed to be associated with 5 µl of cell volume (Mannery et al., 2010). R is the gas constant, T is temperature, n is the number of electrons transferred, F is the faraday constant, and *Eo* = - 264 mV at a pH of 7.4. Data are presented as mean ± SD, n = 3.

Chapter Five

The effect of DOX on expression of ECSOD/SOD3 in CM and CF

Introduction

Three forms of SOD exist in mammalian tissues: Cu,ZnSOD/SOD1, MnSOD/SOD2 and ECSOD/SOD3. While Cu/Zn SOD is localized in cytosol, and MnSOD in mitochondria, the ECSOD is the only SOD secreted into the extracellular environment. It catalyzes the dismutation of $\bullet O_2^-$ to H_2O_2 and O_2, and maintains relatively low levels of $\bullet O_2^-$ in the extracellular environment. Due to its special cellular localization, it has unique and irreplaceable roles in maintaining the normal redox status in tissue.

SOD structure characteristics

The *ECSOD/SOD3* gene has been mapped to human chromosome 4 and mouse chromosome 5 and share 60% identity. In most species, ECSOD exists as a 135 KDa homotetramer composed of two disulfide-linked dimers. As shown in Figure 5.1, each subunit has a molecular weight of 24 KD and is composed of (1) an amino-terminal signal peptide, which permits its secretion from the cell; (2) an active domain binding copper and zinc with a strong homology with Cu,ZnSOD; (3) a heparin-binding domain, which is a C-terminal domain containing a group of six positively charged amino acids (4 arginine, 2 lysine). This domain interacts with the negatively charged heparin sulfate proteoglycans

on the cell surface or in the extracellular matrix (ECM).

ECSOD has a proteolytic cleavage site next to the heparin binding domain. The proteolysis of the heparin binding domain can occur partially, to produce a tetramer with low affinity for heparin (type B), or completely, so all of the 4 subunits lack the heparin-binding domain to produce tetramer with no affinity for heparin (type A). If none of the subunits undergo proteolysis, the tetramer has a strong affinity for heparin (type C). Type A and type B are found circulating in plasma, while type C remains bound to the ECM, but can be released into circulation by displacing it with heparin. The tissue bound forms constitute ~ 99% of the total ECSOD (Fukai et al., 2002).

ECSOD tissue distribution and expression regulation

In contrast to the ubiquitous expression of Cu,ZnSOD and MnSOD, ECSOD expression is restricted to several tissues. In mammalians, ECSOD expression is highest in lung, kidney and aorta, while the heart and brain have lesser amounts (Folz et al., 1997). On the cellular level, a higher level of ECSOD expression was observed in alveolar type II cells, lung macrophages, vascular smooth muscle cells, endothelial cells and some fibroblast cells.

The mechanism involved in ECSOD expression regulation is not well-understood. SP1/SP3 regulates ECSOD expression in human and mouse liver cell lines and lung fibroblast cell lines (Zelko et al, 2004; 2008). In human vascular smooth muscle cells and lung alveolar type II cells, inflammatory cytokines such as interferon (IFN)-γ and lL-4 upregulate the expression of

ECSOD mRNA and protein while tumor necrosis factor (TNF)-α downregulates the expression of ECSOD. Vasoactive factors such as histamine, vasopressin, oxytocyn, endothelin-1, serotonin, and heparin markedly increase enzyme levels in cultured arterial smooth muscle cells (Fukai et al., 1999). Also, exercise training and Angiotensin II upregulate ECSOD expression in smooth muscle cells (Fukai at al., 1999, 2000). In addition, ECSOD expression is uniformly downregulated by a wide variety of oxidizing agents, such as xanthine oxidase, paraquat, and t-butyl hydroperoxide in fibroblasts, although the mechanisms involved are not clear (Stralin and Marklund, 1994).

ECSOD and cardiovascular disease

In the cardiovascular system, ECSOD is highly expressed in blood vessels, particularly arterial walls. Also, ECSOD activity is 10-fold higher in the vessel wall than in other tissues and constitutes up to 70 % of the total SOD activity in aorta. A body of evidence shows the protective role of ECSOD in the cardiovascular system. ECSOD expression is reported to be reduced in patients with coronary artery disease while overexpression of ECSOD in vascular endothelial cells can protect against the oxidation of low-density lipoprotein (LDL), a major contributing factor to the formation of atherosclerosis (Takatsu et al., 2001; Laukkanen et al., 2001). These data suggest that the low ECSOD expression/activity contributes to the endothelial dysfunction in patients with this disease. ECSOD also plays an important role in reducing myocardial infarct size and preserving cardiac function. For example, recombinant human ECSOD

preserves cardiac function and reduces the level of tissue ROS following ischemia/reperfusion in rat isolated hearts (Sioquist et al., 1991). ECSOD-transgenic mice show greater preservation of myocardial function after global ischemia/reperfusion than their wild-type counterparts (Chen et al., 1996). In addition, ECSOD can limit the interaction of $\bullet O_2^-$ with NO• to preserve the bioavailability of NO. Cardiac-specific ECSOD overexpression attenuates ROS levels and increases NO bioavailability in response to ischemia/reperfusion, thus protecting against reperfusion injury (Obal et al., 2012). This action also prevents the excessive formation of the highly reactive and toxic peroxynitrite.

Our questions and research goal

Kliment et al (2009) reported that lack of ECSOD leads to increases in myocardial apoptosis and significantly more left ventricle fibrosis in mice treated with DOX. This means that ECSOD likely plays an important role in normal heart defense against DOX induced cardiotoxicity. Thus, investigating the regulation of SOD3 expression in heart, especially when heart is exposed to DOX, may help us better understand how DOX causes heart damage. However, there are no reports regarding how DOX affects SOD3 expression in heart, especially in different cell types of heart tissue. Here, neonatal cardiomyocytes and cardiac fibroblastsfrom WT mice were treated with a range of DOX concentrations, and SOD3 mRNA and protein expression measured. This study characterized the effects of DOX on SOD3 expression in these two cell types.

Materials and Methods

Cell culture and treatment

Primary CM and CF were obtained from WT C57BL neonatal mice at 1–3 days of age and cultured as described in Chapter 3. Cells were treated with varying concentrations of DOX for the indicated times and cells harvested for detection of SOD3 expression.

RNA extraction and real-time quantitative PCR (qRT-PCR)

Total RNA extraction, cDNA preparation and RT-PCR were conducted as described in Chapter 2. Primers and UPL probes used to detect SOD3 are shown in Table 4.1.

Immunoblot Assay

Immunoblot assays were conducted as described in Chapter 4. Rabbit anti-ECSOD pAb was a generous gift from Dr. Ladislav Dory, University of North Texas.

Statistical analysis

All data are expressed as the mean ± SD for n = 3 per group, as detailed in the Figure Legends. In studies comparing multiple groups to the same control group, statistical analysis was performed with one-way ANOVA followed by Dunnett's post-test.

Results

DOX decreased expression of SOD3 in CM

CM were treated with different concentrations of DOX for 24 h. DOX concentrations were chosen based on the results of the MTT assay to avoid the high DOX concentrations that cause excessive cell death. DOX decreased ECSOD mRNA (Figure 5.2A) and protein (Figure 5.2B) expression in a dose-dependent manner. In contrast, DOX significantly increased MnSOD protein expression levels, while it had no significant effects on Cu,ZnSOD expression (Figure 5.2B). DOX-induced cell apoptosis was demonstrated by PARP cleavage.

CM further treated with 0.5 μM DOX for various time periods showed that the down-regulation of ECSOD mRNA and protein level occurred at 8 h, 16 h and 24 h after DOX treatment (Figure 5.3).

DOX affectss on the expression of SOD3 in CF

CF were treated with various concentrations of DOX for 24 h, and showed that the lowest concentration of DOX (0.5 μM) decreased ECSOD mRNA and protein expression. However, the high concentration of DOX (3 μM) significantly increased the expression of ECSOD protein, with no significant change in ECSOD mRNA expression. Dox treatment also increased MnSOD expression at high concentrations (1 and 3 μM) of DOX (Figure 5.4). DOX-induced cell apoptosis was demonstrated by PARP cleavage.

CF were further treated with 3 μM DOX for various time periods, and showed that the increase of ECSOD protein expression began about 16 h after DOX

treatment. However, there was no obvious change in the mRNA expression (Figure 5.5).

Discussion

A number of studies suggest that the administration of a wide variety of enzymatic and nonenzymatic antioxidants can protect against oxidant-induced tissue injury, both in animal models and in human. Since ECSOD expression and/or activity are decreased in multiple diseases, it is interesting to entertain the idea of ECSOD as a potential target for therapy to improve antioxidant capacity and restore the redox balance. Thus, a further understanding of the role of ECSOD in the pathogenesis of oxidant-mediated diseases as well as the regulatory mechanism of ECSOD expression will provide insight into the potential therapeutic possibilities of this protein.

Our study is the first to show the effects of DOX treatment on ECSOD expression in CM and CF. It is important to note that the ECSOD expression in CM and CF showed different responses to DOX treatment. This means that there must be different machinery that controls ECSOD expression in these two cell types. We expect the decrease of ECSOD expression in CM to exacerbate the DOX-induced oxidative stress, while the increase of ECSOD in CF could present the cellular response to this stress. How these two sources of ECSOD coordinate with each other and how these ECSOD from different sources contribute to DOX-induced pathological changes in heart will be an important avenue to investigate.

In addition, compared to CMs, CFs have much higher ECSOD expression at both mRNA and protein levels (Figure 5.6). The different basal levels of ECSOD expression and different expression regulation mechanisms in CM and CF indicate that ECSOD expression in whole heart tissue needs to be evaluated carefully because measuring total ECSOD expression in heart is not able to distinguish changes of ECSOD expression in these two different cell populations.

Another interesting finding is the inconsistent changes of ECSOD mRNA expression and protein expression in CF treated with 3 μM DOX. The disparity between ECSOD mRNA and protein expression are also reported in other cells (Folz et al., 1994). These data indicate a role of post-transcriptional regulation in maintaining optimal enzyme levels in various tissues and in response to various stressors.

Based on these data, many further studies will be important, such as investigating post-transcriptional modulation of ECSOD, rates of protein synthesis and secretion, and the extent of protein degradation following DOX treatment. These studies will help us better understand the expression regulation of ECSOD, and how this contributes to DOX induced cardiotoxicity.

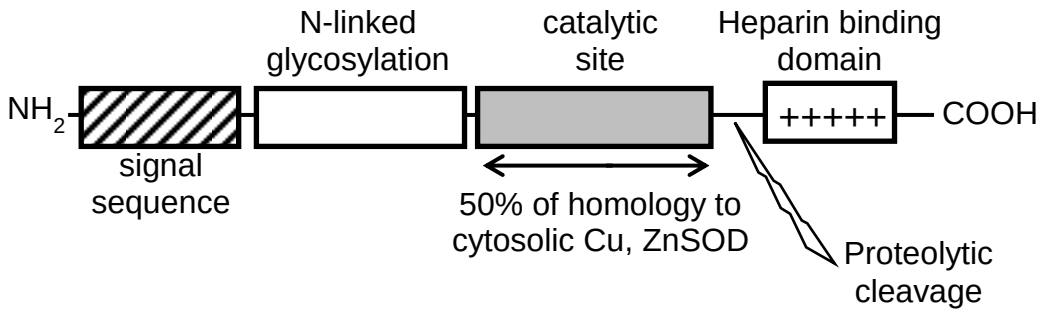

Figure 5.1. Schematic diagram of ECSOD functional domains in protein. The ECSOD protein can be divided into four functional domains: (1) the signal sequence, cleaved during synthesis; (2) the glycosylated N-terminus; (3) the catalytic region, which bears the highest level of homology to Cu,Zn SOD; (4) the positively charged heparin-binding domain.

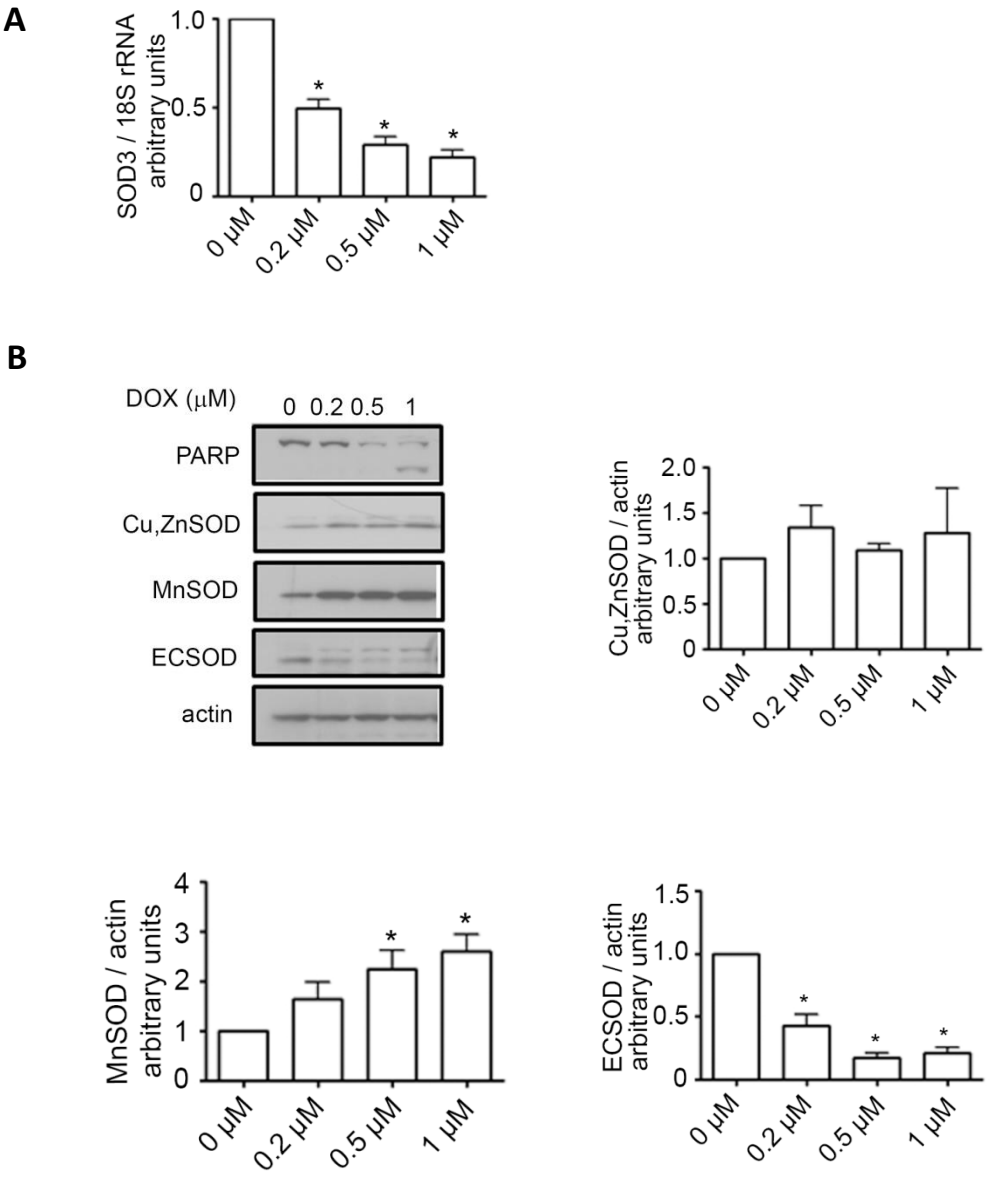

Figure 5.2. DOX treatment increased MnSOD but decreases ECSOD expression in CM culture in a dose-dependent manner. CMs were treated with varying concentrations of DOX for 24 hr, then mRNA expression of SOD3 was measure by real-time PCR (A) and protein expression of Cu,ZnSOD, MnSOD and ECSOD was detected by Western blot (B). DOX-induced cell apoptosis was demonstrated by PARP cleavage. Each bar represents the mean ± SD. (n=3, *, $p < 0.05$ by Dunnett's post-test after one-way ANOVA).

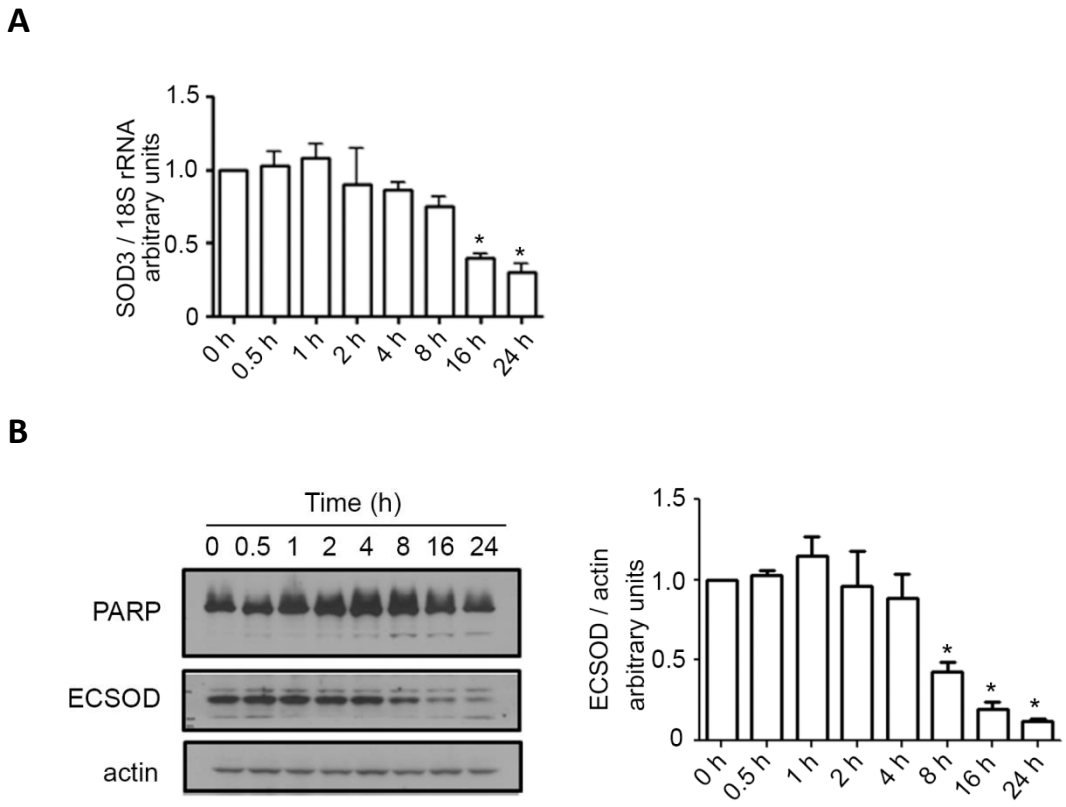

Figure 5.3. DOX treatment decreased ECSOD expression in CM culture. CMs were treated with 0.5 μM DOX for varying time periods, and mRNA expression of ECSOD was measured by real-time PCR (A). Protein expression of ECSOD was detected by Western blot (B). DOX-induced cell apoptosis was demonstrated by PARP cleavage. Each bar represents the mean ± SD. (n=3, *, $p < 0.05$ by Dunnett's post-test after one-way ANOVA).

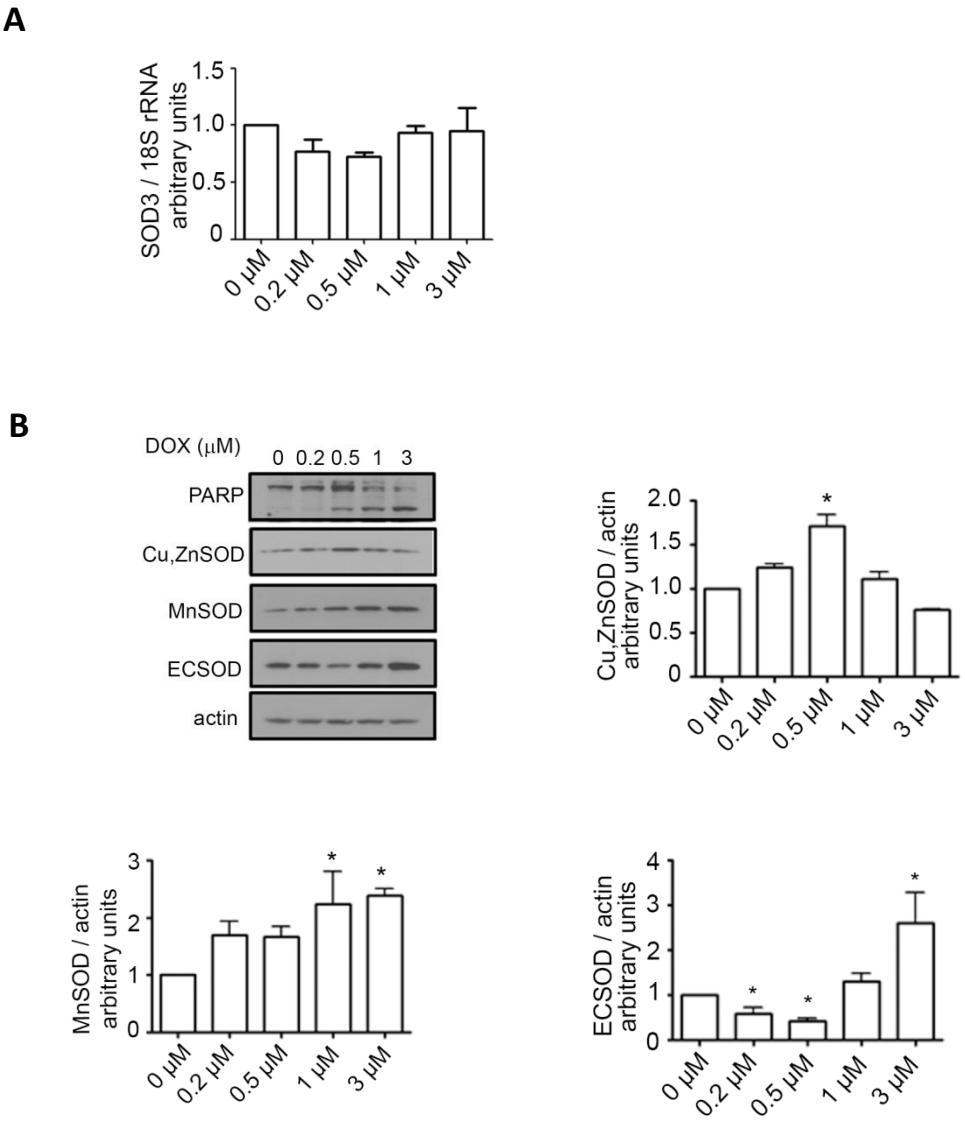

Figure 5.4. DOX treatment changes expression of superoxide dismutases in CF culture in a dose-dependent manner. CFs were treated with varying concentrations of DOX for 24 hr, and mRNA expression of ECSOD was measured by real-time PCR (A) and protein expression of Cu,ZnSOD, MnSOD and ECSOD was detected by Western blot (B). DOX-induced cell apoptosis was demonstrated by PARP cleavage. Each bar represents the mean ± SD. (n=3, *, $p < 0.05$ by Dunnett's post-test after one-way ANOVA).

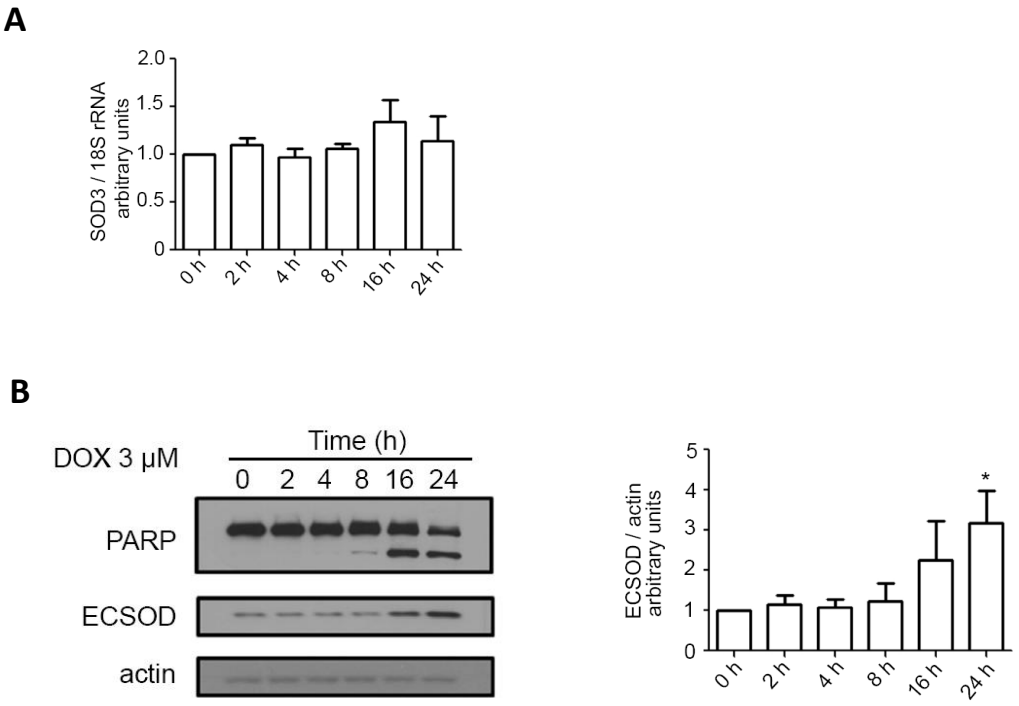

Figure 5.5. DOX (3 μM) treatment increased ECSOD expression in CF culture. CFs were treated with 3 μM DOX for varying time periods, and mRNA expression of ECSOD was measured by real-time PCR (A). Protein expression of ECSOD was detected by Western blot (B). DOX-induced cell apoptosis was demonstrated by PARP cleavage. Each bar represents the mean ± SD. (n=3, *, $p < 0.05$ by Dunnett's post-test after one-way ANOVA).

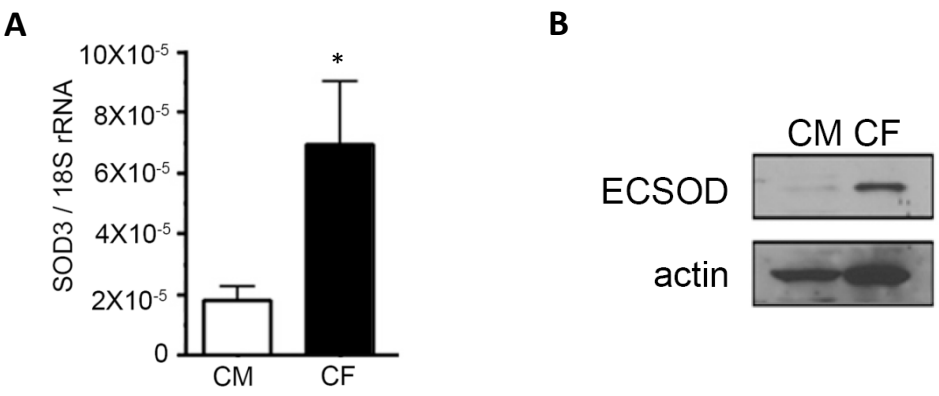

Figure 5.6. CF has higher ECSOD expression compared to CM. mRNA expression of ECSOD was measure by real-time PCR (A) while protein expression of ECSOD was detected by Western blot (B). Each bar represents the mean ± SD. (n=3, *, $p < 0.05$ by Student t test).

Chapter Six

Conclusion, general discussion and future studies

Conclusion and general discussion

The ATP-dependent efflux transporter MRP1 has been a major subject of scientific and clinical interest ever since its first characterization in 1992 (Cole et al., 1992). Due to its role in multidrug resistance development in cancer cells, MRP1 is considered as a diagnostic marker and a therapeutic target to increase the efficacy of a variety of chemotherapy drugs, including anthracyclines (Schaich et al., 2005; Faggad et al., 2009; He et al., 2011). In those situations, inhibiting MRP1 through pharmacological inhibitors is a potential approach to overcome the anti-cancer drug resistance. However, based on its ability to efflux a wide range of endo-/xenobiotics, MRP1 has important physiological functions in normal tissues in unstressed or stressed conditions. Thus, generally inhibiting MRP1 through pharmacological inhibitors may impair the normal tissues' defense ability. So far, the functions of MRP1 in normal tissue defense have not been investigated in depth compared to its effects on drug therapy efficacy in cancer. The work presented in this dissertation investigated the role of MRP1 in the defense of the normal mouse heart. Specific emphasis was put on its potential protective function in chemotherapy drug DOX-induced cardiotoxicity, since DOX-induced cardiotoxicity is a severe dose-limiting side effect in cancer patients receiving this effective anti-cancer medicine.

DOX-induced heart failure is now widely recognized as a high risk complication of cancer chemotherapy experienced by a growing number of cancer survivors. However, there are very few approaches with limited positive effects to prevent or alleviate this life-threatening toxicity. DOX causes oxidative stress in cardiac tissue by promoting the generation of ROS, which further induces the damage to macromolecules, including protein, DNA and lipid. Thus, identifying and studying the genes that may be involved in the oxidative stress regulation will be useful to find the potential strategies to reduce or even prevent DOX-induced cardiotoxicity.

The clinical data showing the correlation between SNPs of MRP1 and patients' susceptibility to DOX-induced cardiotoxicity are informative (Cole., 2014b). These data imply that MRP1 is involved in the heart's defense against DOX toxicity. Further functional studies in our laboratory show that HEK cells that overexpress an MRP1 SNP (Gly671Val) are more sensitive to DOX toxicity compared to cells expressing WT MRP1. This MRP1 SNP actually impairs more than 85% of MRP1's ability to efflux GS-HNE, resulting in a significantly higher intracellular accumulation of GS-HNE (Jungsuwadee et al., 2012). These data suggest that MRP1 modulates the cells' sensitivity to DOX, and this is accomplished not simply by effluxing DOX, but by effluxing other important substrates, such as GS-HNE. To test this hypothesis in heart tissue, WT and Mrp1-/- mice were used as a model. The unique advantage of this model is that unlike human MRP1, murine Mrp1 is not able to efflux DOX, but murine Mrp1 retains the ability to efflux other substrates of human MRP1, such as GSH,

GSSG and GS-HNE. Therefore, the Mrp1-/- mouse provides a good model to examine the role of Mrp1 in DOX-induced cardiotoxicity separately from Mrp1 effects on DOX retention.

The role of Mrp1 in normal heart defense against DOX toxicity

The data presented in this dissertation provide insights into the role of Mrp1 in heart defense against DOX toxicity using both in vivo and in vitro model systems. In Chapter 2 of this dissertation, WT and Mrp1-/- mice were treated chronically with DOX, followed by measurement of cardiac function and heart damage. Mrp1-/- mice showed more severe body weight loss and delayed recovery from hemotoxicity. These data imply that Mrp1 could play important protective roles in organs other than the heart. These findings are consistent with the published data demonstrating that Mpr1 protects normal tissues like skin and brain against xenobiotics. Further echocardiogram studies showed that there is no difference in left ventricular function between saline treated WT and Mrp1-/- mice. However, following chronic DOX treatment, Mrp1-/- mice had significantly more severe left ventricle dysfunction compared to WT mice, presenting as significantly lower fractional shortening and ejection fraction. This functional change was consistent with the higher BNP expression level found in DOX treated Mrp1-/- mouse heart. These observations suggest that under normal physiological conditions, loss of Mrp1 does not affect cardiac function; however, under stressful conditions, such as treatment with DOX, and when the stress exceeds a certain threshold, the heart of Mrp1-/- mice showed an impaired defensive ability to respond to the

stress, consequently resulting in functional damage. These data well support our initial hypothesis regarding the protective role of Mrp1 in heart.

The extent of apoptosis was also measured in heart sections from mice chronically-treated with DOX. The quantitative data showed that following DOX treatment, Mrp1-/- mouse heart had significantly more apoptotic cells than WT mice. We believe this higher apoptosis contributes to the more severe cardiac functional damage in Mrp1-/- mice. This is consistent with our previous electron microscopy studies, which show that compared to WT mice, Mrp1-/- mice have more nuclear injury, including early apoptotic changes in nuclei in heart after a single intravenous administration of DOX. The effects of Mrp1 on DOX-induced apoptosis were also observed in our in vitro study, which used isolated neonatal mice cardiomyocytes and cardiac fibroblasts from WT and Mrp1-/- pups. In CM and CF cultures, the same concentration of DOX showed that compared to WT cells, Mrp1-/- cells are more sensitive to DOX toxicity, indicated by lower cell survival, more PARP cleavage, more caspase3 cleavage and more γH2A.X expression. Those data indicate that Mrp1 similarly protects CM and CF against DOX cytotoxicity. Taken together, these data demonstrate the cardiac protective role of MRP1 in both in vivo and in vitro model systems.

The role of Mrp1 in GSH/GSSG homeostasis

The work presented in this dissertation further examined the mechanisms by which Mrp1 protects in the heart following DOX treatment, especially in GSH homeostasis, GS-HNE accumulation and protein oxidative damage.

In Chapter 4 of this dissertation, loss of Mrp1 increased basal intracellular levels of GSH and GSSG in treatment-naïve and saline-treated heart tissue, CM culture and CF culture. However, no differences were observed in the expression of GSH enzymes between genotypes in the absence of DOX treatment. These data are consistent with the reported function of Mrp1 to efflux GSH and GSSG.

DOX treatment further increased intracellular levels of GSH and GSSG in Mrp1-/- CM and CF. This is likely due to the increased GSH synthesis since the expression of GSH synthetic enzymes, GCLc, GCLm and GSS, was increased in DOX-treated Mrp1-/- cells only. Since all the three enzymes are regulated by Nrf2, we examined whether the Nrf2 pathway was activated in DOX treated Mrp1-/- cells. We found that the expression of Nqo1 and HO-1, two additional downstream genes in the Nrf2 pathway, were also significantly higher in DOX treated Mrp1-/- cells compared to WT cells. We concluded that in response to DOX treatment, the Nrf2 pathway was activated in Mrp1-/- cells, and increased the transcription of its downstream genes, including the GSH synthesis enzymes and finally contributed to the elevated intracellular level of GSH and GSSG. However, the elevated GSH was not able to protect Mrp1-/- cells against DOX-induced oxidative stress. Finally, although the elevated GSH level was not able to protect Mrp1-/- mouse heart or Mrp1-/- cells against DOX toxicity, we found a significantly lower GS-HNE level in treatment-naïve mouse heart (Deng et al., submitted). These data mean that the higher GSH level in Mrp1-/- mouse heart does protect against ‘background’ levels of oxidative stress.

An important observation is that Mrp1 deficiency increases the GSH level in the heart and in CM/CF. This means that MRP1-mediated efflux of GSH plays an important role in maintaining the normal intracellular GSH level. Usually, GCL is recognized as the major determinant of cellular GSH homeostasis. It catalyzes the first and rate-limiting step in de novo synthesis of GSH. The expression and activity of GCL is tightly controlled by a complex regulation at several levels, including: transcriptional activation by oxidative stress; reversible formation of the disulfide bond between its two subunits (GCLc and GCLm); and feedback inhibition by GSH. In out study, without a significant difference in GCLc and GCLm expression, the treatment-naïve and saline-treated Mrp1-/- mice heart and Mrp1-/- CM/CF have a higher GSH level compared to WT mice heart and cells. These data indicate the importance of Mrp1-mediated efflux in intracellular GSH level regulation, regardless of the GCL expression and activity changes. In addition, compared to WT cells, the DOX treated Mrp1-/- cells have significantly higher expression of GCLc and GCLm, which caused a further increase in the GSH pool, although there is already a higher basal level of GSH in Mrp1-/- cells. All of these data indicate that GCL is not the only sensor and factor that is responsible for the intracellular GSH level, and that Mrp1-mediated efflux is another important determinant.

The role of Mrp1 in HNE detoxification

Another important consequence of DOX-induced oxidative stress is lipid peroxidation. HNE is one of the major toxic products of lipid peroxidation and

conjugation with GSH is its major metabolism pathway. GS-HNE was investigated in this study because our previous work demonstrated that Mrp1 is the sole, or at least the most important, transporter in mouse heart to efflux GS-HNE. We expected that loss of Mrp1 would cause GS-HNE accumulation in mouse heart, especially under the oxidative stress induced by DOX. In Chapter 4, DOX treatment significantly increased the GS-HNE detected in mice heart tissue. These data were consistent with the expectation that DOX cause oxidative stress in cardiac tissue, leading to lipid peroxidation. However, unlike our expectation, there was no difference in GS-HNE levels between WT and Mrp1-/- mouse heart. We believe this could be due to the complex compensating effects in Mrp1-/- mouse heart. Thus, Mrp1 deficiency may saturate other detoxification pathways of HNE. To answer this question, we would need to quantitate other metabolites of HNE, such as DHN, HNA, GS-DHN and GS-HNA. More information regarding the biological activities of these HNE metabolites and whether they are substrates of Mrp1 will also be helpful in evaluating the effects of Mrp1 on HNE detoxification.

The role of MRP1 in cellular compartments

In Chapter 2 and 3, our studies show that the loss of Mrp1 causes more nuclear injury in mouse heart following acute DOX treatment, more apoptosis in hearts of mice treated chronically with DOX, and more cell apoptosis and DNA damage in CM/CF culture. Thus, it appears that the most severe damage caused by Mrp1 deficiency mainly occurs in the nucleus. This raises a question

regarding the potential function of Mrp1 in nucleus. A previous study in our laboratory has shown that Mrp1 is localized in sarcolemmal membrane of cardiomyocytes in heart in untreated mice. However, upon treatment with DOX, the expression of Mrp1 is significantly increased in the heart mitochondrial fraction. However, we did not examine the nuclear localization of Mrp1 in heart tissue. Although a nuclear localization sequence was not found in MRP1, two publications from the same research group reported that the nuclear MRP1 contributes to multidrug resistance in human mucoepidermoid carcinoma cell lines (Cai et al., 2011; Cai et al., 2013). In addition, Rajagopal et al (2003) reported that human MRP1 is present in a perinuclear region positive for lysosomal markers, and may rescue cancer cells by sequestering the toxic substance away from the nucleus. However, further studies are needed to determine whether this occurs in heart.

In addition, loss of Mrp1 impairs GSH efflux and could cause lower GSH levels in the extracellular environment and finally accelerate oxidative damage in the extracellular environment. Extracellular GSH can also be broken down in the extracellular space by γGT and dipeptidase, thus producing cysteine. The lower extracellular GSH concentration could affect the cysteine/cystine balance, which is also critical for maintaining extracellular redox status. In Chapter 4, our in vitro studies found that exogenous cell impermeable GSH (10 mM) eliminated the difference in cell viability between DOX treated-WT and Mrp1-/- cells. Also, the expression of ECSOD, the only SOD existing in the extracellular environment, is reduced in saline and DOX-treated Mrp1-/- CM. The lower ECSOD expression

may contribute to the Mrp1-/- CM's sensitivity to DOX. These data imply potential effects of Mrp1 on redox status in the extracellular environment, and indicate the need for further studies.

Clinical significance of this study

During the past two decades, the focus of MRP1 research has been on the negative effects of MRP1 expression, especially its contributions to multidrug resistance in cancer cells. Therefore, the use of MRP1 inhibitors in the treatment of cancer has been the main therapeutic goal (Burkhart et al., 2009; Sirisha et al., 2011; Zhang et al., 2014; Ma et al., 2014). Although this may be beneficial to sensitize multidrug resistant cancer cells to anticancer drugs, our research shows that inhibiting MRP1 in the heart may potentiate the chemotherapy drug-induced cardiotoxicity. These studies provide critical information regarding the potential adverse sequelae of introduction of MRP1 inhibitors as adjuncts to clinical chemotherapy of multidrug resistant tumors. In addition, genetic variants of the *MRP1* gene have been found in clinical patients and multiple SNPs are found to be associated with cancer patients' susceptibility to DOX-induced cardiotoxicity. Our study may provide some explanations for these clinical observations if the SNPs impair MRP1's expression or activity. It will potentially further help to identify these susceptible patients and modify chemotherapy strategies for these individuals and thus prevent such drug-induced toxicity.

Future studies

Based on the results in this dissertation, the following experiments warrant

future investigation:

What are the consequences of increased GSSG in Mrp1-/- mouse heart?

In addition to the higher GSH level, we also demonstrated a significantly higher GSSG level in DOX-treated Mrp1-/- mouse heart and Mrp1-/- CM/CF. Reversible protein S-glutathionylation as a common feature of redox signal transduction is able to regulate the activities of several redox sensitive proteins. Increased intracellular GSSG concentration following microinjection or inhibition of the efflux through Mrp1 has been shown to cause glutathionylation of cysteine-containing proteins, and consequently change their cellular function, finally causing cell death (Park et al., 2009). Investigating the effects of elevated GSH and GSSG levels in Mrp1-/- mouse heart and cells on glutathionylation modification of proteins could provide new insights regarding how Mrp1 modulates the sensitivity to DOX induced cardiotoxicity.

What are the concentrations of HNE and HNE metabolites?

As we discussed above, in addition to conjugation with GSH, HNE has other detoxification pathways. Measurement of the concentration of other HNE metabolites, such as HNA, DHN, GS-HNA, GS-DHN and HNE itself will help to better understand how loss of Mrp1 affects the detoxification of HNE and the consequence of lipid peroxidation.

Does Mrp1 protect heart through other functions in addition to its transport

activity?

Another ABC transporter, P-glycoprotein (Pgp) /MDR1, has been demonstrated to have anti-apoptotic activity independent of its transporter activity (Tainton et al., 2004). In that study, lymphoma cells expressing ATPase-mutant Pgp cannot efflux chemotherapeutic drugs but remained relatively resistant to apoptosis induced by vincristine. In addition, the anti-apoptotic effect of this mutant Pgp is not affected by antibodies that inhibit the efflux function of the protein. Those data are consistent with a dual activity model for Pgp-induced MDR involving both ATPase-dependent drug efflux and ATPase-independent inhibition of apoptosis. It would be important to investigate whether other functions of Mrp1 beyond its transport activity could contribute to the protective role of Mrp1 in DOX toxicity. Use of an Mrp1-specific inhibitor or development of cells expressing Mrp1 with mutations that delete its ability to transport will help to answer this question. Further investigation of Mrp1's localization especially in mitochondria or nucleus and Mrp1's interaction with anti-apoptotic proteins may provide more insight.

Use human induced pluripotent stem (iPS) cells derived CM to study the role of human MRP1 against DOX toxicity.

Since murine Mrp1 does not efflux DOX, here we took advantage of the mouse model to investigate the potential function of Mrp1 in oxidative stress regulation. However, this difference between human MRP1 and mouse Mrp1 may limit the clinical significance of this study. Human induced pluripotent stem

(iPS) cell-derived cardiomyocytes provide a good model to aid drug discovery and improve the predictability of drug efficacy and toxicity screens. Investigation of the function of human MRP1 in these cells would/could provide valuable insight regarding the importance of MRP1 in DOX-induced cardiotoxicity in patients.

What are the concentrations of GSH and GSSG in specific intracellular organelles?

In recent years, increasing evidence demonstrates the existence of well-defined compartments of redox systems within cells, each exhibiting a unique redox environment (Circu et al., 2008). Intracellular GSH is compartmentalized within the mitochondria, nucleus and endoplasmic reticulum (ER), all of which constitute separate redox pools that are distinct from the cytoplasmic pool in terms of distribution of the GSH and GSSG forms, their redox potential and their control of cellular activities. Mrp1 is localized in plasma membrane and in the membrane of intracellular organisms, including lysosome, trans-Golgi vesicles and mitochondria, as shown in studies using techniques such as Western blot, immunofluorescence, and immunogold electron microscopy (Rajagopal et al., 2003; Gennuso et al., 2004; Jungsuwadee et al., 2009). Thus, it will be very important to determine whether such localized expression of Mrp1 affects GSH/GSSG homeostasis in these distinct cell compartments. However, precise quantification of the GSH and GSSG in specific intracellular compartment is difficult.

In summary, this study is the first to document a protective role of Mrp1 in DOX-induced cardiotoxicity despite equal DOX concentrations. It gives critical information regarding the potential adverse sequelae of introduction of MRP1 inhibitors as adjuncts to clinical chemotherapy of multidrug resistant tumors. It will also potentially help to identify the susceptible patients and modify chemotherapy strategies for these individuals and thus prevent such drug-induced toxicity. Further studies as we discussed above will provide essential information to elucidate the mechanism of Mrp1-mediated cardiac protection.

Appendices

Appendix A

List of abbreviations

ABC	ATP-binding cassette
ADP	Adenosine diphosphate
ARE	Antioxidant response element
ATP	Adenosine triphosphate
BNP	B-type natriuretic peptide
CM	Cardiomyocytes
CF	CDHNardiac fibroblasts
Cu,ZnSOD/SOD1	Cu,Zn-superoxide dismutase
DHN	1,4-dihydroxy-2-nonene
DOX	Doxorubicin
ECSOD/SOD3	Extracellular superoxide dismutase
EF	Ejection fraction
Eh	Redox potential
FS	Fractional shortening
GAPDH	Glyceraldehyde-3-phosphate dehydrogenase
GCLc	Glutamate-cysteine ligase catalytic subunit
GCLm	Glutamate-cysteine ligase regulatory subunit
Gpx	Glutathione peroxidase
GR	Glutahione reductase
Grx	Glutaredoxin
GST	Glutathione S-transferase
GSS	Glutathione synthetase
GSH	Glutathione
GSSG	Glutathione disulfide
GS-HNE	Glutathione conjugates of 4-Hydroyx-2-nonenal
γGT	γ glutathione transpeptidase
HO-1	Heme oxygenase 1
HNA	4-hydroxy-2-nonenoic acid
HNE	4-Hydroyx-2-nonenal
HPLC	High performance liquid chromatography
HRP	Horseradish peroxidase

iPS cells	induced pluripotent stem cells
LVEF	Left ventricular ejection fraction
LVFS	Left ventricular fractional shortening
LVIDd	Left ventricular end-diastolic dimension
LVIDs	Left ventricular end-systolic dimension
LVPWd	Left ventricular diastolic posterior wall thickness
LVPWs	Left ventricular systolic posterior wall thickness
LTC4	Leukotriene C4
LY	Lymphocyte
MDA	Malondialdehyde
MnSOD/SOD2	Mn superoxide dismutase
MBB	Monobromobimane
Mrp1/Abcc1	Multidrug resistance-associated protein 1
Mrp1-/-	Mrp1 knock out
MRM	Multiple reaction monitoring
MSD	Membrane spanning domain
NBD	Nucleotide binding domain
NQO1	NAD(P)H dehydrogenase, quinone 1
Nrf2	Nuclear factor-like 2
Pgp	P-glycoprotein
Prx	Peroxiredoxin
RNS	Reactive nitrogen species
ROS	Reactive oxygen species
SNPs	Single nucleotide polymorphisms
TMD	Transmembrane domain
Trx	Thioredoxin
WBC	White blood cell
WT	Wild type

Appendix B

Isolation of neonatal mice cardiomyocytes and cardiac fibroblasts

Solutions:
Hanks balanced salt solution without Ca^{2+} and Mg^{2+} (14185-052, Life Technologies, CA)
Enzyme solution: 10mg collagenase in 30 m l HBSS (collagenase type 2: Worthington Biochemical Corp., Lakewood, NJ)
DMEM (10965, Life Technologies, CA)
Fetal bovine serum (FBS) (10438-026, Life Technologies, CA)
Penicillin/streptomycin (15140-122GIBCO, Grand Island, NY)

Protocol:

1. 1–3 days old pups are sacrificed by cervical dislocation. The hearts are removed and placed in cold HBSS without Ca^{2+} and Mg^{2+}.
2. The hearts are washed with HBSS for several times to remove most of the red blood cells and the atria are removed and discarded.
3. The ventricles are transferred to 1 mL of enzyme solution and minced into small pieces.
4. Tissue is placed into a 10 mL beaker and a small stir bar is added.
5. 4 mL of enzyme solution is added for a total of 5 mL. The beaker is placed in a dish of warm water bath (37°C) on a stir plate and the tissues agitated for 10 min.
6. At the end of each cycle of agitation, the tissue pieces are allowed to settle. Then, the supernatant is removed and added to a 15 mL centrifuged tube with 0.5 mL FBS with a final FBS concentration of 10% and centrifuged for 10 min at 800 rpm. (Note: the supernatant from the first digestion may contain mainly red blood cells and should be discarded)
7. At the end of centrifugation, the supernatant is discarded and the cell pellet is resuspended in 2 mL DMEM and placed in a 6-well culture dish.
8. Step 5 -7 are repeated until all tissue has been digested. This can take up to 10 individual digests for the ventricular tissue.
9. After pre-plating period (about 2 hours) to allow the non-myocytes predominantly fibroblasts to adhere to the plastics, the suspensions mainly including cardiomyocytes are collected form cell culture dish by gently washing with culture medium and collected in a 15 mL centrifuge tube and centrifuged at 800 rpm for 10 min. The cell pellet mainly including cardiomyocytes are resuspended in DMEM medium and plated in cell culture dish with appropriate cell density (about $10^5/cm^2$). The non-myocytes predominantly fibroblasts which adhere to the plastics before are maintained in DMEM medium with 10% FBS.
10. CM numbers are determined by counting living cells (with Trypan blue) using a hemocytometer.
11. For CM culture, 100 μmol/L Bromodeoxyuridine (Sigma Chemical Co) is added during the first 48 h of culture to prevent proliferation of

nonmyocytes.

12. CF cultures are used for experiments after two passages to eliminate other nonmyocytes.

References

Alary J, Guéraud F, and Cravedi JP. (2003) Fate of 4-hydroxynonenal in vivo: disposition and metabolic pathways. *Mol Aspects Med*. 24:177-187.

Arcamone F, Cassinelli G, Fantini G, Grein A, Orezzi P, Pol C, and Spalla C. (1969) Adriamycin, 14-hydroxydaunomycin, a new antitumor antibiotic from S. peucetius var. caesius. *Biotechnol Bioeng.* 11:1101-1110.

Armstrong JS, Steinauer KK, Hornung B, Irish JM, Lecane P, Birrell GW, Peehl DM, and Knox SJ. (2002) Role of glutathione depletion and reactive oxygen species generation in apoptotic signaling in a human B lymphoma cell line. *Cell Death Differ.* 9(3):252-263.

Ballatori N, Hammond CL, Cunningham JB, Krance SM, and Marchan R. (2005) Molecular mechanisms of reduced glutathione transport: role of the MRP/CFTR/ABCC and OATP/SLC21A families of membrane proteins. *Toxicol Appl Pharmacol.* 204:238-255.

Ballatori N, Krance SM, Notenboom S, Shi S, Tieu K, and Hammond CL. (2009) Glutathione dysregulation and the etiology and progression of human diseases. *Biol Chem.* 390:191-214.

Baudouin-Cornu P, Lagniel G, Kumar C, Huang ME, and Labarre J. (2012) Glutathione degradation is a key determinant of glutathione homeostasis. *J Biol Chem.* 287:4552-4561.

Brewer AC, Mustafi SB, Murray TV, Rajasekaran NS, and Benjamin IJ. (2012) Reductive stress linked to small HSPs, G6PD, and Nrf2 pathways in heart disease. *Antioxid Redox Signal* .18:1114-1127.

Burkhart CA, Watt F, Murray J, Pajic M, Prokvolit A, Xue C, Flemming C, Smith J, Purmal A, Isachenko N, Komarov PG, Gurova KV, Sartorelli AC, Marshall GM, Norris MD, Gudkov AV, and Haber M. (2009) Small-molecule multidrug resistance-associated protein 1 inhibitor reversan increases the therapeutic index of chemotherapy in mouse models of neuroblastoma. *Cancer Res.* 69:6573-6580.

Butterfield DA, and Stadtman ER. (1997) Protein oxidation processes in aging brain. *Advantage of Cell Aging Gerontology.* 2:161-191.

Cai B, Miao Y, Liu Y, Xu X, Guan S, Wu J, and Liu Y. (2013) Nuclear multidrug-resistance related protein 1 contributes to multidrug-resistance of mucoepidermoid carcinoma mainly via regulating multidrug-resistance protein 1: a human mucoepidermoid carcinoma cells model and Spearman's rank correlation analysis. *PLoS One.* 8:e69611.

Cai BL, Xu XF, Fu SM, Shen LL, Zhang J, Guan SM, and Wu JZ. (2011) Nuclear translocation of MRP1 contributes to multidrug resistance of mucoepidermoid carcinoma. *Oral Oncol.* 47:1134-1140.

Camelliti P, Borg TK, and Kohl P. (2005) Structural and functional characterisation of cardiac fibroblasts. *Cardiovasc Res.* 65:40-51.

Chaiswing L, Cole MP, St Clair DK, Ittarat W, Szweda LI, and Oberley TD. (2004) Oxidative damage precedes nitrative damage in adriamycin-induced cardiac mitochondrial injury. *Toxicol Pathol* .32, 536-547.

Chatterjee K, Zhang J, Honbo N, and Karliner JS. (2010) Doxorubicin

cardiomyopathy. *Cardiology.* 115:155-162.
Chen EP, Bittner HB, Davis RD, Folz RJ, and Van Trigt P. (1996) Extracellular superoxide dismutase transgene overexpression preserves postischemic myocardial function in isolated murine hearts. *Circulation.* 94:II412-417.
Chen Y, Shertzer HG, Schneider SN, Nebert DW, and Dalton TP. (2005). Glutamate cysteine ligase catalysis: dependence on ATP and modifier subunit for regulation of tissue glutathione levels. *J. Biol. Chem.* 280:33766-33774.
Christiansen S, and Autschbach R. (2006) Doxorubicin in experimental and clinical heart failure. *Eur J Cardiothorac Surg.* 30: 611–616.
Circu ML, and Aw TY. (2008) Glutathione and apoptosis. *Free Radic Res.* 42: 689-706.
Circu ML, Stringer S, Rhoads CA, Moyer MP, and Aw TY. (2009) The role of GSH efflux in staurosporine-induced apoptosis in colonic epithelial cells. *Biochem Pharmacol.* 77:76-85.
Cole MP, Chaiswing L, Oberley TD, Edelmann SE, Piascik MT, Lin SM, Kiningham KK, and St Clair DK. (2006) The protective roles of nitric oxide and superoxide dismutase in adriamycin-induced cardiotoxicity. *Cardiovasc Res.* 69:186-97.
Cole SP. (2014a) Multidrug Resistance Protein 1 (MRP1, ABCC1): A 'Multitasking' ABC Transporter. *J Biol Chem.* 289:30880-30888.
Cole SP. (2014b)Targeting the multidrug resistance protein (MRP1, ABCC1): past, present and future. *Annu. Rev. Pharmacol. Toxicol.* 54:95-117.
Cole SP, Bhardwaj G, Gerlach JH, Mackie JE, Grant CE, Almquist KC, Stewart AJ, Kurz EU, Duncan AM, and Deeley RG. (1992) Overexpression of a transporter gene in a multidrugresistant human lung cancer cell line. *Science* 258:1650-1654.
Cole SP, Downes HF, Mirski SE, and Clements DJ. (1990) Alterations in glutathione and glutathione-related enzymes in a multidrug-resistant small cell lung cancer cell line. *Mol Pharmacol.* 37:192-197.
Cole SP, and Deeley RG. (1998) Multidrug resistance mediated by the ATP-binding cassette transporter protein MRP. *Bioessays.* 20:931-940.
Cole SP, and Deeley RG. (2006) Transport of glutathione and glutathione conjugates by MRP1.*Trends Pharmacol Sci.* 27:438-446.
Couture L, Nash JA, and Turgeon J. (2006) The ATP-binding cassette transporters and their implication in drug disposition: a special look at the heart. *Pharmacol Rev.* 58:244-258.
Dalleau S, Baradat M, Guéraud F, and Huc L. (2013) Cell death and diseases related to oxidative stress: 4-hydroxynonenal (HNE) in the balance. *Cell Death Differ* .20:1615-1630.
Dasuri K, Zhang L, and Keller JN. (2013) Oxidative stress, neurodegeneration, and the balance of protein degradation and protein synthesis. *Free Radic Biol Med.* 62:170-185.
Deng J, Coy DJ, Zhang W, Sunkara M, Morris A, Wang C, Chaiswing L, Oberley TD, Vore M, Jungsuwadee P. Elevated glutathione in multidrug resistance associated protein 1 (Mrp1/Abcc1) null mice does not protect

against doxorubicin-induced cardiotoxicity. (Submitted)
Diah SK, Smitherman PK, Townsend AJ, and Morrow CS (1999) Detoxification of 1-chloro-2,4-dinitrobenzene in MCF7 breast cancer cells expressing glutathione S-transferase P1-1 and/or multidrug resistance protein 1. *Toxicol Appl Pharmacol.* 157:85-93.
Dolye JJ, Neugut AI, Jacobson JS, Grann VR, and Hershman DL. (2005) Chemotherapy and cardiotoxicity in older breast cancer patients: a population-based study. *J Clin Oncol.* 23:8597-8605.
Dong J, Yang G, and McHaourab HS. (2005) Structural basis of energy transduction in the transport cycle of MsbA. *Science.* 308:1023-1028.
Ducroq J, Moha ou Maati H, Guilbot S, Dilly S, Laemmel E, Pons-Himbert C, Faivre JF, Bois P, Stücker O, and Le Grand M. (2010) Dexrazoxane protects the heart from acute doxorubicin-induced QT prolongation: a key role for I(Ks). *Br J Pharmacol.* 159:93-101.
Ellison I, and Richie JP Jr. (2012) Mechanisms of glutathione disulfide efflux from erythrocytes. *Biochem Pharmacol.* 83:164-169.
Esterbauer H, Schaur RJr, and Zollner H. (1991) Chemistry and biochemistry of 4- hydroxynonenal, malonaldehyde and related aldehydes. *Free Radical Biology and Medicine.* 11:81-128.
Faggad A, Darb-Esfahani S, Wirtz R, Sinn B, Sehouli J, Könsgen D, Lage H, Noske A, Weichert W, Buckendahl AC, Budczies J, Müller BM, Elwali NE, Dietel M, and Denkert C. (2009) Expression of multidrug resistance-associated protein 1 in invasive ovarian carcinoma: implication for prognosis. *Histopathology.* 54:657-666.
Flens M, Zaman G, van der Valk P, Izquierdo M, Schroeijers A, Scheffer G, van der Groep P, de Haas M, Meijer C, and Scheper R. (1996) Tissue distribution of the multidrug resistance protein. *Am J Pathol.* 148:1237-1247.
Fogli S, Nieri P, and Breschi MC. (2004) The role of nitric oxide in anthracycline toxicity and prospects for pharmacologic prevention of cardiac damage. *FASEB J.* 18:664-675.
Folz RJ, and Crapo JD. (1994) Extracellular superoxide dismutase (SOD3): tissue-specific expression, genomic characterization, and computer-assisted sequence analysis of the human EC SOD gene. *Genomics.* 22:162-171.
Forman HJ, Fukuto JM, and Torres M. (2004). Redox signaling: thiol chemistry defines which reactive oxygen and nitrogen species can act as second messengers. *Am. J. Physiol. Cell Physiol.* 287:C246-256.
Franco AA, Odom RS, and Rando TA. (1999) Regulation of antioxidant enzyme gene expression in response to oxidative stress and during differentiation of mouse skeletal muscle. *Free Radic Biol Med.* 27:1122-1132.
Franco R, Bortner CD, Schmitz I, and Cidlowski JA. (2014) Glutathione depletion regulates both extrinsic and intrinsic apoptotic signaling cascades independent from multidrug resistance protein 1. *Apoptosis.* 19:117-34.
Franco R, Panayiotidis MI, and Cidlowski JA. (2007) Glutathione depletion is necessary for apoptosis in lymphoid cells independent of reactive oxygen species formation. *J Biol Chem.* 282:30452–30465.
Franklin CC, Backos DS, Mohar I, White CC, Forman HJ, and Kavanagh TJ.

(2009) Structure, function, and post-translational regulation of the catalytic and modifier subunits of glutamate cysteine ligase. *Aspects Med.* 30:86-98.

Fraser JA, Kansagra P, Kotecki C, Saunders RD, and, McLellan LI. (2003) The modifier subunit of Drosophila glutamate-cysteine ligase regulates catalytic activity by covalent and noncovalent interactions and influences glutathione homeostasis in vivo. *J Biol Chem.* 278:46369-46377.

Frohnert BI, and Bernlohr DA. (2014) Glutathionylated products of lipid peroxidation: A novel mechanism of adipocyte to macrophage signaling. *Adipocyte.* 3:224-229.

Fromm MF. (2004) Importance of P-glycoprotein at blood-tissue barriers. *Trends Pharmacol Sci.* 25:423-429.

Fukai T, Folz RJ, Landmesser U, and Harrison DG. (2002) Extracellular superoxide dismutase and cardiovascular disease. Cardiovasc Res. 55:239-249.

Fukai T, Siegfried MR, Ushio-Fukai M, Griendling KK, and Harrison DG. (1999) Modulation of extracellular superoxide dismutase expression byangiotensin II and hypertension. *Circ. Res.* 85:23-28.

Fukai T, Siegfried MR, Ushio-Fukai M, Cheng Y, Kojda G, and Harrison DG. (2000) Regulation of the vascular extracellular superoxide dismutase by nitric oxide and exercise training. *J. Clin. Invest.*105:1631-1639.

Ganguli D, Kumar C, and Bachhawat AK. (2007) The alternative pathway of glutathione degradation is mediated by a novel protein complex involving three new genes in Saccharomyces cerevisiae. *Genetics.* 175:1137-1151.

Gao J, Xiong Y, Ho YS, Liu X, Chua CC, Xu X, Wang H, Hamdy R, and Chua BH. (2008) Glutathione peroxidase 1-deficient mice are more susceptible to doxorubicin-induced cardiotoxicity. *Biochim Biophys Acta.* 1783:2020-2029.

Gennuso F, Fernetti C, Tirolo C, Testa N, L'Episcopo F, Caniglia S, Morale MC, Ostrow JD, Pascolo L, Tiribelli C, and Marchetti B. (2004) Bilirubin protects astrocytes from its own toxicity by inducing up-regulation and translocation of multidrug resistance-associated protein 1 (Mrp1). *Proc Natl Acad Sci U S A.* 101:2470-145.

Gewirtz DA. (1999) A critical evaluation of the mechanisms of action proposed for the antitumor effects of the anthracycline antibiotics adriamycin and daunorubicin. *Biochem Pharmacol.* 57:727-741.

Ghibelli L, Fanelli C, Rotilio G, Lafavia E, Coppola S, Colussi C, Civitareale P, and Ciriolo MR. (1998) Rescue of cells from apoptosis by inhibition of active GSH extrusion. *FASEB J.* 12:479-486.

Green PS, and Leeuwenburgh C. (2002) Mitochondrial dysfunction is an early indicator of doxorubicin-induced apoptosis. *Biochim Biophys Acta.* 1588:94-101.

Grimble RF, Jackson AA, Persaud C, Wride MJ, Delers F, and Engler R. (1992) Cysteine and glycine supplementation modulate the metabolic response to tumor necrosis factor alpha in rats fed a low protein diet. *J Nutr.* 122:2066-2073.

Hammond CL, Madejczyk MS, and Ballatori N. (2004) Activation of plasma membrane reduced glutathione transport in death receptor apoptosis of

HepG2 cells. *Toxicol Appl Pharmacol.* 195:12-22.

Hammond CL, Marchan R, Krance SM, and Ballatori N. (2007) Glutathione export during apoptosis requires functional multidrug resistance-associated proteins. *J Biol Chem.* 282:14337-14347.

Hansen JM, Go YM, and Jones DP. (2006) Nuclear and mitochondrial compartmentation of oxidative stress and redox signaling. *Annu Rev Pharmacol Toxicol.* 46:215-234.

Hayashi A, Suzuki H, Itoh K, Yamamoto M, and, Sugiyama Y. (2003) Transcription factor Nrf2 is required for the constitutive and inducible expression of multidrug resistance-associated protein1 in mouse embryo fibroblasts. *Biochemical and Biophysical Research Communications*. 310:824-829.

He SM, Li R, Kanwar JR, and Zhou SF. (2011) Structural and functional properties of human multidrug resistance protein 1 (MRP1/ABCC1). *Curr Med Chem.* 18:439-81.

He YY, Huang JL, Ramirez DC, and , Chignell CF. (2003) Role of reduced glutathione efflux in apoptosis of immortalized human keratinocytes induced by UVA. *J Biol Chem.* 278:8058-8064.

Higgins CF. (2001) ABC transporters: physiology, structure and mechanism--an overview. *Res Microbiol.* 152:205-210.

Higgins CF, and Linton KJ. (2004) The ATP switch model for ABC transporters. *Nat Struct Mol Biol* .11:311-322.

Hirrlinger J, and Dringen R. (2005) Multidrug resistance protein 1-mediated export of glutathione and glutathione disulfide from brain astrocytes. *Methods Enzymol.* 400:395-409.

Hirrlinger J, König J, Keppler D, Lindenau J, Schulz JB, and Dringen R. (2001) The multidrug resistance protein MRP1 mediates the release of glutathione disulfide from rat astrocytes during oxidative stress. *J Neurochem.* 76:627-636.

Hogg N. (2002) The biochemistry and physiology of S-nitrosothiols. *Annu Rev Pharmacol Toxicol.* 42:585-600.

Hsia, TC, Lin, CC, Wang, JJ, Ho, ST, and Kao, A. (2002) Relationship between chemotherapy response of small cell lung cancer and P-glycoprotein or multidrug resistance-related protein expression. *Lung.* 180:173-179.

Huang CS, Chang LS, Anderson ME, and, Meister A. (1993) Catalytic and regulatory properties of the heavy subunit of rat kidney gamma-glutamylcysteine synthetase. *J Biol Chem.* 268:19675-19680.

Ijiri K, and Potten CS. (1987) Further studies on the response of intestinal crypt cells of different hierarchical status to eighteen different cytotoxic agents. *Br J Cancer.* 55:113-123.

Itoh K, Wakabayashi N, Katoh Y, Ishii T, O'Connor T, and, Yamamoto M. (2003) Keap1 regulates both cytoplasmic-nuclear shuttling and degradation of Nrf2 in response to electrophiles. *Genes to Cells.* 8:379-391.

Jones DP. (2008) Radical-free biology of oxidative stress. *Am J Physiol Cell Physiol.* 295:C849-868.

Jungsuwadee P, Cole MP, Sultana R, Joshi G, Tangpong J, Butterfield DA,

St. Clair DK, and Vore M. (2006) Increase in Mrp1 expression and 4-hydroxy-2-nonenal adduction in heart tissue of Adriamycin-treated C57BL/6 mice. *Mol Cancer Ther.* 5:2851-2860.

Jungsuwadee P, Nithipongvanitch R, Chen Y, Oberley TD, Butterfield DA, St. Clair DK, and Vore M. (2009) Mrp1 Localization and Function in Cardiac Mitochondria after Doxorubicin. *Mol Pharmacol.* 75:1117-1126.

Jungsuwadee P, Zhao T, Stolarczyk EI, Paumi CM, Butterfield DA, St Clair DK, and Vore M. (2012) The G671V variant of MRP1/ABCC1 links doxorubicin-induced acute cardiac toxicity to disposition of the glutathione conjugate of 4-hydroxy-2-trans-nonenal. *Pharmacogenet Genomics.* 22:273-284.

Kamkin A, Kiseleva I, Lozinsky I, and Scholz H. (2005) Electrical interaction of mechanosensitive fibroblasts and myocytes in the heart. *Basic Res Cardiol.* 100:337-345.

Kang YJ. (2007) Antioxidant defense against anthracycline cardiotoxicity by metallothionein. *Cardiovasc Toxicol.* 7:95-100.

Kim SR, Saito Y, Itoda M, Maekawa K, Kawamoto M, Kamatani N, Ozawa S, and Sawada J. (2009) Genetic variations of the ABC transporter gene ABCB11 encoding the human bile salt export pump (BSEP) in a Japanese population. Drug Metab. *Pharmacokinet.* 24: 277-281.

Kliment CR, Suliman HB, Tobolewski JM, Reynolds CM, Day BJ, Zhu X, McTiernan CF, McGaffin KR, Piantadosi CA, and Oury TD. (2009) Extracellular superoxide dismutase regulates cardiac function and fibrosis. *J Mol Cell Cardiol.* 47:730-742.

Krohn M, Lange C, Hofrichter J, Scheffler K, Stenzel J, Steffen J, Schumacher T, Brüning T, Plath AS, Alfen F, Schmidt A, Winter F, Rateitschak K, Wree A, Gsponer J, Walker LC, and Pahnke J. (2011) Cerebral amyloid-β proteostasis is regulated by the membrane transport protein ABCC1 in mice. J Clin Invest. 21:3924-3931.

Laberge RM, Karwatsky J, Lincoln MC, Leimanis ML, and Georges E. (2007) Modulation of GSH levels in ABCC1 expressing tumor cells triggers apoptosis through oxidative stress. *Biochem Pharmacol.* 73:1727-1737.

Lambrechts S, Lambrechts D, Despierre E, Van Nieuwenhuysen E, Smeets D, Debruyne PR, Renard V, Vroman P, Luyten D, Neven P, Amant F, Leunen K, Vergote I; Belgian and Luxembourg Gynaecological Oncology Group (BGOG). (2015) Genetic variability in drug transport, metabolism or DNA repair affecting toxicity of chemotherapy in ovarian cancer. *BMC Pharmacol Toxicol.* 16:2.

Laukkanen MO, Leppänen P, Turunen P, Porkkala-Sarataho E, Salonen JT, and Ylä-Herttuala S. (2001) Gene transfer of extracellular superoxide dismutase to atherosclerotic mice. *Antioxid Redox Signal.* 3:397-402.

Lebovitz RM, Zhang H, Vogel H, Cartwright J Jr, Dionne L, Lu N, Huang S, and Matzuk MM. (1996) Neurodegeneration, myocardial injury, and perinatal death in mitochondrial superoxide dismutase-deficient mice. *Proc Natl Acad Sci U S A.* 93: 9782-9787.

Leier I, Jedlitschky G, Buchholz U, Cole SP, Deeley RG, and Keppler D

(1994) The MRP gene encodes an ATP-dependent export pump for leukotriene C4 and structurally related conjugates. *Journal of Biological Chemistry.* 269:27807-27810.

Leonard GD, Fojo T, and Bates SE. (2003) The role of ABC transporters in clinical practice. *Oncologist.* 8:411-424.

Leslie EM, Deeley RG, and Cole SP. (2005) Multidrug resistance proteins: role of P-glycoprotein, MRP1, MRP2, and BCRP (ABCG2) in tissue defense. *Toxicol Appl Pharmacol.* 204:216-237.

Leslie EM, Ito K, Upadhyaya P, Hecht SS, Deeley RG, and Cole SP. (2001) Transport of the β-O-glucuronide conjugate of the tobacco-specific carcinogen 4-(methylnitrosamino)-1-(3-pyridyl)-1-butanol (NNAL) by the multidrug resistance protein 1 (MRP1). Requirement for glutathione or a non-sulfur-containing analog. *J Biol Chem*. 276:27846-27854.

Levonen AL, Landar A, Ramachandran A, Ceaser EK, Dickinson DA, Zanoni G, Morrow JD, and Darley-Usmar VM. (2004) Cellular mechanisms of redox cell signalling: role of cysteine modification in controlling antioxidant defences in response to electrophilic lipid oxidation products. *Biochem J.* 378: 373-82.

Li Q, Bolli R, Qiu Y, Tang XL, Murphree SS, and French BA. (1998) Gene therapy with extracellular superoxide dismutase attenuates myocardial stunning in conscious rabbits. *Circulation.* 98:1438-1448.

Li Q, Bolli R, Qiu Y, Tang XL, Guo Y, and French BA. (2001) Gene therapy with extracellular superoxide dismutase protects conscious rabbits against myocardial infarction. *Circulation.* 103:1893-1898.

Li Q, Kato Y, Sai Y, Imai T, and Tsuji A. (2005) Multidrug resistance-associated protein 1 functions as an efflux pump of xenobiotics in the skin. *Pharm Res* 22:842-846.

Li T, Singal PK. (2000) Adriamycin-induced early changes in myocardial antioxidant enzymes and their modulation by probucol. *Circulation.* 102:2105-2110.**Li T, and Singal PK.** (2000) Adriamycin-induced early changes in myocardial antioxidant enzymes and their modulation by probucol. *Circulation.* 102: 2105-2110.

Li Y, Huang TT, Carlson EJ, Melov S, Ursell PC, Olson JL, Noble LJ, Yoshimura MP, Berger C, Chan PH, Wallace DC, and Epstein CJ. (1995) Dilated cardiomyopathy and neonatal lethality in mutant mice lacking manganese superoxide dismutase. *Nat Genet.* 11:376-381.

Linton KJ. (2007) Structure and function of ABC transporters. *Physiology* 22:122-30.

Liu J, Mao W, Ding B, and Liang CS. (2008) ERKs/p53 signal transduction pathway is involved in doxorubicin-induced apoptosis in H9c2 cells and cardiomyocytes. *Am J Physiol Heart Circ Physiol.* 295:H1956-1965.

Liu QY, and Tan BK. (2003) Relationship between anti-oxidant activities and doxorubicin-induced lipid peroxidation in P388 tumour cells and heart and liver in mice. *Clin Exp Pharmacol Physiol.* 30:185-188.

Loe DW, Deeley RG, and Cole SP. (2000) Verapamil stimulates glutathione transport by the 190-kDa multidrug resistance protein 1 (MRP1). *J*

Pharmacol Exp Ther. 293:530-538.

Lorico A, Rappa G, Finch RA, Yang D, Flavell RA, and Sartorelli AC. (1997) Disruption of the murine MRP (multidrug resistance protein) gene leads to increased sensitivity to etoposide (VP-16) and increased levels of glutathione. *Cancer Res.* 57:5238-5242.

Lou H, Danelisen I, and Singal PK. (2005) Involvement of mitogen-activated protein kinases in adriamycin-induced cardiomyopathy. *Am J Physiol Heart Circ Physiol.* 288:H1925-1930.

Lu SC. (2009) Regulation of glutathione synthesis. *Mol Aspects Med.* 30:42-59.

Lu SC. (2013). Glutathione synthesis. *Biochim. Biophys. Acta.* 1830:3143-3153.

Luo X, Evrovsky Y, Cole D, Trines J, Benson LN, and Lehotay DC. (1997) Doxorubicin-induced acute changes in cytotoxic aldehydes, antioxidant status and cardiac function in the rat. *Biochim Biophys Acta.* 1360:45-52.

Lushchak VI. (2012) Glutathione homeostasis and functions: potential targets for medical interventions. *J Amino Acids.* 2012:736837.

Ma SL, Hu YP, Wang F, Huang ZC, Chen YF, Wang XK, and Fu LW. (2014) Lapatinib antagonizes multidrug resistance-associated protein 1-mediated multidrug resistance by inhibiting its transport function. *Mol Med.* 20:390-399.

Mendoza JL, and Thomas PJ. (2007) Building an understanding of cystic fibrosis on the foundation of ABC transporter structures. *J Bioenerg Biomembr.* 39:499-505.

Miao L, and St Clair DK. (2009) Regulation of superoxide dismutase genes: implications in disease. *Free Radic Biol Med.* 47(4):344-356.

Minich T, Riemer J, Schulz JB, Wielinga P, Wijnholds J, and Dringen R. (2006) The multidrug resistance protein 1 (Mrp1), but not Mrp5, mediates export of glutathione and glutathione disulfide from brain astrocytes. *J Neurochem.* 97:373-384.

Minotti G, Menna P, Salvatorelli E, Cairo G, and Gianni L. (2004) Anthracyclines: Molecular Advances and Pharmacologic Developments in Antitumor Activity and cardiotoxicicty. *Pharmacological Reviews.* 56:185-229.

Mueller CF, Widder JD, McNally JS, McCann L, Jones DP, and Harrison DG. (2005) The role of the multidrug resistance protein-1 in modulation of endothelial cell oxidative stress. *Circ Res.* 97:637-644.

Narasimhan M, and Rajasekaran NS. (2015) Reductive potential - a savior turns stressor in protein aggregation cardiomyopathy. *Biochim Biophys.* 1852:53-60.

Natarajan K, Xie Y, Baer MR, and Ross DD. (2012) Role of breast cancer resistance protein (BCRP/ABCG2) in cancer drug resistance. *Biochem Pharmacol.* 83:1084-1103.

Nguyen T, Sherratt PJ, Nioi P, Yang CS, and Pickett CB. (2005) Nrf2 Controls Constitutive and Inducible Expression of ARE-driven Genes through a Dynamic Pathway Involving Nucleocytoplasmic Shuttling by Keap1. *Journal of Biological Chemistry.* 280:32485-32492.

Nies AT, Jedlitschky G, Konig J, Herold-Mende C, Steiner HH, Schmitt HP, and Keppler D. (2004) Expression and immunolocalization of the multidrug resistance proteins, MRP1-MRP6 (ABCC1-ABCC6), in human brain.

Neuroscience .129:349-360.

Nohl H, Gille L, and Staniek K. (1998) The exogenous NADH dehydrogenase of heart mitochondria is the key enzyme responsible for selective cardiotoxicity of anthracyclines. *Z Naturforsch C.* 53:279-285.

Nooter, K, Brutel de la Riviere, G, Look, M. P, van Wingerden, KE, He nzen-Logmans, SC, Scheper, RJ, Flens, MJ, Klijn, JG, St oter, G, and Foeke ns, JA. (1997a) The prognostic significance of expression of the multidrug resistance-associated protein (MRP) in primary breast cancer. *Br. J. Cancer*. 76:486-493

Nooter, K, de la Riviere, GB, Klijn, J, Stoter, G, and Foekens, J. (1997b) Multidrug resistance protein in recurrent breast cancer. *Lancet.* 349:1885-1886.

Nozaki N, Shishido T, Takeishi Y, and Kubota I. (2004) Modulation of doxorubicin-induced cardiac dysfunction in toll-like receptor-2-knockout mice. *Circulation.* 110:2869-2874.

Obal D, Dai S, Keith R, Dimova N, Kingery J, Zheng YT, Zweier J, Velayutham M, Prabhu SD, Li Q, Conklin D, Yang D, Bhatnagar A, Bolli R, and Rokosh G. (2012) Cardiomyocyte-restricted overexpression of extracellular superoxide dismutase increases nitric oxide bioavailability and reduces infarct size after ischemia/reperfusion. *Basic Res Cardiol.* 107(6):305.

Octavia Y, Tocchetti CG, Gabrielson KL, Janssens S, Crijns HJ, and Moens AL. (2012) Doxorubicin-induced cardiomyopathy: from molecular mechanisms to therapeutic strategies. *J Mol Cell Cardiol.* 52:1213-1225.

Oja SS, Janáky R, Varga V, and Saransaari P. (2000) Modulation of glutamate receptor functions by glutathione. *Neurochem Int.* 37:299-306.

Oliveira PJ, Bjork JA, Santos MS, Leino RL, Froberg MK, Moreno AJ, and Wallace KB. (2004) Carvedilol-mediated antioxidant protection against doxorubicin-induced cardiac mitochondrial toxicity. *Toxicol Appl Pharmacol.* 200:159-68.

Ottaviano FG, and Yee KO. (2011) Communication signals between cardiac fibroblasts and cardiac myocytes. *Journal of Cardiovascular Pharmacology.* 57:513-521.

Pacciarini MA, Barbieri B, Colombo T, Broggini M, Garattini S, and Donelli MG. (1978) Distribution and antitumor activity of adriamycin given in a high-dose and a repeated low-dose schedule to mice. *Cancer Treat Rep.* 62:791-800.

Pappa A, Estey T, Manzer R, Brown D, and Vasiliou V. (2003) Human aldehyde dehydrogenase 3A1 (ALDH3A1): biochemical characterization and immunohistochemical localization in the cornea. *Biochem J.* 376:615-623.

Park AM, Nagase H, Liu L, Vinod Kumar S, Szwergold N, Wong CM, and Suzuki YJ. (2011) Mechanism of anthracycline-mediated down-regulation of GATA4 in the heart. *Cardiovasc Res.* 90:97-104.

Park HA, Khanna S, Rink C, Gnyawali S, Roy S, Sen CK. (2009) Glutathione disulfide induces neural cell death via a 12-lipoxygenase pathway. *Cell Death Differ.* 16:1167-1179.

Park HA, Kubicki N, Gnyawali S, Chan YC, Roy S, Khanna S, Sen CK. (2011) Natural vitamin Eα-tocotrienol protects against ischemic stroke by induction of multidrug resistance-associated protein 1. *Stroke* 42:2308-2314.

Parola M, Leonarduzzi G, Robino G, Albano E, Poli G, and Dianzani MU. (1996) On the role of lipid peroxidation in the pathogenesis of liver damage induced by long-standing cholestasis. *Free Radic Biol Med.* 20:351-359.

Pawłowska J, Tarasiuk J, Wolf CR, Paine MJ, and Borowski E. (2003) Differential ability of cytostatics from anthraquinone group to generate free radicals in three enzymatic systems: NADH dehydrogenase, NADPH cytochrome P450 reductase, and xanthine oxidase. *Oncol Res.* 13:245-252.

Poizat C, Puri PL, Bai Y, and Kedes L. (2005) Phosphorylation-dependent degradation of p300 by doxorubicin-activated p38 mitogen-activated protein kinase in cardiac cells. *Mol Cell Biol.* 25:2673-2687.

Pompella, A, Visvikis, A, Paolicchi, A, De, T, V, and Casini, AF. (2003) *Biochem. Pharmacol.* 66:1499-1503.

Rabbani A, Finn RM, and Ausió J. (2005) The anthracycline antibiotics: antitumor drugs that alter chromatin structure. *Bioessays*. 27:50-56.

Rahman AM, Yusuf SW, Ewer MS. (2007) Anthracycline-induced cardiotoxicity and the cardiac-sparing effect of liposomal formulation. *Int J Nanomedicine.* 2:567-83.

Rajagopal A, and Simon SM. (2003) Subcellular localization and activity of multidrug resistance proteins. *Mol Biol Cell.* 14:3389-3399.

Rajasekaran NS, Connell P, Christians ES, Yan LJ, Taylor RP, Orosz A, Zhang XQ, Stevenson TJ, Peshock RM, Leopold JA, Barry WH, Loscalzo J, Odelberg SJ, and Benjamin IJ. (2007) Human alpha B-crystallin mutation causes oxido-reductive stress and protein aggregation cardiomyopathy in mice. *Cell.* 130:427-439.

Rajasekaran NS, Varadharaj S, Khanderao GD, Davidson CJ, Kannan S, Firpo MA, Zweier JL, and Benjamin IJ. (2011) Sustained activation of nuclear erythroid 2-related factor 2/antioxidant response element signaling promotes reductive stress in the human mutant protein aggregation cardiomyopathy in mice. *Antioxid Redox Signal.* 14:957-971.

Rappa G, Lorico A, Flavell RA, and Sartorelli AC. (1997) Evidence that the multidrug resistance protein (MRP) functions as a co-transporter of glutathione and natural product toxins. *Cancer Research.* 57:5232-5237.

Reddy NM, Kleeberger SR, Yamamoto M, Kensler TW, Scollick C, Biswal S, and Reddy SP. (2007). Genetic dissection of the Nrf2-dependent redox signaling-regulated transcriptional programs of cell proliferation and cytoprotection. *Physiol Genomics.* 32:74-81.

Renes J, de Vries EE, Hooiveld GJ, Krikken I, Jansen PL, and Müller M. (2000) Multidrug resistance protein MRP1 protects against the toxicity of the major lipid peroxidation product 4-hydroxynonenal. *Biochem J.* 350:555-561.

Riad A, Bien S, Gratz M, Escher F, Westermann D, Heimesaat MM, Bereswill S, Krieg T, Felix SB, Schultheiss HP, Kroemer HK, and Tschöpe C. (2008) Toll-like receptor-4 deficiency attenuates doxorubicin-induced cardiomyopathy in mice. *Eur J Heart Fail.* 10:233–243.

Richman PG and, Meister A. (1975) Regulation of gamma-glutamyl-cysteine synthetase by nonallosteric feedback inhibition by glutathione. *J Biol Chem.* 250:1422-1426.

Rush T, Liu X, Nowakowski AB, Petering DH, and Lobner D. (2012) Glutathione-mediated neuroprotection against methylmercury neurotoxicity in cortical culture is dependent on MRP1. *Neurotoxicology.* 33(3):476-481.

Safra T, Muggia F, Jeffers S, Tsao-Wei DD, Groshen S, Lyass O, Henderson R, Berry G, Gabizon A.Lou H, Danelisen I, and Singal PK. (2000) Pegylated liposomal doxorubicin (doxil): reduced clinical cardiotoxicity in patients reaching or exceeding cumulative doses of 500 mg/m2. *Ann Oncol.* 11:1029-1033.

Salerno M, and Garnier-Suillerot A. (2001) *Kinetics of glutathione and daunorubicin efflux from multidrug resistance protein overexpressing small-cell lung cancer cells. Eur J Pharmacol. 421:1-9.*

Sarkadi B, Ozvegy-Laczka C, Német K, and Váradi A. (2004) ABCG2 -- a transporter for all seasons. *FEBS Lett.* 567:116-120.

Saurin, W., M. Hofnung, and E. Dassa. (1999) Getting in or out: early segregation between importers and exporters in the evolution of ATP-binding cassette (ABC) transporters. *J. Mol. Evol.* 48:22-41.

Schaich M, Soucek S, Thiede C, Ehninger G, Illmer T and SHG AML96 Study Group. (2005) MDR1 and MRP1 gene expression are independent predictors for treatment outcome in adult acute myeloid leukaemia. *Br J Haematol.* 128:324-332.

Semsei AF, Erdelyi DJ, Ungvari I, Csagoly E, Hegyi MZ, and Kiszel PS. (2012) ABCC1 polymorphisms in anthracycline-induced cardiotoxicity in childhood acute lymphoblastic leukaemia. *Cell Biol. Int* 36:79-86.

Senft AP, Dalton TP, and Shertzer HG. (2000) Determining Glutathione and Glutathione Disulfide Using the Fluorescence Probe o-Phthalaldehyde. *Analytical Biochemistry.* 280:80-86.

Shi Q, Liu X, Bai Y, Cui C, Li J, Li Y, Hu S, and Wei Y. (2011) In vitro effects of pirfenidone on cardiac fibroblasts: proliferation, myofibroblast differentiation, migration and cytokine secretion. *PLoS One.* 6:e28134.

Sies H. (1997) Oxidative stress: oxidants and antioxidants. *Exp Physiol.* 82:291-295.

Simůnek T, Stérba M, Popelová O, Adamcová M, Hrdina R, and Gersl V. (2009) Anthracycline-induced cardiotoxicity: overview of studies examining the roles of oxidative stress and free cellular iron. *Pharmacol Rep.* 61:154-171.

Singal P, Li T, and Kumar D. (2000) Adriamycin-induced heart failure mechanisms and modulation. *Molecular and Cellular Biochem*. 207:77-86.

Sirisha K, Shekhar MC, Umasankar K, Mahendar P, Sadanandam A, Achaiah G, and Reddy VM. (2011) Molecular docking studies and in vitro screening of new dihydropyridine derivatives as human MRP1 inhibitors. *Bioorg Med Chem.* 19:3249-3254.

Sjöquist PO, Carlsson L, Jonason G, Marklund SL, and Abrahamsson T. (1991) Cardioprotective effects of recombinant human extracellular-

superoxide dismutase type C in rat isolated heart subjected to ischemia and reperfusion. *J. Cardiovasc. Pharmacol.*17:678-683.

Souders CA, Bowers SL, and Baudino TA. (2009) Cardiac fibroblast: the renaissance cell. *Circ Res.* 105:1164-1176.

Sreekumar PG, Spee C, Ryan SJ, Cole SP, Kannan R, and Hinton DR. (2012) Mechanism of RPE cell death in α-crystallin deficient mice: a novel and critical role for MRP1-mediated GSH efflux. *PLoS One.* 7:e33420.

Stěrba M, Popelová O, Lenčo J, Fučíková A, Brčáková E, Mazurová Y, Jirkovský E, Simůnek T, Adamcová M, Mičuda S, Stulík J, and Geršl V. (2011) Proteomic insights into chronic anthracycline cardiotoxicity. *J Mol Cell Cardiol.* 50:849-862.

Stěrba M, Popelová O, Vávrová A, Jirkovský E, Kovaříková P, Geršl V, and Simůnek T. (2013) Oxidative stress, redox signaling, and metal chelation in anthracycline cardiotoxicity and pharmacological cardioprotection. *Antioxid Redox Signal.* 18:899-929.

Stralin, P, and Marklund, SL. (1994) Effects of oxidative stress on expression of extracellular superoxide dismutase, CuZn-superoxidedismutase and mn-superoxide dismutase in human dermal fibroblasts. *Biochem. J.* 298:347-352.

Stride BD, Grant CE, Loe DW, Hipfner DR, Cole SP, and Deeley RG. (1997) Pharmacological characterization of the murine and human orthologs of multidrug-resistance protein in transfected human embryonic kidney cells. *Mol Pharmacol.* 52:344-353.

Sullivan, GF, Amenta, PS, Villanueva, JD, Alvarez, CJ, Yang, JM, and Hait, WN. (1998) The expression of drug resistance gene products during the progression of human prostate cancer. *Clin. Cancer Res.* 4:1393-1403.

Sultana R, Perluigi M, and Allan Butterfield D. (2013) Lipid peroxidation triggers neurodegeneration: a redox proteomics view into the Alzheimer disease brain. Free *Radic Biol Med.* 62:157-169.

Swain S, Whaley F, and Ewer M. (2003) Congestive heart failure in patients treated with doxorubicin: a retrospective analysis of three trials. *Cancer.* 97:2869-2879.

Tainton KM, Smyth MJ, Jackson JT, Tanner JE, Cerruti L, Jane SM, Darcy PK, and Johnstone RW. (2004) Mutational analysis of P-glycoprotein: suppression of caspase activation in the absence of ATP-dependent drug efflux. *Cell Death Differ.* 11:1028-1037.

Takatsu H, Tasaki H, Kim HN, Ueda S, Tsutsui M, Yamashita K, Toyokawa T, Morimoto Y, Nakashima Y, and Adachi T. (2001) Overexpression of EC-SOD suppresses endothelial-cell-mediated LDL oxidation. *Biochem. Biophys. Res. Commun.* 285:84-91.

Taylor C. G., Nagy L. E., and Bray T. M. (1996). Nutritional and hormonal regulation of glutathione homeostasis. Curr. Top. *Cell Regul.* 34, 189–208

Triller, N, Korosec, P, Kern, I, Kosnik, M, and Debeljak, A. (2006) Multidrug resistance in small cell lung cancer: expression of P-glycoprotein, multidrug resistance protein 1 and lung resistance protein in chemo-naive patients and in relapsed disease. *Lung Cancer.* 54:235-240

Vásquez-Vivar J, Martasek P, Hogg N, Masters BS, Pritchard KA Jr, and

Kalyanaraman B. (1997) Endothelial nitric oxide synthase-dependent superoxide generation from adriamycin. *Biochemistry.* 36:11293-11297.

Versantvoort, C.H.M., Broxterman, H.J., Bagrij, T., Scheper, R.J., and Twentyman, P. (1995) Regulation by glutathione of drug transport in multidrug-resistant human lung tumour cell lines overexpressing multidrug resistance-associated protein. *Br. J. Cancer* 72:82-89.

Visscher H, Ross CJ, Rassekh SR, Barhdadi A, Dubé MP, and Al-Saloos H. (2012) Pharmacogenomic prediction of anthracycline-induced cardiotoxicity in children. *J. Clin. Oncol.* 30:1422-1428

Vlaming ML, Mohrmann K, Wagenaar E, de Waart DR, Elferink RP, Lagas JS, van Tellingen O, Vainchtein LD, Rosing H, Beijnen JH, Schellens JH, and Schinkel AH. (2006) Carcinogen and anticancer drug transport by Mrp2 in vivo: studies using Mrp2 (Abcc2) knockout mice. *J Pharmacol Exp Ther.* 318:319-327.

Volkel W, Alvarez-Sanchez R, Weick I, Mally A, Dekant W, and Pahler A. (2005) Glutathione conjugates of 4-hydroxy-2(E)-nonenal as biomarkers of hepatic oxidative stress-induced lipid peroxidation in rats. *Free Radical Biology and Medicine.* 38:1526-1536.

Von Hoff DD, Layard MW, Basa P, Davis HL Jr, Von Hoff AL, Rozencweig M, and Muggia FM.(1979) Risk factors for doxorubicin-induced congestive heart failure. *Ann Intern Med.* 91:710717.

Wahlund G, Marklund SL, and Sjoquist PO. (1992). Extracellularsuperoxide dismutase type C (EC-SOD C) reduces myocardial damage in rats subjected to coronary occlusion and 24 hours of reperfusion. *Free Radic Res Commun.* 17:41-47.

Wang W, and Ballatori N. (1998) Endogenous glutathione conjugates: occurrence and biological functions. *Pharmacol Rev.* 50:335-556.

Westlake CJ, Cole SP, and Deeley RG. (2005) Role of the NH2-terminal membrane spanning domain of multidrug resistance protein 1/ABCC1 in protein processing and trafficking. *Mol Biol Cell.* 16:2483-2492.

Wijnholds J, Evers R, van Leusden MR, Mol CA, Zaman GJ, Mayer U, Beijnen JH, van der Valk M, Krimpenfort P, and Borst P. (1997) Increased sensitivity to anticancer drugs and decreased inflammatory response in mice lacking the multidrug resistance-associated protein. *Nat Med.* 3:1275-1279.

Wijnholds J, Scheffer GL, van der Valk M, van der Valk P, Beijnen JH, Scheper RJ, and Borst P. (1998) Multidrug resistance protein 1 protects the oropharyngeal mucosal layer and the testicular tubules against drug-induced damage. *J Exp Med.* 188:797-808.

Wojnowski L, Kulle B, Schirmer M, Schlüter G, Schmidt A, and Rosenberger A. (2005) NAD(P)H oxidase and multidrug resistance protein genetic polymorphisms are associated with doxorubicin-induced cardiotoxicity. *Circulation* 112:3754-3762.

Woodcock EA, and Matkovich SJ. (2005) Cardiomyocytes structure, function and associated pathologies. *Int J Biochem Cell Biol.* 37:1746-1751.

Xiong Y, Liu X, Lee CP, Chua BH, and Ho YS. (2006) Attenuation of

doxorubicin-induced contractile and mitochondrial dysfunction in mouse heart by cellular glutathione peroxidase. *Free Radic Biol Med* .41:46-55.

Yadav UC, and Ramana KV. (2013) Regulation of NF-κB-induced inflammatory signaling by lipid peroxidation-derived aldehydes. *Oxid Med Cell Longev.* 2013:690545.

Yen HC, Oberley TD, Gairola CG, Szweda LI, and St Clair DK. (1999) Manganese superoxide dismutase protects mitochondrial complex I against adriamycin-induced cardiomyopathy in transgenic mice. *Arch Biochem Biophys.* 362:59-66.

Yen HC, Oberley TD, Vichitbandha S, Ho YS, and St Clair DK. (1996) The protective role of manganese superoxide dismutase against adriamycin-induced acute cardiac toxicity in transgenic mice. *J Clin Invest*. 98:1253-1260

Yoshioka M, Sagara H, Takahashi F, Harada N, Nishio K, Mori A, Ushio H, Shimizu K, Okada T, Ota M, Ito YM, Nagashima O, Atsuta R, Suzuki T, Fukuda T, Fukuchi Y, and Takahashi K. (2009) Role of multidrug resistance-associated protein 1 in the pathogenesis of allergic airway inflammation. *Am J Physiol Lung Cell Mol Physiol.* 296:L30-36.

Zelko IN, and Folz RJ. (2004) Sp1 and Sp3 transcription factors mediate trichostatin A-induced and basal expression of extracellular superoxide dismutase. Free Radic Biol Med. 37:1256-1271.

Zelko IN, Mueller MR, and Folz RJ. (2008) Transcription factors sp1 and sp3 regulate expression of human extracellular superoxide dismutase in lung fibroblasts. Am J Respir Cell Mol Biol. 39:243-251.

Zhang DW, Cole SP, and Deeley RG. (2001) Identification of an amino acid residue in multidrug resistance protein 1 critical for conferring resistance to anthracyclines. *J Biol Chem.* 276:13231-13239.

Zhang H, Limphong P, Pieper J, Liu Q, Rodesch CK, Christians E and Benjamin IJ. (2012) Glutathione-dependent reductive stress triggers mitochondrial oxidation and cytotoxicity. *FASEB J*. 26:1442-1451.

Zhang H, Patel A, Ma SL, Li XJ, Zhang YK, Yang PQ, Kathawala RJ, Wang YJ, Anreddy N, Fu LW, Chen ZS. (2014) In vitro, in vivo and ex vivo characterization of ibrutinib: a potent inhibitor of the efflux function of the transporter MRP1. *Br J Pharmacol.* 171:5845-5857.

Zhang X, Min X, Li C, Benjamin IJ, Qian B, Zhang X, Ding Z, Gao X, Yao Y, Ma Y, Cheng Y, and Liu L. (2010) Involvement of reductive stress in the cardiomyopathy in transgenic mice with cardiac-specific overexpression of heat shock protein 27. *Hypertension.* 55:1412-1417.

Zhang Y, El-Sikhry H, Chaudhary KR, Batchu SN, Shayeganpour A, Jukar TO, Bradbury JA, Graves JP, DeGraff LM, Myers P, Rouse DC, Foley J, Nyska A, Zeldin DC, and Seubert JM. (2009) Overexpression of CYP2J2 provides protection against doxorubicin-induced cardiotoxicity. *Am J Physiol Heart Circ Physiol.* 297:H37-46.

Zhu W, Shou W, Payne RM, Caldwell R, and Field LJ. (2008) A mouse model for juvenile doxorubicin-induced cardiac dysfunction. *Pediatr Res.* 4:488-494.

VITA

Wei Zhang

Education

Ph.D.: Toxicology, University of Kentucky, Lexington, KY
08/2010–Present

MSc: Cell biology, Peking Union Medical College, Beijing, China
09/2007–07/2010

BS: Biotechnology, Beijing Normal University, Beijing, China
09/2003–06/2007

Grant

American Heart Association (AHA) Pre-doctoral Fellowship 07/2013 –06/2015

Publication

Zhang W, Deng J, Coy DJ, Sunkara M, Morris A, Wang C, St Clair DK, Vore M. Loss of Abcc1 (Mrp1) potentiates chronic doxorubicin-induced cardiac dysfunction in mice. (Under review)

Deng J, Coy DJ, **Zhang W**, Sunkara M, Morris A, Wang C, Chaiswing L, St Clair DK, Vore M, Jungsuwadee P. Elevated glutathione in multidrug resistance associated protein 1 (Mrp1/Abcc1) null mice does not protect against doxorubicin-induced cardiotoxicity. (Under review)

Zhang W, St Clair DK, Vore M. Loss of Mrp1 potentiates Doxorubicin-induced cardiotoxicity in neonatal mouse cardiomyocytes and cardiac fibroblasts. (In preparation)

Zhao T, Hou CX, Zhang Y, **Zhang W,** Yan B, Thompson SR, Vore M. Translation of multidrug resistance protein (MRP2, ABCC2) is regulated by insulin-like growth factor 2 mRNA binding protein 1. (Under review)

Zhang W, Chen X, Luo A, Lin D, Tan W, Liu Z. Genetic variants of C1orf10 and risk of esophageal squamous cell carcinoma in a Chinese population. *Cancer Sci.* 2009; 100 (9): 1695-700

Chen X, He J, **Zhang W.** Ecological factors affecting choice of Pica pica sericea nest location in Universities in Beijing. *Sichuan Journal of Zoology* 2006; 125 (14): 855-61

Oral presentation
Title: Mrp1 protects doxorubicin-induced cardiotoxicity in mice.
Great Lakes Drug Metabolism and Disposition Group meeting, 2014, Indianapolis, IN.

Poster Presentation
Zhang W, Deng J, Coy DJ, Wang C, Vore M. Loss of Mrp1 potentiates doxorubicin-induced cardiotoxicity in mice.
Society of Toxicology (SOT) meeting, 2015, San Diego.

Zhang W, Deng J, Coy DJ, Wang C, Vore M. Loss of Mrp1 in transgenic mice potentiates doxorubicin-induced cardiotoxicity.
Annual Meeting of the Great Lakes Drug Metabolism Discussion Group, 2014, Indianapolis, IN.

Zhang W, Deng J, Coy DJ, Wang C, Vore M. Loss of Mrp1 in transgenic mice potentiates doxorubicin-induced cardiotoxicity.
Markey Cancer Research Day, 2014, Lexington, KY.

Zhang W, Deng J, Coy DJ, Chaiswing L, Vore M. Loss of Mrp1 potentiates doxorubicin-induced cardiotoxicity in mice.
Society of Toxicology (SOT) meeting, 2014 Phoenix,

Zhang W, Deng J, Coy DJ, Wang C, Vore M. Loss of Mrp1 potentiates doxorubicin-induced cardiotoxicity in mice.
Gill Heart Research Day, 2014, Lexington, KY.

Zhang W, Deng J, Coy DJ, Chaiswing L, Vore M. Mrp1 protects against doxorubicin-induced cardiotoxicity in vitro.
Gill Heart Research Day, 2013, Lexington, KY.

Zhang W, Deng J, Coy DJ, Chaiswing L, Vore M. Mrp1 protects against doxorubicin-induced cardiotoxicity in vitro.
Markey Cancer Research Day, 2013, Lexington, KY.

Zhang W, Coy DJ, Deng J, Vore M. Mrp1 protects against doxorubicin-induced cardiotoxicity in vitro.
Experimental Biology (EB) meeting, 2013 Boston, MA.